Assessment of Hydrological Responses to Climate Change in Mt. Elgon Sub-Watersheds, Kenya

John Mwanzia Musau

A thesis Submitted in Partial Fulfillment for the Degree of Master of Science in Environmental Engineering and Management in the Jomo Kenyatta University of Agriculture and Technology

2015

DECLARATION

This thesis is my original work and has not been presented for a degree in any other university.

Signature…….. Date……..

John Mwanzia Musau

This thesis has been submitted for examination with our approval as university supervisors.

Signature…….. Date……..

Prof. John Gathenya

JKUAT, Kenya

Signature…….. Date……..

Dr. Eike Luedeling

World Agroforestry Centre (ICRAF), Kenya

Signature…….. Date……..

Mr. Joseph Sang

JKUAT, Kenya

Signature…….. Date……..

Prof. Patrick Home

JKUAT, Kenya

DEDICATION

To my parents Mr. and Mrs. Musau, my wife Grace and spiritual father Fr. Lance Nadeau for their guidance and support.

ACKNOWLEDGEMENT

First of all I thank the almighty God for the wisdom and courage to reach this far. I extend my deepest gratitude to my family, their encouragement and care made it possible to persist to the end.

Thank you Jomo Kenyatta University of Agriculture and Technology, Biomechanical and Environmental Engineering Department (BEED) for the opportunity to be part of the Msc Environmental Engineering and Management class of 2012. I express my sincere gratitude to my supervisors for their valuable guidance and support throughout my research.

Financial support for this research was provided by the World Agro-forestry Centre (ICRAF). I am thankful to ICRAF for providing the funding for this project. I acknowledge intellectual discussions with my colleagues at JKUAT and the World Agro-forestry Centre, Nairobi. I am greatly indebted to Water Resources Management Authority (WARMA) and Kenya Meteorological Department (KMD) for providing the hydrological and climatic data respectively.

TABLE OF CONTENTS

LIST OF TABLES

LIST OF FIGURES

LIST OF APPENDICES

LIST OF ABBREVIATIONS

ANN	Artificial Neural Network
CCCSN	Canadian Climate Change Scenarios Network
CN	Curve Number
DEM	Digital Elevation Model
GCM	General Circulation Model
GHGs	Greenhouse Gases
GLUE	Generalized Likelihood Uncertainty Estimation
HRU	Hydrological Response Unit
IPCC	Intergovernmental Panel on Climate Change
IWRM	Integrated Water Resources Management
KSS	Kenya Soil Survey
LH-OAT	Latin Hypercube One-factor-At-a-Time
NSE	Nash Sutcliffe Efficiency
SCS	Soil Conservation Service
SOTER	Soil Terrain Database
SRES	IPCC Special Report on Emissions Scenarios
SRTM	Shuttle Radar Topography Mission
SUFI	Sequential Uncertainty Fitting
SWAT	Soil and Water Assessment Tool
USDA-ARS	United States Department of Agriculture–Agricultural Research Service

ABSTRACT

Watershed hydrology is responsive to changing climatic patterns. Sustainable resource planning and management at watershed scale therefore requires consideration of climate change impacts, which may result in future changes in water resources quantity and quality. Climate change is a major threat to agriculture-based livelihoods and natural resource management regimes in East Africa. Communities which rely mainly on climate-sensitive sectors for their livelihoods are the severely affected by impacts of climate change.

Mt. Elgon, which is the study area for this project, is a key water tower endowed with a rich diversity of flora and fauna which influence lives and livelihoods of thousands of people through provision of ecosystem services. The main objective of this study was to assess potential impacts of climate change on the hydrology of the four main sub-watersheds on the eastern slopes of Mt. Elgon namely Kuywa, Kimilili, Rongai and Koitobos. More specifically, this study sought to (i) calibrate and validate SWAT model which could be used to simulate the hydrological processes in Mt. Elgon sub-watersheds, (ii) simulate climate change scenarios reflecting expected rainfall and temperature change for the 2011-2040 (2020s), 2041-2070 (2050s) and 2071-2100 (2080s) periods, and (iii) assess potential hydrological impacts of the climate change scenarios.

In this study, the 2009 version of the SWAT model was used. 29-year long records (1970-1998) of daily hydro-climatic data in the upper Nzoia River basin were utilized for model setup. Model calibration was conducted using the sequential uncertainty fitting version 2 (SUFI-2) algorithm in the SWAT CUP software. Statistical downscaling was used to develop climate scenarios in form of additive and ratio anomalies between the baseline period (1960-1990) and three future periods: 2020s (2011-2040), the 2050s (2041-2070) and the 2080s (2071-2100).

The SWAT model performed well in simulating monthly stream flow with R^2 values of 0.68 and 0.70 and NSE values of 0.58 and 0.70 for the calibration (1986-1998) and validation (1973-1985) periods, respectively. The delta-change method was used to generate monthly temperature and precipitation change scenarios for the future periods based on output from ten GCMs and three emissions scenarios (A1B, A2 and B1). Different magnitudes of change in climate showed varied streamflow responses in the four watersheds. The results indicated that annual rainfall is likely to increase by between 1.4% and 4.6% by the 2020s, 3.3% and 6.4% by the 2050s, and 7.3% and 15.1% by the 2080s. Projected monthly changes varied strongly depending on GCM, GHGs emissions scenario and time period. Results on streamflow response suggested potential dramatic changes in streamflow. The overall relative changes in annual mean flow in the whole catchment ranged from -2.9% to +8.9% by 2020s, -9.3% to -0.2% by 2050s and 1.7% to 22.6% by 2080s depending on the emission scenario. This implies a likely increase in floods in the area in the 2020s and 2080s. At sub-basin level, the streamflow response to precipitation and temperature change was nonlinear.

In conclusion, the sub-watersheds depicted distinct variation in their response to climate change despite their proximity. The projected climate change scenarios and streamflow change depicted wide uncertainty. However, there is need to compare results from different climate and hydrological models as well as more detailed model calibration to minimize on the parameter uncertainty. To counter the potential hydrological impacts, there is need for local and regional policy to facilitate mitigation and adaption to climate change impacts. This includes policies on water resource abstraction, flood management as well as disaster preparedness and mitigation. These policies should also include community livelihood improvement and sustainability, forest management as well agricultural management components. In addition, infrastructure development in the area should consider detailed analysis of the potential climate changes to mitigate impacts.

CHAPTER ONE

INTRODUCTION

1.0 Background of the study

The increasing concentration of atmospheric greenhouse gases (GHGs) and consequent global warming are almost certainly responsible for significant changes in global climatic patterns (Xu et al., 2011). According to the Intergovernmental Panel on Climate Change (IPCC, 2007), average global surface temperature during the 1906 to 2005 period increased by 0.56 to 0.92ºC. Towards the end of the 21st century, a further 1.1-2.9ºC increase is expected for the low emissions scenario (SRES B1) and 2.4-6.4ºC for the high emissions scenario (A1FI) relative to the 1980-1999 baseline period. Climate change impacts are likely to affect African countries due to their geographical location, high poverty levels, low technological and institutional capacity to adapt to rapid changes in the environment, high dependency on subsistence agriculture and rapid population growth (IPCC, 2001). The impacts of changing climate are likely to be exacerbated by unsustainable land use practices such as deforestation, wetland drainage and poor land use systems which affect water storage and regulation capacity.

Communities which rely mainly on climate-sensitive sectors for their livelihoods are more likely to be highly affected by the impacts of climate change (Xu et al., 2013). Shifts in the availability of water resources are expected to be among the most significant consequences of the projected climate changes (IPCC, 2007; Kingston & Taylor, 2010). One possible implication of climate change is an intensification of hydrological processes at global, regional and local levels (Labat et al., 2004; Lu et al., 2010; Luo et al., 2013). These hydrological changes will have dire implications on runoff volume and timing, ecosystems dynamics, social and economic systems (Dibike & Coulibaly, 2005; Xu et al., 2013). According to the Intergovernmental Panel on

Climate Change (IPCC, 2007), at high latitudes as well as in some wet tropical regions, a 10-40% increase in annual average river runoff and water availability is expected while in mid-latitudes and dry areas, a 10-30% decrease in river runoff is expected. The intensity of the impacts at local level and the vulnerability of communities and ecosystems to these impacts are related to the particular features of the area, as well as the magnitude and spatial distribution of the changes that will be experienced (Hagg et al., 2007; Matondo et al., 2004). In Mt. Elgon sub-watersheds, the target area of this study, historical occurrences of extreme hydrological conditions with impacts on local populations have exposed the vulnerability of human and natural systems to hydrological changes. Given the vital role of water resources in socio-economic development, the potential hydrological impacts of climate change pose a major challenge for water resource planning and management. Consequently, such impacts have been widely studied mainly using water balance models coupled with General Circulation Models (GCMs) (Chien et al., 2013).

Despite the growing interest in assessing the hydrological impacts of climate change, the underlying uncertainties in simulation of hydrological responses to climate change are still a challenge. In stationary climate conditions and/or physical characteristics, errors in model structure, calibration procedure, and calibration data errors are the main sources of uncertainties (Bastola et al., 2011; Brigode et al., 2013; Yang et al., 2008). In contrast, in non-stationary conditions such as those caused by climate change, the coarse resolution of the climate models and their representation of the atmospheric and other processes, and differences in results of downscaling methods are additional sources of uncertainties (Braga et al., 2013; Chiew et al., 2010; Ficklin et al., 2009; Minville et al., 2008; Teng et al., 2012; Xu et al., 2011). Although the relative significance of the different uncertainty sources has not been strictly defined, studies have shown that uncertainties from GCMs outputs are more significant than those from hydrological models (Arnell, 2011; Chen et al., 2011; Teng et al., 2012). A multi-model, scenario-based approach has been recommended to allow investigation of uncertainty between

different GCMs and GHGs emission scenarios (Xu et al., 2013). This study seeks to address the need for improved understanding of climate change impacts in the upper reaches of the Nzoia river basin and the uncertainty associated with such projections. In order to improve on the predictions from previous studies, simulations from 10 out of 23 GCMs included in the IPCC 4th Assessment Report (IPCC, 2007) with three different GHGs emission scenarios, were used to drive the SWAT model.

1.1 Statement of the Problem

Mt. Elgon is considered one of the five water towers in Kenya (Akotsi, 2006). The high potential slopes of the mountain support a range of productive activities including tourism, irrigated and rain-fed agriculture, livestock production, environmental conservation, and forestry. The area is endowed with a rich biodiversity which influence lives and livelihoods of thousands of people through provision of ecosystem services (Petursson et al., 2006). However, climate change is likely to affect hydrological processes thus increasing the vulnerability of the communities to natural variations. Land degradation due to soil erosion has stripped the fertile soil leading to decline in agricultural production. Due to declining yields, the income levels are low. Hence farmers do not invest adequately in land management which aggravates the land degradation.

Poor agricultural practices, intensification of land use, and cultivation of formerly forested areas are causing changes in the patterns of natural variability of the catchment hydrology (Petursson et al., 2006). These factors are increasing the vulnerability of the water resources in the area to changing climate. As a result, there is need for the analysis of the natural hydrological processes as well as understanding of the variations due to anthropogenic activities and climate changes on the natural system. In order to mainstream an Integrated Water Resources Management (IWRM) framework in the area, hydrological modeling is required to harmonize the economic, social and

environmental dimensions of water resources to support sustainable development in the catchment.

Sustainable management and development of water resources in the catchment requires knowledge of the distribution of water resources both in space and time. In Mt. Elgon, pressure on water resources due to small-holder farming and logging practices, and the impacts of institutional innovations of community participation in forest management have not been studied adequately. Although hydrological modeling has the potential to fill the existing knowledge gaps, lack of adequate hydro-climatic data and uncertainties in simulation of the hydrological processes is a major challenge. The Mt. Elgon sub-watersheds have not yet received adequate attention in the field of climate and hydrological research hence there is inadequate understanding of the hydro-climate processes in this area. This can be addressed through scenario-based hydrological modeling and uncertainty analysis.

1.2 Justification of the study

Mountainous regions are significant natural water towers (Immerzeel et al., 2010; Viviroli et al., 2007). Hence, simulating hydrology in these areas is essential in appreciating the dominant processes controlling the water balance to facilitate informed decision making in water resource management in the surrounding areas (Chaponniere et al., 2008). However, the hydrology of mountainous areas is often not given adequate attention. In Mt. Elgon area, the livelihoods of the poor subsistence farmers are highly dependent on exploitation of natural resources (Petursson et al., 2006). Consequently, a managerial challenge of balancing conservation and resource use amid climate change adaptation strategies is inevitable.

Spatial and temporal variations of the hydrological processes in this area have important consequences on the socioeconomic stability and sustainability of the area. Hydrological

modeling is essential for a comprehensive analysis of the mechanisms associated with dynamical processes influencing the various aspects of water resources in the catchment such as precipitation, evapo-transpiration, runoff and river base flow. This will help to estimate the catchment's water balance, including runoff rates and volumes, and the impacts of climate change on the catchment. These estimates will be useful in decision making to promote sound land use practices and optimize agricultural production while ensuring environmental sustainability.

The ongoing global climate change and uncertainties compounding future climate are a major concern in the planning and management of natural resources. Therefore, in-depth understanding of the potential climate and land use change impacts on the hydrology of Mt. Elgon sub-watersheds is critical for sustainable development in the region. Although the impact of different climate change scenarios has been projected at a global scale, the type and magnitude of the impact in Mt. Elgon sub-watersheds has not been fully studied. Consideration of the long-term variability of hydrological processes with regard to varying climate require sophisticated modeling tools, which couple hydrological models and GCMs. This study explores the potential hydrological changes in the area which is needed to plan for appropriate adaptation measures.

1.3 Objectives of the study

The overall objective of this study was to simulate the potential hydrological responses to climate change in the four main sub-watersheds on the eastern slopes of Mt. Elgon namely Kuywa, Kimilili, Rongai and Koitobos sub-watersheds. The specific objectives of the study were:

i. To calibrate and validate the Soil and Water Assessment Tool (SWAT) model for the sub-watersheds
ii. To develop climate change scenarios for the watersheds using the delta change approach

iii. To assess the hydrological impacts of climate change scenarios in the four sub-watersheds

1.4 Research questions

This study sought to answer the following questions:

i. What are the optimum parameter values for the simulation of hydrological responses in Mt. Elgon sub-watersheds using the SWAT model?
ii. What are the projected climate change scenarios for Mt. Elgon sub-watersheds?
iii. What are the potential hydrological impacts of the climate change scenarios in Mt. Elgon sub-watersheds?

1.5 Study area

Figure 1.1 shows the study area consisting of the upper reaches of the Nzoia river basin. The river flows from south-eastern slopes of Mt Elgon and the western slopes of the Cherangani Hills in western Kenya and drains to the south-west into Lake Victoria. The total area used for model calibration is about 10,154 km^2 while the four sub-watersheds studied cover about 2,961 km^2. The area has high topographic relief characterized by steeply sloping uplands and elevation ranging from 1250 to 4300 m.a.s.l. The climate of the area is mainly tropically humid, with mean annual rainfall of about 1000 to 1500 mm and average temperature of about 16 to 19º C. The annual rainfall pattern is generally unimodal with no distinct dry season throughout the year. However, the rainfall is highest during April –May and August–September periods. Mean temperature is lowest in June to September while potential evapotranspiration decreases with increasing altitude (Githui et al., 2009). The soil in the area is characterized by clay, as well as loamy and sandy soil types. In terms of land use, the area is characterized by intensive agricultural activities, forest area and significant presence of shrub land. The upper

reaches of Mt. Elgon are covered by protected afro-montane forests (Petursson et al., 2006).

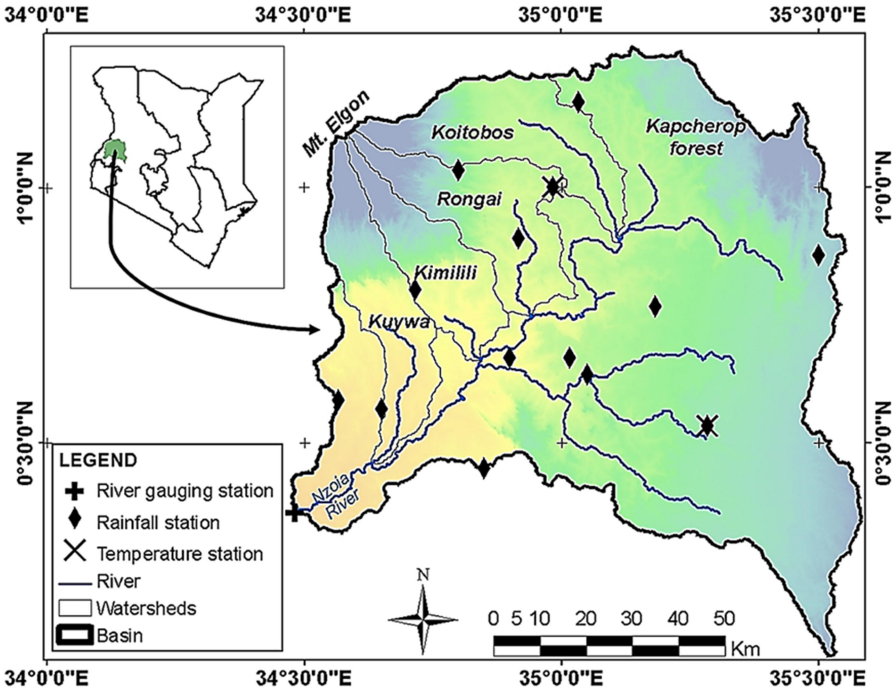

Figure 1.1: Location of the study region and hydrological and meteorological stations in the Upper Nzoia River basin

1.6 Significance of the study

This study is significant not only for its contribution towards stressing the suitability of SWAT model in simulating streamflow in the upper Nzoia basin but also for providing the much needed knowledge on the potential impacts of climate change in Mt. Elgon sub-watersheds. Although impacts of climate change in the entire Nzoia river basin have been studied, the magnitude of the impacts at a sub-watershed scale, particularly Mt. Elgon sub-watersheds, has not been investigated. The results from this study are therefore a major contribution to the existing pool of knowledge on the potential impacts of climate change in one of Kenya's significant water towers. In addition, conclusions from this study will inform policy measures to ensure effective adaptation and mitigation of the climate change impacts.

CHAPTER TWO

LITERATURE REVIEW

2.0 A Brief on the chapter

This chapter comprises a review of the literature relevant to this study. First the hydrological modeling approach is discussed with focus on the model application process. The assessment of the hydrological impacts of climate change is then discussed with emphasis on the methodologies for generating climate change scenarios and the analysis of the different uncertainties involved in the process. Lastly, a brief description of the SWAT model and its suitability in Mt. Elgon sub-watersheds is provided.

2.1 Hydrological modeling

The simulation of hydrological processes at local, regional and global scales is vital in addressing a wide range of environmental, social and water resources problems. Generally, hydrological models are unique tools applied in water resource management endeavors such as flood and drought prediction, climate and land use change impacts assessment as well as water pollution analysis. The emphasis in the development of these models has been the representation of quantitative relationships between inputs (such as land use, temperature, precipitation) and outputs (such as discharge, sediments, nutrients) using the least number of parameters and yet achieve the best possible estimate of the actual state of the hydrological variables (Singh & Woolhiser, 2002). Consequently, these models have advanced over time to multifaceted decision support tools which are applied in elucidating the likely condition and performance of hydrological systems under different land use and cover characteristics, climatic conditions, land management alternatives and other socioeconomic components (Tang et al., 2007).

2.1.1 Classification of hydrological models

A plethora of hydrological models of varying nature, complexity and purpose have been developed in the recent past to aid understanding of hydrological processes and their uncertainty. Different authors have adopted different classification schemes for these hydrological models. Consequently, a massive collection of comprehensive literature, both published and unpublished, exists on the classification hydrological models (Daniel et al., 2011; Jajarmizadeh et al., 2012b; Pechlivanidis et al., 2011; Rosbjerg & Madsen, 2006).

Based on Daniel et al. (2011) and Lastoria (2008), hydrological models can be categorized based on the model characteristics, temporal description in the model, and spatial specification. Under the model characteristics, considerations include the employed algorithms (physically-based, conceptual, empirical and hybrid models), description of the hydrological processes (stochastic, deterministic and deterministic-stochastic models), model parameter specification approach (calibrated and measured parameter models), and the extent to which they simulate the hydrologic cycle (complete or partial). The temporal description criterion can refer to models which simulate short events such as a single storm (event-driven models) or those that simulate continuous input-output relationships over a longer period (continuous-processes models). On the other hand, the spatial description criterion categorizes hydrological models into lumped models, semi-distributed models and distributed models (Daniel et al., 2011).

This study is based on the application of the SWAT model, which is a semi-distributed hydrological model. More than 1230 publications have been published based on the application of the SWAT model (Galván et al., 2014). The performance of the SWAT model has been compared widely to other models. Borah and Bera (2003) compared SWAT model with other 10 models namely Agricultural NonPoint Source pollution model (AGNPS), Annualized Agricultural NonPoint Source model (AnnAGNPS), Areal

Nonpoint Source Watershed Environment Response Simulation (ANSWERS), ANSWERS-Continuous, CASCade of planes in 2-Dimensions (CASC2D), Dynamic Watershed Simulation Model (DWSM), Hydrological Simulation Program - Fortran (HSPF), KINematic runoff and EROSion model (KINEROS), the European Hydrological System model (MIKE SHE), and Precipitation-Runoff Modeling System (PRMS). Singh et al. (2005) compared the performance of SWAT and HSPF. Both studies concluded that SWAT model simulated runoff better.

The HBV model (Bergström & Forsman, 1973; Lindström et al., 1997) has also been applied to assess climate change impacts in Nyando river basin (Taye et al., 2010). However the SWAT model was considered in this study because unlike the HBV model, SWAT model represents surface-groundwater interactions better through baseflow and recharge. In addition, canopy interception and energy balance fluxes are well simulated in SWAT compared to the HBV model. The hydrological processes, watershed characteristics, and outputs in SWAT model are subdivided into smaller entities to reflect spatial heterogeneities in land cover, soil types, topography and weather conditions in the study area (Muleta & Nicklow, 2005). Therefore, significant features of catchments are more effectively represented than in lumped models while less input data and computation time is required compared to fully distributed models (Boyle et al., 2001; Orellana et al., 2008). As a result, the SWAT model has been recommended as it combines the strengths of both lumped and fully distributed models.

2.1.2 Model parameterization and calibration

In order to optimize the performance of hydrologic models in depicting watershed hydrology, adjustment of the model parameters using a reliable model calibration technique is crucial (Bahremand & De Smedt, 2008; Liu et al., 2005; Uhlenbrook et al., 1999). The two significant steps in model calibration are parameter identification and parameter estimation. Parameter identification involves selection of parameters that need

to be adjusted, while parameter estimation involves identifying the 'optimal' or 'near-optimal' values of the selected parameters (Muleta & Nicklow, 2005). The commonly used approach in selecting parameters of interest for model calibration is sensitivity analysis, which involves assessment of the parameters' influence on the values of the hydrological variable to be simulated such as runoff, baseflow and sediment yield (Liang & Guo, 2003; Sieber & Uhlenbrook, 2005; Wagener et al., 2001). This approach helps to quantify the influence of changes in individual or a combination of model inputs such as model parameters, forcing, initial conditions and boundary conditions, on a particular model output. This process plays a key role in the identification of important model parameters, testing the model conceptualization and improving on the model structure (Tang et al., 2007).

Parameter sensitivity analysis methods have been broadly categorized into local and global procedures (Muleta & Nicklow, 2005; Saltelli et al., 1999; Tang et al., 2007). Both categories involve a sampling strategy applied to the parameter space as well as an objective function to measure the impacts of the sampled parameter values on a particular model output (Tang et al., 2007). In local procedures, each of the input factors is sequentially perturbed, while all other factors are fixed to constant nominal values. Hence, the value of the objective function (in direct methods) or inclusion of derivative information (in gradient–based methods) is used to control the search in the parameter space (Blasone et al., 2007). These procedures do not account for any existing interaction between inputs and the reliability of the analysis declines as the perturbation moves away from the nominal value. In addition, the application of these procedures is constrained by the nonlinear nature of the relationship between inputs and output variables in hydrologic systems (Muleta & Nicklow, 2005).

The global methods, on the other hand, use deterministic and stochastic rules to broadly search the parameter space and then progressively converge into the subregion(s) containing the best value of the objective function (Blasone et al., 2007). As a result, the

effects of interactions between different inputs is accounted for by examining the effects of varying inputs on the outputs in the entire permissible range of the input space (Muleta & Nicklow, 2005). The performance of different sensitivity analysis approaches has been compared in several studies (Blasone et al., 2007; Gan & Biftu, 1996; Madsen et al., 2002; Marshall et al., 2004; Thyer et al., 1999). The studies have concluded that the global population-evolution-based algorithms perform better than multi-start local search procedures, which in turn are more effective than pure local search methods. In this study, Latin hypercube one-factor-at-a-time (LH-OAT, van Griensven et al., 2006) method within ArcSWAT interface for SWAT2009 was applied for initial manual calibration and Sequential Uncertainty Fitting version 2 (SUFI-2, Abbaspour et al., 1997, 2007) method in the SWAT-CUP software was used for the auto-calibration to facilitate effective identification and estimation of the most sensitive parameters.

Parameter estimation methods can be categorized into manual and automatic approaches. The manual approach involves trial-and-error adjustment of model parameters hence requires a high degree of expert knowledge of the model and the system. The adjustment of parameter values and judgment of the goodness-of-fit of the model simulation is therefore based on a subjective strategy which is tedious and time consuming (Blasone et al., 2007). The automatic approach involves the use of a search algorithm to determine the best parameter values. This approach is fast, less subjective and most likely to give better results compared to manual calibration (Bahremand & De Smedt, 2008). In this study, manual calibration was used to first fine tune the parameters to acceptable ranges prior to automatic calibration which was used to estimate the optimal parameter values.

In model calibration, different parameter sets can be used to obtain similarly good fits between observed and simulated values (Uhlenbrook et al., 1999). Singh and Frevert (2006) outlined four main issues focused on recent advances in automated watershed model calibration: (i) advanced management of data errors; (ii) pursuit for the best

parameter estimation algorithm; (iii) determination of the most appropriate amount of data required; and (iv) efficient depiction of the calibrated model uncertainty and propagation of the uncertainty into the model outcome.

2.2 Assessment of climate change impacts

Given the vital role of water resources in socio-economic development in Mt. Elgon area, the potential hydrological impacts of climate change pose a major challenge for water resource planning and management. The complex interplay between hydrological and climatic components influencing the spatial and temporal variability of water resources has been widely studied mainly using hydrological models coupled with GCMs. The GCMs developed in the past two decades have received wide recognition as viable tools for the assessment of the potential climate change impacts (Chen et al., 2012; Gao et al., 2013; Kienzle et al., 2012; Zhang et al., 2012). The hydrological impacts of climate change have mainly been attributed to change in the dominant climate variables namely precipitation and temperature (Chien et al., 2013; Githui et al., 2009; Lee et al., 2013; Xu et al., 2013). However, other studies have also coupled the precipitation and temperature change effects with effects of increased concentrations of atmospheric carbon dioxide (Ficklin et al., 2009; Nunes & Pacheco, 2008), urbanization factors (Franczyk & Chang, 2009) and land cover (Githui et al., 2009; Mango et al., 2011; Wilson & Weng, 2011).

Despite the substantial improvement in the depiction of present and past global and continental climate by GCMs, their depiction of local scale conditions is constrained (Rahman et al., 2012; Varis et al., 2004). The spatial resolution of GCMs is very coarse. On the other hand, hydrological models often focus on process occurring at spatial scales much smaller than those resolved in GCMs (Chen et al., 2012). In addition, local-scale physical processes such as runoff, soil moisture and evapotranspiration, which are significant to hydrologic regimes are not well parameterized in GCMs (Kite et al., 1994;

Loaiciga et al., 1996). Therefore, determination of climate scenarios necessitates the application of methods to transform the coarse climate model outputs to fine spatial and temporal resolutions.

2.2.1 Determination of climate change scenarios

The assessment of climate change impacts on hydro-meteorological variables necessitates a definition of future climate scenarios. These include time series or statistical measures of expected future climatic variables, such as temperature and precipitation. These scenarios can be generated by downscaling GCMs or using hypothetical scenarios. Downscaling approaches have been broadly categorized into dynamical and statistical methods. With emphasis on hydrology, a broad overview of downscaling methods and their applications can be found in Fowler et al. (2007), Xu (1999), Hewitson and Crane (1996) and Murphy (1998).

Dynamical downscaling methods involves use of Regional Climate Models (RCMs) which have been developed to attain a fine computational grid using initial conditions, time-dependent lateral meteorological conditions derived from GCMs and surface boundary conditions. Thus, a GCM is used to simulate global circulation response to large-scale forcing while the RCM accounts for sub-GCM grid-scale forcing to enhance the simulation of local scale atmospheric circulations and climate variables (Jiang et al., 2007). Spatially complete fields of climate variables are created while maintaining some spatial correlation as well as physically reasonable relationship between variables (Kilsby et al., 2007; Maurer & Hidalgo, 2008; Rahman et al., 2012). However, the application of this approach is restricted by: the inheritance of systematic errors in the GCMs into the downscaled values, complicated design, inflexibility in the sense that increasing or changing the region necessitates repeating the entire experiment, and the need to downscale the results further to individual sites or localities for impact studies (Ghosh & Misra, 2010; Xu, 1999).

On the other hand, statistical downscaling methods use quantitative relationships between the large-scale variables (predictors) and local-scale variables (predictands) to predict climatic variables at a given site (Xu, 1999). Thus, the set of predictors and the relationships considered influence efficiency of the method. In addition the effectiveness of the downscaling method varies depending on the variable, season as well as different periods of records considered (Wetterhall et al., 2007). Statistical downscaling methods can be categorized into regression methods, weather-pattern based approaches and stochastic weather generators. These methods are computationally inexpensive, flexible, can directly incorporate observed data, and are based on accepted statistical procedures. However, they require long time series of observed data and they are a based on the assumption that the predictor/predictand relationships will remain constant in the future periods (Jiang et al., 2007).

Due to the limitations of the GCMs and downscaling methods, hypothetical scenarios based on reasonably but arbitrarily specified changes in climate variables have often been used (Engeland et al., 2001; Xu, 2000). In this method, a qualitative interpretation of climate model predictions or the analyses of changes in climate characteristics in the past are used to adjust climate variables, such as temperature and precipitation. Adjustments in temperature and precipitation can be made independently or in combination.

The downscaling technique applied in this study is based on the use of change factors (multiplicative or additive) obtained from the climate models simulations and applied to observed series to simulate future conditions (Chen et al., 2011; Hijmans et al., 2005; Minville et al., 2008). This method was selected because the spatial variability in climate conditions in the study area is not well simulated by GCMs. The method is based on the assumption that biases inherent in the baseline period are similar to the biases in the future periods and that the relative changes obtained from the climate models are more representative than the absolute changes (Ogiramoi, 2011). This method is suitable

because it requires less data inputs and computing requirements and can simulate climate change scenarios for a relatively small study area as the one considered in this study.

2.2.2 Uncertainty analysis in hydrological impact assessment

Uncertainty is an intrinsic characteristic of all hydrological processes which is further intensified by the errors in data measurement and processing, insufficient depiction of hydrologic processes in model structures, or the creation of too complex representations which are not fully supported by the current understanding of the physical system (Efstratiadis et al., 2008). The identification, quantification, and minimization of the uncertainties in the assessment of the hydrological impacts of climate change is vital for adaptive water resource planning and management (Jung et al., 2012). Despite the systematic consideration of the uncertainties related to simulation of hydrological impacts of climate change in recent research, quantitative assessment of these uncertainties is still a major challenge.

Previous studies have categorized these uncertainties into three categories: climate projection uncertainties which relates to GHGs emission scenario, and GCM structure and initial conditions (Hawkins & Sutton, 2009; Tebaldi et al., 2005); downscaling uncertainties (Chen et al., 2013; Im et al., 2009) and hydrologic model structure and parameters identification uncertainties (Bae et al., 2011; Chang & Jung, 2010; Clark et al., 2008; Jiang et al., 2007; Najafi et al., 2011; Wilby & Harris, 2006). However, the relative significance of these sources of uncertainty has not been adequately assessed. Moreover, only a few studies have considered the whole cascade of uncertainty sources in their analysis.

In their assessment of the relative weights of the sources of uncertainty in future low flows for the River Thames, Wilby and Harris (2006) found that the GCM structure and

downscaling method uncertainties affected the low flow change more than the uncertainties due to hydrological model parameters and emission scenarios. In their study on error estimation for future temperature and precipitation projections, Woldemeskel et al. (2012) concluded that, based on the total uncertainty from GCMs, GHGs emission scenarios, and initial conditions (or ensemble runs), GCMs contributed 80% and 75% of the total uncertainty for precipitation and temperature respectively. Based on four hydrologic models of varying complexity, Najafi et al. (2011) showed that in rainfall-dominated Tualatin River Basin in Oregon, USA, hydrologic model selection uncertainty was more prominent than the GCM uncertainty during the dry season as compared to the wet season. This is comparable to results obtained by Tian et al. (2015) who compared uncertainty sources for future high flows based on three hydrological models (modèle du Génie Rural à 4 paramètres Journalier (GR4J), Hydrologiska Byråns Vattenbalansavdelning (HBV), and Xinanjiang); three emission scenarios (A1B, A2, and B2) and the Providing Regional Climates for Impacts Studies (PRECIS) regional climate model. They concluded that the major source of uncertainty was parameters followed by model structure and emission scenarios contributed the least amount of uncertainty.

Lack of knowledge about the future human development and the sensitivity of the climate system to all the feed-back mechanisms influenced by increasing emissions causes uncertainties about future GHGs emissions (Roosmalen, 2009). On the other hand, the simplification of complex, highly non-linear climate systems by GCMs causes uncertainties due to: inadequate depiction of unresolved scales and the varying climate sensitivity of single GCMs, variability of the climate system to small perturbations responsible for unexpected conditions, the initial boundary conditions used at the start of a GCM experiment, and the sub-decadal to multi century scale impact of volcanoes (Viner, 2002). The downscaling methods cause uncertainty due to location and variable-specific performance of the different downscaling methods.

The hydrological model uncertainties have been attributed to inadequate depiction of the temporal and spatial variability of meteorological data driving the model (Andreassian et al., 2001), the assumed conceptual model for the system (Butts et al., 2004; Wagener et al., 2001), the sensitive model parameters found by calibration, which may be influenced by the choice of calibration period, and use of statistically inadequate fitting criteria (Gan & Biftu, 1996; Gan et al., 1997; Yapo et al., 1996), and the limitation of most optimization methods in handling response surfaces of irregular topography (Duan et al., 1992).

The hydrological model prediction uncertainties have been widely studied in recent years. Consequently, a multiplicity of mathematical methods embedded in calibration techniques have been developed to facilitate identification of best model outputs that correspond to multiple, "behavioral" parameter sets. These include analytical and approximation methods (Melching, 1992), Bayesian and Monte Carlo (MC) sampling based methods (Thiemann et al., 2001; Vrugt et al., 2003), and model error analysis methods (Montanari & Brath, 2004; Solomatine & Shrestha, 2009). The application of these techniques is compounded by concerns, such as the computational effort for multidimensional applications, approval by policy makers and the public, and the failure to provide a final decision regarding a single best parameter set. Therefore, the heterogeneity of processes and the unknown scale dependencies of parameters were identified by Efstratiadis et al. (2008) as the reason for optimization of small portions of the parameters by many studies. Other emerging methods which can deal with multiple uncertainties sources include Markov chain Monte Carlo (MCMC) techniques (Vrugt et al., 2008), Bayesian approaches (Kavetski et al., 2006; Kuczera et al., 2006), multi model averaging techniques (Georgakakos et al., 2004; Vrugt & Robinson, 2007), and data assimilation techniques (Moradkhani et al., 2005).

In the context of climate change impact assessment, authors have used different approaches to address uncertainties. Bastola et al. (2011) considered model structure and

parameter set uncertainty in a non-stationary context using multiple emission scenarios and GCMs, four conceptual rainfall-runoff models and two parameter uncertainty evaluation methods (Generalized Likelihood Uncertainty Estimation and Bayesian Model Averaging). Jiang et al. (2007) employed six conceptual rainfall–runoff models and a total of fifteen hypothetical climate change scenarios, comprising of a combination of three temperature increases and five precipitation changes, in a Chinese watershed to assess hydrological model structure uncertainty. They concluded that performance of models can vary under future climate conditions although they may show similar behaviors under historical climatic conditions. Other studies have also concluded that the GCM structure is the main source of uncertainty in hydrological impact studies (Arnell, 2011; Chang & Jung, 2010; Chen et al., 2011; Prudhomme & Davies, 2009; Teng et al., 2012).

Using three different GCMs, two GHGs emissions scenarios, two downscaling techniques and two different versions of the Probability Distributed Moisture model (PDM), Prudhomme and Davies (2009) concluded that the choice of the GCM was the largest source of uncertainty although the downscaling technique was also a significant source of uncertainty. Kay et al. (2009) assessed six uncertainty sources of climate change impact on flood frequency for two river basins in England. In their study, they considered five different GCMs, four emissions scenarios with the delta change approach and a RCM to assess GCM uncertainty. They considered downscaling method uncertainty by using the delta change approach and an RCM nested within a single GCM, while 9 RCMs nested within a single GCM were used to assess RCM structure uncertainty. They also examined model structure uncertainty by using a spatially distributed and a lumped conceptual hydrological model. For one of the models, a jack-knife method was used to generate multiple calibrated parameter sets to assess parameter uncertainty. Internal climate variability uncertainty was considered by resampling of rainfall series and using a three-member initial condition ensemble of the same GCM.

The hydrological simulations based on climatic projections have shown relatively minor dependence on the choice of hydrological model compared to the choice of climate models (Bates et al., 2008; Kay et al., 2009). The impact analysis methods used in previous studies differ depending on the indicators considered such as water quality, surface flow, lateral flow and groundwater flow or a combination of more than one indicator. Impacts on streamflow have been analyzed based on flow duration, timing and magnitude, flow variability, frequency and rate of change for hydrologic events.

2.3 Climate change in East Africa region

The potential impacts of projected regional climate change in the East Africa region have been studied (Adhikari & Hong, 2013; Anyah & Semazzi, 2007; Christy et al., 2009; Githui et al., 2009; Mango et al., 2011; Schreck & Semazzi, 2004; Shongwe et al., 2011; Taye et al., 2010). Recent climate models show a likely increase in the seasonal temperature for the east Africa region in the forthcoming decades (IPCC, 2007). The minimum temperature has particularly shown a rapid rate of increase compared to the maximum temperature while the mean temperature has remained constant since 1905 (Anyah & Semazzi, 2007). The climate variability, particularly above average rainfall intensity during short rains, in east Africa region has shown correlation to the El-Nino–southern oscillation (Schreck & Semazzi, 2004). In addition, the climate models have indicated significant influence of the mountainous regions as well as the rift valley on regional climate. IPCC (2007) indicated that during the wet seasons, extreme rainfall events will increase by the year 2100 thus increasing the frequency and severity of flood events. The precipitation and temperature projection results obtained by Shongwe et al. (2011) are shown in appendices 1and 2.

2.4 The SWAT model

SWAT is a physically based, semi-distributed, catchment-scale model developed by the United States Department of Agriculture–Agricultural Research Service (USDA–ARS). Its main objective is to simulate, on daily time scale, the impacts of land management decisions on water, sediment and agricultural chemical yields in ungauged river basins. The main components of the model are hydrology, weather, sedimentation, soil temperature, crop growth, nutrients, pesticides, and agricultural management. The hydrological processes simulated by SWAT include surface runoff (using SCS curve number or Green and Ampt infiltration equation), percolation, lateral flow, groundwater flow from shallow aquifers to streams, evapotranspiration (using Hargreaves, Priestley-Taylor or PenmanMonteith method), transmission losses from streams and water storage, losses from ponds, and snowmelt (Arnold et al., 1998).

The SWAT model has gained wide recognition as demonstrated by its many applications (Anand et al., 2007; Gassman et al., 2007). In this model, basins are subdivided into multiple sub-watersheds which are further subdivided into hydrologic response units (HRUs) based on unique combinations of soil, land use and slope. These HRUs are homogeneous spatial units characterized by similar geomorphologic and hydrological properties and are the fundamental spatial units for water balance simulation in SWAT. User specified thresholds of land cover, soil area, and slope can be applied to limit the number of HRUs in each sub-watershed. Storage volumes representing the water balance of each HRU are canopy interception, snow, soil profile (0–2 m), shallow aquifer (2–20 m), and deep aquifer (more than 20 m), (Ficklin et al., 2009; Jha, 2011).

The watershed hydrology in SWAT consists of two major phases namely the land and water or routing phases. The land phase focuses on the quantity of water, sediment, nutrient, and pesticide from each sub-basin while the water or routing phase considers the movement of such quantities through the channel network to the watershed outlet.

The water balance equation shown in Equation 1.1 is used to simulate the land phase of the hydrologic cycle. A more detailed description of SWAT can be found in Arnold et al. (1998) and Neitsch et al. (2011).

$$SW_t = SW_0 + \sum_{i=1}^{t}\left(R_{day} - Q_{surf} - E_a - w_{seep} - Q_{gw}\right)_t \qquad \textbf{Equation 1.1}$$

Where SW_t (in mm) is the final soil water content; SW_0(in mm) is the initial soil water content on day i, t (day) is the time; R_{day} (in mm) is the amount of precipitation on day i, Q_{surf} (in mm) is the amount of surface runoff on day i, , E_a (in mm) is the amount of evapotranspiration on day i, w_{seep} (in mm) is the amount of water entering the vadose zone from the soil profile on day i, and Q_{gw} (in mm) is the amount of return flow on day i.

The SWAT model was selected for this study due to its widespread successful application in regions of varying topography, climatic and land use characteristics to simulate both climate and land management impacts on the quantity and quality of water resources. According to Arnold et al. (1998), the model uses readily available data inputs; is computationally efficient hence can operate on large basins; and is capable of simulating long periods to assess effects of management changes on continuous time-steps. The model offers different weather input options namely: simulation of elevation bands to account for precipitation and temperature changes with altitude; adjustments to climate inputs; and forecasting of future weather patterns (Gassman et al., 2007). However, the model was mainly designed for evaluation of long-term periods and not extreme events (Arnold et al., 1998) hence it may not reflect adequately potential climate change impacts on extreme hydrological events in the study area. In addition, the model overestimates low flows and underestimates high flows due to inadequate consideration of precipitation duration and intensity (Jeong et al., 2010). This is likely to affect its performance in Mt. Elgon sub-watersheds.

CHAPTER THREE

MATERIALS AND METHODS

3.0 A Brief on the chapter

This chapter comprises a description of the overall research design, materials and methods used in this study. The datasets used as well as the model set-up, calibration and validation procedure are described. The procedure used to generate climate change scenarios and analysis of the hydrological impacts of these scenarios is also discussed.

3.1 Overall research design

A three stage approach was used in this study to assess the potential hydrological impacts of climate change. This approach entails hydrological model calibration and validation using observed hydro-climatic data; definition of climate change scenarios to be applied to the observed climate data; and model simulation using the climate change scenarios. The overall procedures and data sets used in the study are summarized in Figure 3.1.

3.2 Input datasets used in the study

The simulation of spatially distributed hydrological processes using SWAT requires spatial and temporal datasets. The spatial datasets include a digital elevation model (DEM), land cover/use data and soil type data. The climate inputs consist of daily rainfall, maximum and minimum temperatures, solar radiation, wind speed, and relative humidity (Arnold et al., 2011). The use of daily time step input datasets enables better expression of the simulated hydrologic processes based on changes in daily discharge.

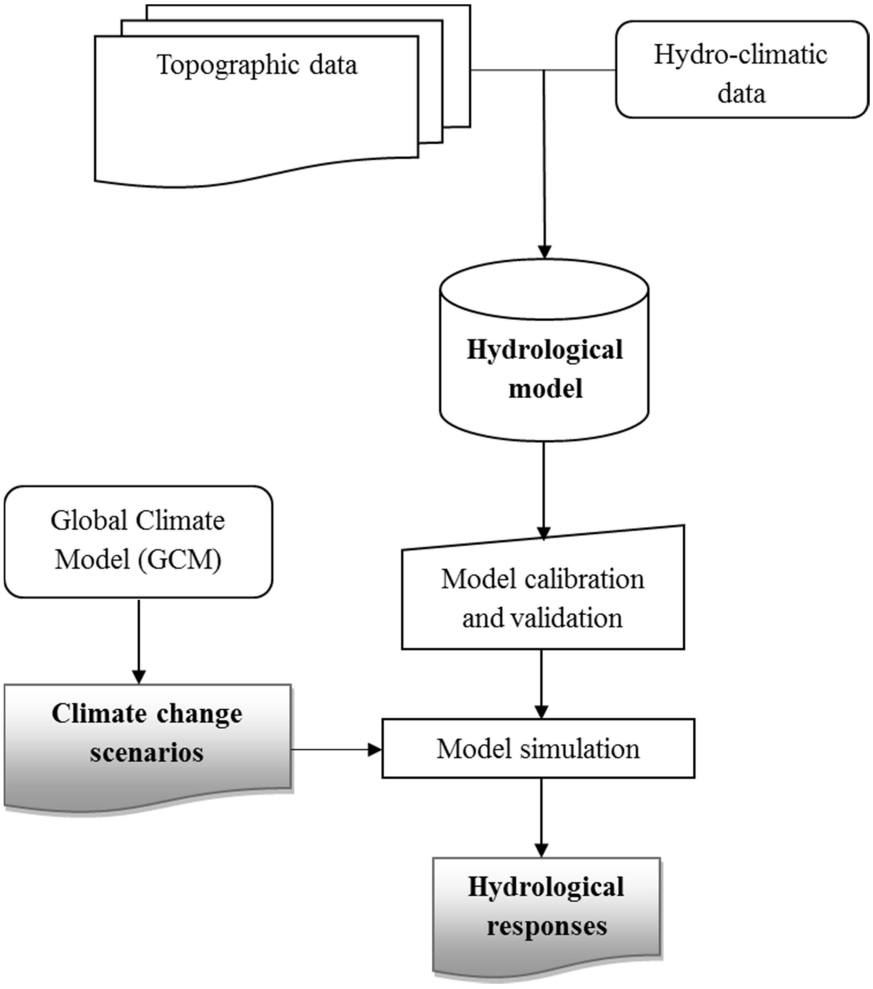

Figure 3.1: Overall study design

3.2.1 Topographic data

The topographic characteristics and spatial distribution of land cover/use and soil types are required for delineation of hydrological response units in the SWAT model. In hydrological modeling, DEMs play an important role in generating topographic parameters such as slope, drainage network and catchment area. These parameters are essential in understanding the watershed hydrological processes such as infiltration, evaporation and heat exchange. In this study, a DEM with a resolution of 90 m obtained

from the NASA Shuttle Radar Topography Mission (SRTM) dataset was used to represent topography.

A Land cover map with a resolution of 1 km was obtained from the European Commission Global Land Cover 2000 dataset and reclassified according to SWAT model input requirements. Forests are spread widely in the upper and middle parts of the area, while cropland is located in the middle and lower parts. A soil map at 1:1,000,000 scale was obtained from the Kenya Soil and terrain database (KENSOTER). The combination of these topographic datasets provides a depiction of the physical characteristics of the study area at varying spatial resolutions.

3.2.2 Hydro-climatic data

Daily rainfall data (14 stations), and minimum and maximum temperature data (2 stations) covering the 1970-1998 period were obtained from the Kenya Meteorological Department (KMD). The WXGEN weather generator inbuilt in SWAT model was used to generate solar radiation, wind speed, and relative humidity data as well as filling missing rainfall and temperature data (Neitsch et al., 2011; Sharpley & Williams, 1990). The generated weather data was based on long-term monthly statistical information for rainfall, maximum and minimum temperature, dew point temperature, solar radiation and wind speed obtained from Kitale and Eldoret meteorological stations. A first-order Markov chain is used to define wet and dry days based on probability of occurrence of rain day on basis of occurrence of rain in previous day while Markov chain-skewed model (Nicks, 1974) or Markov chain-exponential model (Williams, 1995) is used to generate rainfall amount. A stationary generating process (Matalas, 1967) based on previous day's values is used to generate temperature and solar radiation while a triangular distribution (Sharpley & Williams, 1990) is used to generate relative humidity from temperature and average dew point temperature. Adjustments are then applied to all the parameters using a continuity equation to account for the presence or absence of

rainfall. A modified exponential distribution is used to generate wind speed from average monthly values.

Daily river discharge data for the 1DD01A station were obtained from the Water Resources Management Authority (WRMA) for model calibration and validation. Missing stream flow data values were filled by computing the average for the missing day in the previous years where there were existing data values. The stations used in this study are shown in Table 3.1. Graphical presentation of average monthly total rainfall from a sample of four stations is show in Figure 3.2. The rainfall data indicates a unimodal rainfall pattern in the area with April to August being the wettest months.

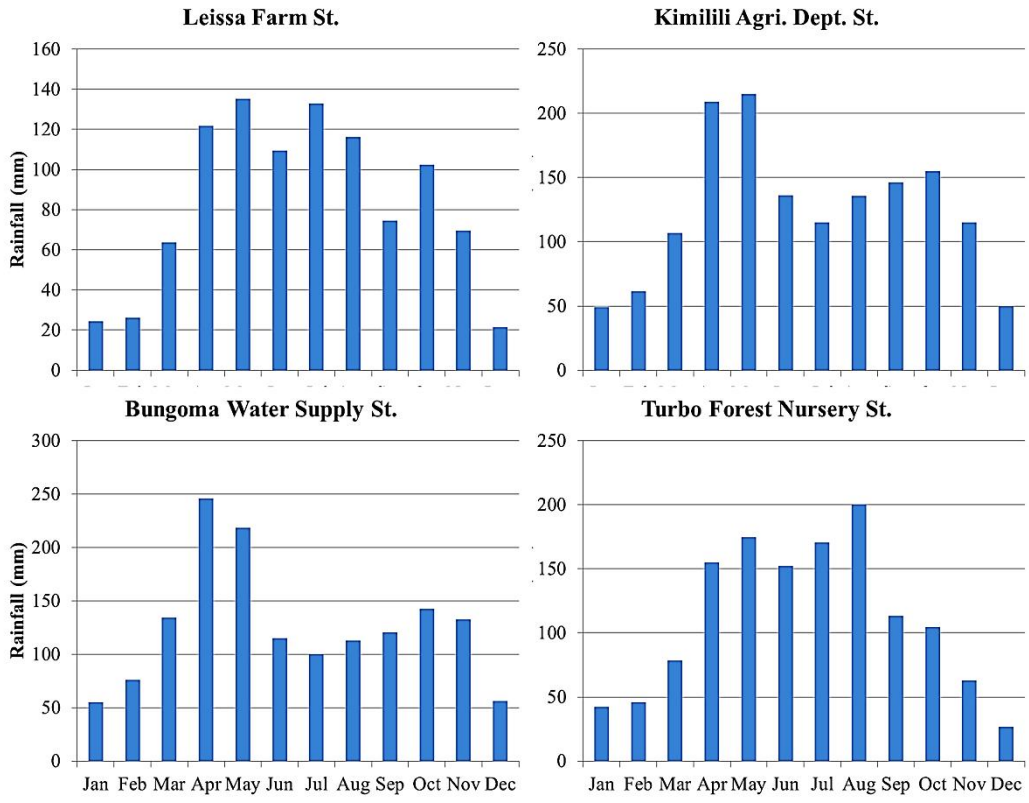

Figure 3.2: Mean Monthly total rainfall from a sample of four stations in the study area.

Table 3.1: Weather and discharge stations used in this study

	Station Name	Station ID	Lat.	Long.	Alt. (m)	% missing
Climatic	Chorlim A.D.C. farm	8834013	1.0333	34.8000	1340	14.1
	Kitale met. station	8834098	1.0000	34.9833	2073	52.6
Data	Leissa farm, Kitale	8835039	1.1667	35.0333	1829	2.0
	Gloucester vale estate	8934008	0.9000	34.9167	1829	2.0
(1970-	Lugari forest station	8934016	0.6667	34.9000	1680	55.8
1998)	Kimilili agr. department	8934060	0.8000	34.7167	1676	2.6
	Malava forest guard post.	8934130	0.4500	34.8500	1707	11.8
	Bungoma water supply	8934134	0.5833	34.5667	1402	1.2
	Nzoia sugar factory	8934183	0.5667	34.6500	1462	62.9
	Turbo forest res. Station	8935076	0.6667	35.0167	1890	4.9
	Turbo forest nursery	8935170	0.6333	35.0500	1859	3.8
	Eldoret met. station	8935181	0.5333	35.2833	2120	52.3
Flow data (1970-1998)	Nzoia	1DD01A	0.3720	34.4880		12.6

3.3 SWAT model setup

3.3.1 Watershed delineation

The first step in the watershed delineation was loading the DEM with appropriate projection (WGS_1984_UTM_ZONE_36N) into the ArcSWAT interface and delineating a mask file for the study area. The initial stream network and sub-basin outlets were generated by varying the drainage area based on the threshold approach. This approach defines the minimum, maximum and suggested drainage area required to form the origin of a stream. The modeling process and the subsequent results on the water balance components in SWAT are impacted by size, scale, and number of sub-basins used (FitzHugh & Mackay, 2000; Jha et al., 2004; Tripathi et al., 2006).

Based on a successive re-run of the stream and outlet definition routine, 25,000 hectares was selected as the threshold area. A smaller threshold area results in a more detailed

drainage network but slows down the processing speed (Jha et al., 2004). In order to automatically delineate the study basin, the 1DD01A River gauging station (Lat 0.37º N, Long 34.49º E) was used as the main outlet. A total of 25 sub-basins were created based on the automatically created outlets.

3.3.2 Hydrologic Response Unit analysis

The land use and soil data were then loaded into the ArcSWAT interface to define the hydrologic characteristics of each simulated land use-soil combination. The land cover and soil classes were defined using look up tables. These tables were prepared prior so as to relate the land use grid and soil shape file values to SWAT land cover/land use and soil classes to facilitate reclassification and calculation of the area covered by each of the classes. The land slope classes were defined based on the DEM data for slope classification. The multiple slope discretization option was selected as the slopes in the different sub-basins vary. Four slope classes (0-3, 3-6, 6-9 and >9) were applied based on the slope statistics of the watershed. The overlay operation was then performed after the reclassification of the land use, soil and slope grids.

The HRU definition is the last step in the HRU analysis. HRUs reflect the variation in climatic and topographic features of sub-basins which are used by the model to estimate the runoff which is then routed to stream channels to obtain the total runoff for the watershed. Therefore, HRUs provides a much better physical description of the watershed's water balance than sub-basins thus facilitating accurate prediction of the flow. The multiple HRUs were defined in each sub-watershed based on combinations of land use, soil type and slope. In this approach, a threshold level is used to eliminate minor land uses, soils or slope classes in each sub-basin. Thresholds levels of 20% for land use, 20% for soil types and 5% for slope were used to subdivide the sub-watershed which led to a total of 200 HRUs.

The modified SCS curve number method (US-Soil Conservation Service Engineering Department, 1972) was used to estimate surface runoff. This method estimates surface runoff from precipitation summed across all HRUs in a sub-watershed based on soil, land use, and management information. This method has shown significant performance in simulating daily runoff compared to the Green-Ampt method (King et al., 1999). The curve number is adjusted at each time step based on the amount of soil water present. The SCS curve number equation is expressed as shown in Equations 3.1 and 3.2:

$$\boldsymbol{Q_{surf} = \frac{(R_{day} - I_a)^2}{(R_{day} - I_a + S)}} \qquad \textbf{Equation 3.1}$$

$$\boldsymbol{S = 25.4\left(\frac{1000}{CN} - 10\right)} \qquad \textbf{Equation 3.2}$$

Where $\boldsymbol{Q_{surf}}$ is the accumulated runoff (mm H_2O), $\boldsymbol{R_{day}}$ is the rainfall depth for the day (mm H_2O), $\boldsymbol{I_a}$ is the initial abstractions (commonly approximated as $0.2\boldsymbol{S}$) which include surface storage, interception and infiltration before runoff (mm H_2O), $\boldsymbol{S}$ is the retention parameter (mm H_2O) which varies in space due to heterogeneity in soils, land use, management and slope, and in time due to variability in soil water content, $\boldsymbol{CN}$ is the curve number of the day.

The Hargreaves method (Hargreaves et al., 1985) was used for estimating potential evapotranspiration as it requires less input data compared to the Priestley-Taylor and Penman-Monteith methods. This method is expressed as shown in Equation 3.3 (Neitsch et al., 2011):

$$\boldsymbol{\lambda E_O = 0.0023 \cdot H_0 \cdot (T_{mx} - T_{mn})^{0.5} \cdot (\overline{T}_{av} + 17.8)} \qquad \textbf{Equation 3.3}$$

Where $\boldsymbol{\lambda}$ is the latent heat of vaporization (MJ kg^{-1}), $\boldsymbol{E_O}$ is the potential evapotranspiration (mm d^{-1}), $\boldsymbol{H_0}$ is the extraterrestrial radiation (MJ m^{-2} d^{-1}), $\boldsymbol{T_{mx}}$ is the

maximum air temperature for a given day (ºC), $\boldsymbol{T_{mn}}$ is the minimum air temperature for a given day (ºC), and $\overline{\boldsymbol{T}}_{\boldsymbol{av}}$ is the mean air temperature for a given day (ºC).

The variable storage method developed by Williams (1969) was used to simulate channel water routing. In this method, the outflow volume is a function of inflow volume, volume stored and the coefficient of storage. The channel parameters considered include reach length, slope of the channel, side slope, flood plain slope, width and depth of full channel, and the Manning's coefficient for the channel and flood plain. The manning's equation is used to compute the flow rate and average velocity, while the channel length is divided by the velocity to give the travel time (Arnold & Allen, 1996).

3.4 Model calibration and validation

Both manual and automatic calibration approaches were used in this study. The 1986-1998 and 1973-1985 were used for stream flow calibration and validation respectively. These periods were selected because they coincide with the period of available climatic data. The first three years were used for model warm-up to estimate initial conditions in the watershed at the beginning of the simulation (Bekiaris et al., 2005; Larose et al., 2003). The warm-up period also helps to reduce the influence of the initial state variables estimated by the user through multiple model cycles (Shrestha et al., 2013). The calibration was based on streamflow data for a single station (1DD01A station) due to lack of reliable flow data upstream.

3.4.1 Sensitivity analysis

The sensitivity analysis, in this study, involved identification of the most sensitive parameters based on an automatic procedure in SWAT; and perturbation of the identified sensitive parameters using a manual approach. The Latin hypercube one-factor-at-a-time (LH-OAT) sampling technique described by van Griensven et al. (2006)

and incorporated in the ArcSWAT interface for SWAT2009 was used to identify the sensitive parameters. The LH-OAT technique is based on loops whereby for N intervals, the technique takes N sample points and varies each of the selected P parameters by changing each LH sample point P times. Each loop requires P+1 runs thus for the user defined N intervals, a total of N*(P+1) runs are required. Starting with a Latin Hypercube sample point$\boldsymbol{j}$, a partial effect $\boldsymbol{S_{i,j}}$ for each parameter $\boldsymbol{e_i}$ is computed (in percentage) as shown in Equation 3.4 (van Griensven et al., 2006). The final effect is the average of partial effects of each loop for all the sample points (total of N loops) and can be ranked from one (for largest effect) to a value equal to the selected parameters.

$$\boldsymbol{S_{i,j}} = \left| \frac{\boldsymbol{100} * \left(\frac{\boldsymbol{M(e_1,\ldots,e_i*(1+f_i),\ldots,e_p) - M(e_1,\ldots,e_i,\ldots,e_p)}}{\boldsymbol{[M(e_1,\ldots,e_i*(1+f_i),\ldots,e_p) + M(e_1,\ldots,e_i,\ldots,e_p)]/2}} \right)}{\boldsymbol{f_i}} \right| \qquad \textbf{Equation 3.4}$$

Where $\boldsymbol{M}(\blacksquare)$ is the model functions, $\boldsymbol{j}$ is a LH point and $\boldsymbol{f_i}$ is a predefined fraction by which the parameter $\boldsymbol{e_i}$ is changed.

A total of 13 parameters (shown in Table 3.2) representing groundwater, soil, runoff, evaporation and channel components of the watershed hydrological process were obtained from the sensitivity analysis in SWAT. The ArcSWAT interface allows modification of parameter values lumped across the catchment or by a distributed approach based on the sub-basins and HRUs. In addition, parameters can be modified by replacement of the initial value, addition of an absolute change or multiplication of a relative change within a pre-defined range to obtain the optimum value. Lumped sensitivity analysis approach was used while parameters were varied by replacement and multiplication of relative changes. For a comprehensive explanation of each parameter and value ranges see Neitsch et al. (2011).

Table 3.2: Parameters selected for SWAT model calibration

Name	Definition	Range	Process
CN2	SCS moisture condition II curve number for pervious areas	±25%	Runoff
ESCO	Soil evaporation compensation coefficient	0-1	Evaporation
SURLAG	Surface runoff lag coefficient	0.05-24	Runoff
RCHRG_DP	Deep aquifer percolation fraction.	0-1	Groundwater
GWQMN	Threshold water level in shallow aquifer for base flow (mm H_2O)	0-500	Groundwater
GW_REVAP	Groundwater "revap" coefficient.	0.02-2	Groundwater
GW_DELAY	Groundwater delay (days)	0-90	Groundwater
ALPHA_BF	Baseflow recession constant (days)	0-1	Groundwater
SOL_K	Saturated hydraulic conductivity (mm/hr)	±8%	Runoff
SOL_AWC	Soil available water storage capacity (mm H2O/mm soil)	0-1	Runoff
CH_N2	Manning's n value for main channel	0-0.3	Routing
CH_K2	Effective hydraulic conductivity in main channel alluvium (mm/hr).	5-130	Routing
OV_N	Manning's ''n'' value for overland flow	0.01-30	Runoff

3.4.2 Manual calibration

After the sensitivity analysis, manual calibration process was carried out for the period 1986 to 1998. The sensitive runoff and base flow parameters were perturbed within their absolute range while keeping the others constant to adjust volume and timing of the simulated runoff hydrograph. The surface runoff parameters were first adjusted followed by base flow parameters. This method has been successfully applied in previous studies (Shrestha et al., 2013; Yang et al., 2008).

3.4.3 Auto-calibration and uncertainty analysis

According to Beven and Binley (1992), manual calibration of distributed models is constrained by the large number of parameters determining the simulated hydrologic response. Thus, auto-calibration is essential for identification of the optimum parameter values. The sequential uncertainty fitting version 2 (SUFI-2) algorithm in the SWAT CUP software was used for auto-calibration and uncertainty analysis (Abbaspour et al., 1997, 2007). SUFI-2 is an accepted tool for combined calibration and uncertainty

analysis of the SWAT model (Chien et al., 2013; Faramarzi et al., 2010; Setegn et al., 2008; Strauch et al., 2012). As shown by Yang et al. (2008), SUFI-2 requires fewer simulations compared to the Generalized Likelihood Uncertainty Estimation (GLUE), Parameter Solution (ParaSol), and Bayesian inference techniques to achieve a similar level of performance. A step-by-step description of the SUFI-2 optimizing algorithm is outlined by Yang et al. (2008). First, a suitable objective function $\boldsymbol{g(b)}$ is defined. Different formulations of objective functions yield different optimum parameter values and require different set of parameter ranges. Consequently, there has been emphasis in the development of multi-objective formulations which combine different functions to overcome the non-uniqueness problem. In this study, the Nash-Sutcliffe coefficient (NSE) (Nash & Sutcliffe, 1970) was selected as the objective function. Then, physically meaningful ranges of minimum and maximum values for the parameters to be optimized [$\boldsymbol{b_{absmin}, b_{absmax}}$] are defined. The parameters are assumed to be uniformly distributed within a region bounded by the minimum and maximum values.

A latin hypercube sampling is then carried out within the hypercube [$\boldsymbol{b_{min}, b_{max}}$] (initially set as[$\boldsymbol{b_{absmin}, b_{absmax}}$]), and the corresponding objective function is evaluated using a parameter sensitivity matrix and parameter covariance matrix. The parameter sensitivity matrix $\boldsymbol{J}$ and parameter covariance matrix $\boldsymbol{C}$ are computed as shown in Equations 3.5 and 3.6:

$$\boldsymbol{J_{i,j} = \frac{\Delta g_i}{\Delta b_i}, i = 1, \dots, C_2^n, j = 1, \dots, m} \qquad \textbf{Equation 3.5}$$

$$\boldsymbol{C = S_g^2 (J^T J)^{-1}} \qquad \textbf{Equation 3.6}$$

Where $\boldsymbol{C_2^n}$ is the number of rows in the sensitivity matrix (equivalent to all possible combinations of two simulations), $\boldsymbol{j}$ is the number of columns (equal to the number of parameters) and $\boldsymbol{S_g^2}$ is the variance of the objective function values resulting from the $\boldsymbol{m}$ model runs.

Parameter uncertainty analysis in SUFI-2 accounts for all sources of uncertainties based on a multivariate uniform distribution within a parameter hypercube. In this method, the model output uncertainty is quantified using the 95% prediction uncertainty band (95PPU) calculated by the 2.5th and 97.5th percentiles of the cumulative distribution of every simulated point of output variable obtained through the sampled parameter sets (Abbaspour et al., 2007). A large parameter uncertainty is initially assumed such that the 95PPU encloses all the measured data. Then, this uncertainty is decreased in steps until the 95PPU band encloses "most of the observations", and the average distance between the upper (at 97.5 % level) and the lower (at 2.5 % level) parts of the 95PPU is "small" (Chien et al., 2013). For parameter $\boldsymbol{b_j}$, a 95% predictive interval is computed as shown in Equations 3.7 and 3.8:

$$\boldsymbol{b_{j,lower} = b_j^* - t_{v,0.025}\sqrt{C_{jj}}}, \qquad \textbf{Equation 3.7}$$

$$\boldsymbol{b_j, upper = b_j^* + t_{v,0.025}\sqrt{C_{jj}}} \qquad \textbf{Equation 3.8}$$

Where $\boldsymbol{b_j^*}$ is the parameter $\boldsymbol{b_j}$ for the best parameter estimates which produce the optimal objective function, $\boldsymbol{v}$ is the degrees of freedom $(\boldsymbol{m-n})$ and $\sqrt{\boldsymbol{C_{jj}}}$ is the estimated standard deviation. The parameter value range is then used to compute the 95PPU. The p-factor is calculated as the percent of observations bracketed by the 95PPU while the r-factor is calculated based on Equation 3.9:

$$\boldsymbol{r-factor = \frac{\frac{1}{n}\sum_{t_i=1}^{n}\left(y^M_{t_i,9\ 75\%} - y^M_{t_i,2.5\%}\right)}{\sigma_{obs}}} \qquad \textbf{Equation 3.9}$$

Where $\boldsymbol{y^M_{t_i,9\ 75\%}}$ and $\boldsymbol{y^M_{t_i,2.5\%}}$ is the upper and lower boundaries of the 95PPU, respectively, while $\boldsymbol{\sigma_{obs}}$ is the standard deviation of the measured data.

The ultimate goal is to enclose the majority of the observed data within the smallest possible uncertainty bound (*p*-factor close to 100 % and *r*-factor close to 1) as this

ensures that all other uncertainties are accounted for by the parameter uncertainties. If the values of the two factors are satisfactory, a uniform distribution in the parameter hypercube[$\boldsymbol{b_{min}}$, $\boldsymbol{b_{max}}$] is assumed as the posterior parameter distribution. If otherwise, is updated as shown in Equations 3.10 and 3.11 and another iteration is performed.

$$\boldsymbol{b'_{j,min} = b_{j,lower} - max\left(\frac{(b_{j,lower} - b_{j,min})}{2}, \frac{(b_{j,max} - b_{j,upper})}{2}\right)} \quad \textbf{Equation 3.10}$$

$$\boldsymbol{b'_{j,max} = b_{j,upper} + max\left(\frac{(b_{j,lower} - b_{j,min})}{2}, \frac{(b_{j,max} - b_{j,upper})}{2}\right)} \quad \textbf{Equation 3.11}$$

3.4.4 Model performance evaluation

Both graphical and statistical techniques have been recommended for performance evaluation in relation to calibration, validation and application of hydrological models. Based on previous recommendations (Krause et al., 2005; Moriasi et al., 2007), a combination of statistical and graphical methods were used to evaluate the goodness-of-fit between the simulated and observed values, both during the calibration and verification period.

The statistics used to compare the observed and simulated streamflow are: the Nash-Sutcliffe efficiency (NSE) (Nash & Sutcliffe, 1970), the coefficient of determination (R^2), the mean error (ME), the mean absolute error (MAE), the root mean squared error (RMSE), the percent bias (PBIAS) (Yapo et al., 1996), the ratio of the root mean squared error to the standard deviation of the observations (RSR) (Moriasi et al., 2007), the coefficient of persistence (P) (Kitanidis & Bras, 1980), the index of agreement (d) (Willmott et al., 1985), and the weighted coefficient of determination (Br^2) (Krause et al., 2005).

The two indexes proposed by Abbaspour et al. (2007) were also used to quantify the performance of the uncertainty analysis: (i) the p-factor, which represents the percentage of observed data embraced by the 95PPU; and (ii) the r-factor, which measures how

wide the uncertainty bounds are with respect to the variability of the observations, computed as the average width of the 95PPU divided by the standard deviation of the observations.

3.5 Future climate data and scenarios

In this study, temperature and rainfall change over three future periods, namely the 2020s (2011-2040), the 2050s (2041-2070) and the 2080s (2071-2100), were downscaled using the delta-change approach. In this approach, monthly anomalies were calculated for the temperature and precipitation amounts between the future and reference periods for each GCM simulation. This method is stable, robust and simple in generating climate scenarios from a group of global climate models hence its wide application in previous studies (Andréasson et al., 2004; Boyer et al., 2010; Merritt et al., 2006; Minville et al., 2008). As stated by Boyer et al. (2010), the delta-change method assumes that the GCMs biases remain similar across the reference and that the future periods and temporal variability (daily to inter annual) of the observed climate variables during the reference period is maintained for the simulated series. The future climate scenarios were generated using ten GCMs (shown in Table 3.3) and three GHGs emissions scenarios (A1B, A2 and B1). The selection of the models was based on the studies by (Akurut et al., 2014; Conway et al., 2007; Githui et al., 2009; McHugh, 2005).

The climate scenarios generated consisted of monthly percentage change for rainfall (multiplicative factor) and degrees Celsius change for temperature (additive factor) in the future periods relative to the baseline period (1961-1990) for each GCM. In order to address the uncertainties in the projections of individual GCMs, the monthly anomalies were averaged per GHGs emissions scenarios and per future period to make a total of nine scenarios (three scenarios per future period) namely A1B2020s, A1B2050s, A1B2080s, A22020s, A22050s, A22080s, B12020s, B12050s, and B12080s. The monthly rainfall and mean temperature anomalies were then applied to observed daily

data in the SWAT model. The model data was obtained from the Canadian Climate Change Scenarios (CCCSN, http://ccds-dscc.ec.gc.ca/?page=dd-gcm).

Table 3.3: Global climate models used to generate climate scenarios.

Model	Modeling Group (Country)
CGCM3T63	Canadian Centre for Climate Modelling and Analysis (Canada)
CNRMCM3	Centre National de Recherches Meteorologiques (France)
CSIROMk3.0	Commonwealth Scientific and Industrial Research Org. (Australia)
ECHO-G	University of Bonn, Meteorological Research Institute (Germany)
GISS-ER	Goddard Institute for Space Studies (USA)
MRI CGCM2.3.2	Meteorological Research Institute (Japan)
IPSLCM4	Institut Pierre Simon Laplace (France)
GFDLCM2.1	NOAA Geophysical Fluid Dynamics Lab (United States)
ECHAM50M	Max Planck Institute for Meteorology (Germany)
HadCM3	Hadley Centre for Climate Prediction and Research (UK)

3.6 Analysis of hydrological impacts

The main objective of this study was to generate an approximation of expected changes in streamflow in the study area for a given scenario characterizing the future climate. Consequently, the calibrated SWAT model was used to simulate the impacts of the projected rainfall and temperature changes on stream flow.

The SWAT interface was used to apply the monthly adjustment factors to climatic data by editing the rainfall adjustment factor (RFIN, %) and temperature adjustment factor (TMPIN, ºC) in the .SUB files of the SWAT model. Rainfall amount was perturbed by multiplying observed rainfall with monthly change factors while temperature was perturbed by adding the prescribed monthly changes to the monthly baseline conditions to obtain daily data (Bouraoui et al., 2002; Mengistu & Sorteberg, 2012). The simulated streamflow for the 1973-1998 period was considered as the baseline period against which the simulations for the 2020s, 2050s and 2080s periods were compared.

3.6.1 Mean streamflow changes

The expected changes were analyzed in terms of mean monthly, seasonal and annual values. The projected impacts of rainfall and temperature change (ΔP, ΔT) were determined according to Equation 3.12 where $\boldsymbol{\Delta Q}$ is the monthly, seasonal or annual stream flow change.

$$\boldsymbol{\Delta Q_{\Delta P,\Delta T}} = \frac{\left(\boldsymbol{Q_{\Delta P,\Delta T} - Q_{\Delta P=0,\Delta T=0}}\right)}{\boldsymbol{Q_{Q_{\Delta P=0,\Delta T=0}}}} * \mathbf{100} \qquad \textbf{Equation 3.12}$$

3.6.2 Analysis of extreme flows

Due to the expected changes in precipitation and temperature, climate change will affect high and low flows hence affecting aquatic ecosystems as well as hydrologic regimes. Flow Durations Curves (FDCs) based on annual maximum and minimum flows computed for the 2020s, 2050s and 2080s were used to illustrate the percentage of time that streamflow is likely to equal or exceed a given value.

CHAPTER FOUR

RESULTS AND DISCUSSION

4.0 A Brief on the chapter

This chapter consists of three main sections which present the results of the study and discussions. The first section focuses on the SWAT model sensitivity analysis, calibration and validation results and their discussion. The second section gives the results of the climate change scenarios and their discussion while the third section comprises the analysis of the projected hydrological impacts of climate change.

4.1 Hydrological modeling

4.1.1 Watershed delineation

The delineation of the watershed area upstream of the 1DD01A River gauging station (Lat 0.37ºN, Long 34.49ºE) gave a total of 22 sub-basins and 200 HRUs. The minimum, maximum and mean elevations in the area were 1277, 4286 and 2020 m.a.s.l, respectively. The four sub-watersheds covered a total area of about 2,961 km^2. As shown in Figure 4.1 and Figure 4.2, the four sub-watersheds depicted differences in size, land cover, topography and soil types. These differences are expected to influence streamflow response in the sub-watersheds hence the spatial variations in the overall streamflow changes in the sub-watersheds are not only due to climatic changes but also due to the physical differences. Specifically, the Kuywa sub-watershed depicted a wide variation in physical characteristics compared to the other three sub-watersheds.

Figure 4.1 shows the percentage area covered by each land cover type in each sub-watershed. The land cover classes in the sub-watersheds based on SWAT model land cover classification were deciduous forest (FRSD), close grown agricultural land

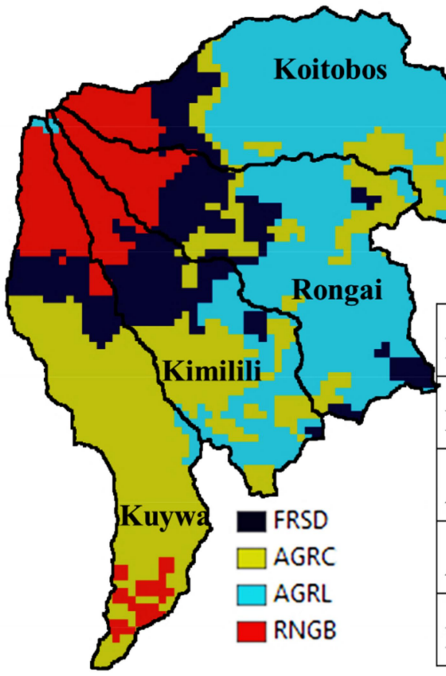

Landcover	% coverage			
	Koitobos	Rongai	Kimilili	Kuywa
FRSD	7.88	18.63	23.89	11.82
AGRC	16.87	15.60	34.95	64.13
AGRL	66.93	53.36	27.29	1.96
RNGB	8.32	12.40	13.88	22.08

Figure 4.1: Land use types and their areal coverage in Mt. Elgon sub-watersheds

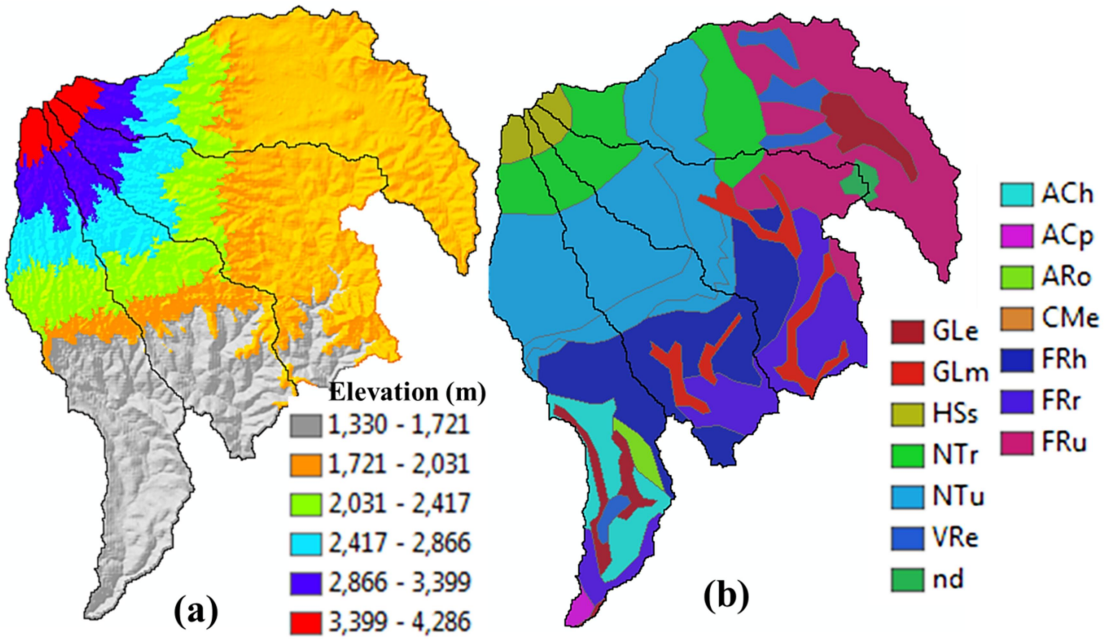

Figure 4.2: (a) Topography and (b) Soil types in Mt. Elgon sub-watersheds

(AGRC), generic agricultural land (AGRL) and range land (RNGB). In Koitobos sub-watershed, which covered an area of about 866.75 km^2, the major land cover types were AGRC and AGRL while in Rongai which covered about 796.97 km^2, FRSD and AGRL were the major land cover types. In Kimilili sub-watershed, which covers 576.45 km^2, the main land cover types are FRSD, AGRC and AGRL while in Kuywa sub-watershed (about 720.37 km^2), major land cover types were FRSD, AGRC and RNGB.

Topography in the Koitobos and Rongai is similar while in Kimilili, and Kuywa, elevation classes are similar. In Kuywa, a large area is covered by elevation between 1330 and 1721 m.a.s.l which makes the sub-watershed distinct from the other three sub-watersheds. In addition, the distribution of soil types is different across the sub-watersheds. As a result of these variation in the characteristics of the sub-watersheds, the response to climate change conditions are expected to be different.

4.1.2 Model auto-calibration

Four iterations with 500 model simulations each were undertaken in SWAT-CUP based on the SUFI-2 approach using daily observed flow for the 1981-1998 period. After each iteration, parameter ranges were adjusted to the improved parameter ranges from the previous iteration. The sensitivity analysis results gave the degree of sensitivity of 13 parameters and the parameter bounds which were essential for the manual and auto-calibration activities. In the fourth iteration, 61% of the observations were bracketed within the 95PPU brackets and an r-factor of 0.97 was obtained indicating that SUFI-2 is capable of capturing the observations. The p-values indicated that the sensitivity of 6 parameters (shown in Table 4.1) was significant. The p-value for each of these parameters was less than 0.01 suggesting that their sensitivity is significant.

Table 4.1: The most sensitive parameters and final auto-calibration results

Parameter	Fitted value	Final range	
RCHRG_DP.gw	0.38	0	1
GW_DELAY.gw	40.16	30	45
GW_REVAP.gw	0.09	0.02	2
ESCO.hru	0.84	0.80	1
GWQMN.gw	0.76	0.50	1.50
CN2.mgt	-15.90%	-30%	20%

Using the optimal parameter combinations, the model reproduced monthly flows better than daily flows. This is consistent with the observation of Geza et al., (2009) that simulations for shorter time steps are poorer than for longer time steps. Table 4.2 shows the statistical measures used to evaluate the model performance. Figure 4.3 shows the daily and monthly flow hydrographs for the calibration (1986-1998) and validation (1973-1985) periods respectively. The R^2 values for daily flow simulation were 0.63 and 0.61 and NSE values were 0.54 and 0.61 for the calibration and validation periods respectively. The simulated monthly flow showed a good correlation with observed flow with R^2 values of 0.68 and 0.70 and NSE values of 0.58 and 0.70 for the calibration and validation periods, respectively.

Table 4.2: Goodness-of-fit between observed and simulated daily and monthly streamflow

		NSE	R^2	ME	MAE	RMSE	PBIAS	RSR	d	Br^2
Daily	Cal.	0.54	0.63	13.51	24.40	33.31	22.70	0.67	0.86	0.62
	Val.	0.61	0.61	2.57	19.62	29.14	4.40	0.63	0.87	0.54
Monthly	Cal.	0.58	0.68	13.52	21.38	28.81	22.70	0.65	0.88	0.64
	Val.	0.70	0.70	2.64	16.38	23.02	4.50	0.55	0.91	0.65

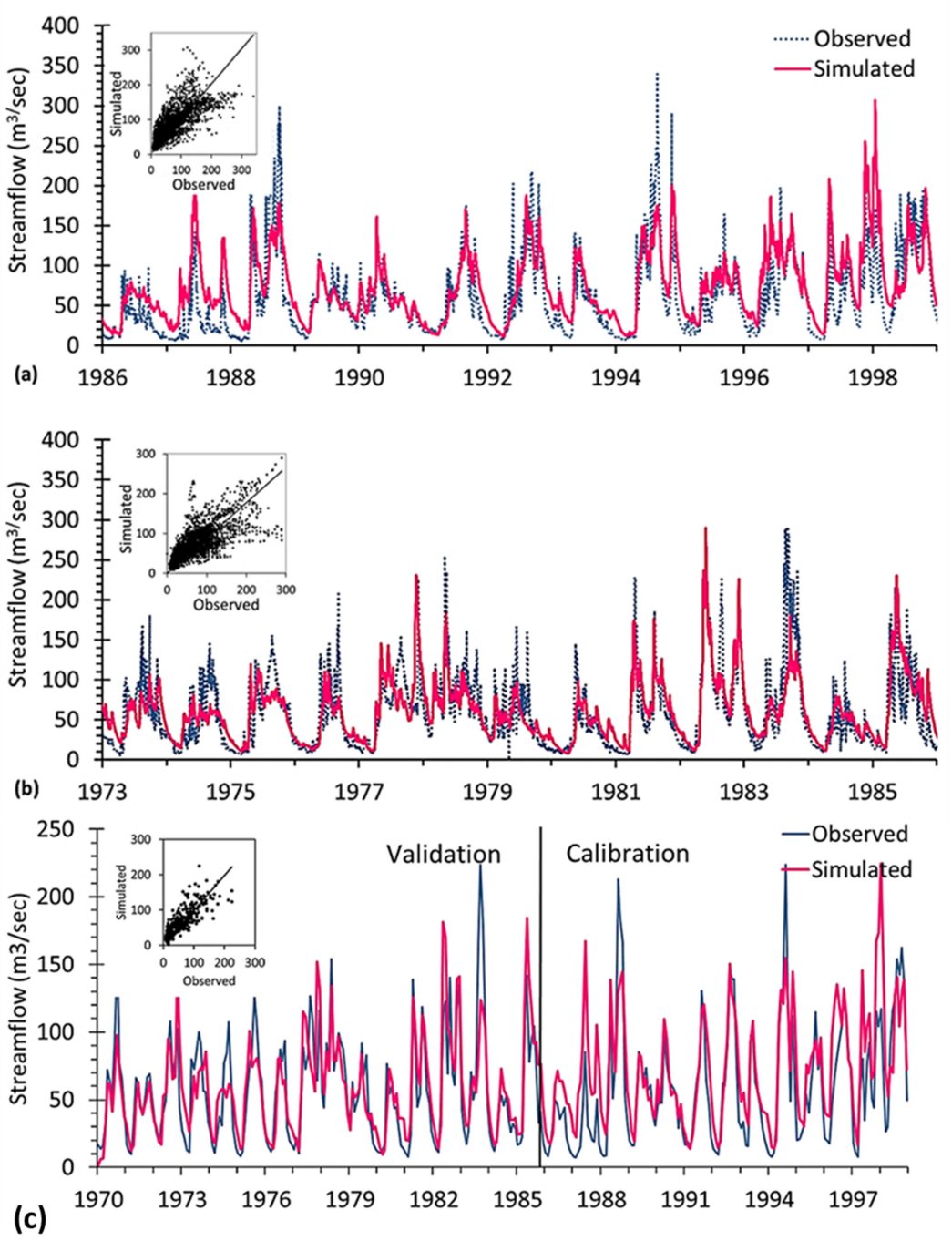

Figure 4.3: (a) Hydrographs and scatter plots for daily calibration, (b) daily validation and (c) monthly calibration and validation.

Good correspondence exhibited between monthly observed and simulated flows implies that the model captured well the seasonality of flow. A scatter plot and 1:1 line for the observed and simulated monthly flows for the entire period shown in Figure 4.4 shows good correlation between the observed and simulated flow for the entire period. The monthly simulated flow is generally higher than the observed flow values for the entire study period. The average daily flow hydrographs in Figure 4.5 and Figure 4.6 shows that the SWAT model overestimated low flows and underestimated high flows. This has also been observed in other studies (Benaman & Shoemaker, 2005; Jajarmizadeh et al., 2012; Jeong et al., 2010; Lubini & Adamowski, 2013; Nie et al., 2011; Tian et al., 2014). This shortcoming in SWAT model has mainly been attributed to lack of consideration of precipitation duration and intensity by the SCS curve number method for simulation of stream flow (Jeong et al., 2010; Nie et al., 2011). In addition, the model was mainly developed for evaluation of long-term periods and not modelling of storm-events hence does not simulate high flows adequately (Arnold et al., 1998). Moreover, estimation of missing meteorological data by the weather generator and errors in the streamflow data could also lead to poor correlation between observed and simulated flows (Lubini & Adamowski, 2013). However, based on the generally good performance shown in Table 4.2, the calibrated model was considered suitable for simulating the impact of projected climate change scenarios on stream flow in the study area.

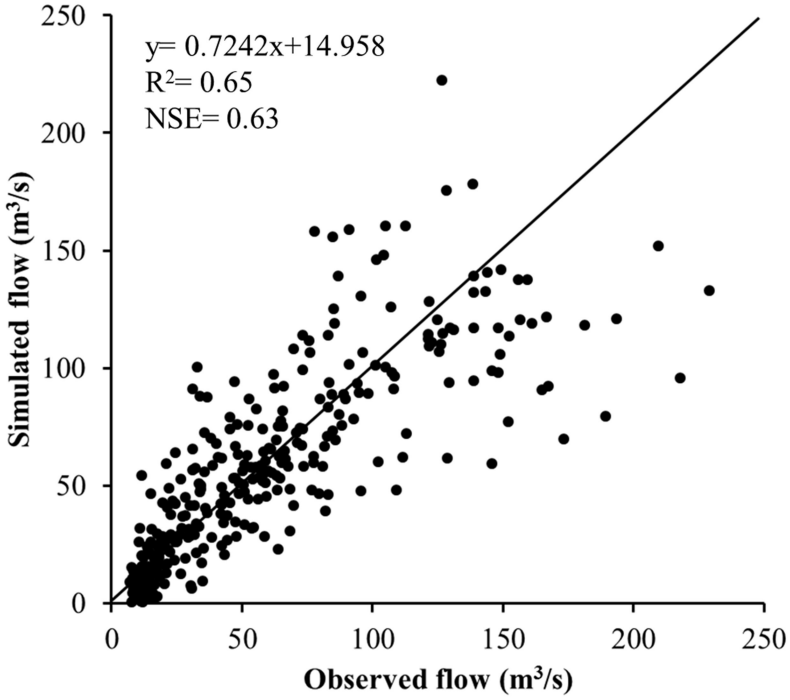

Figure 4.4: Scatter plot and 1:1 line of the observed and simulated monthly flows for the entire simulation period (1973-1998).

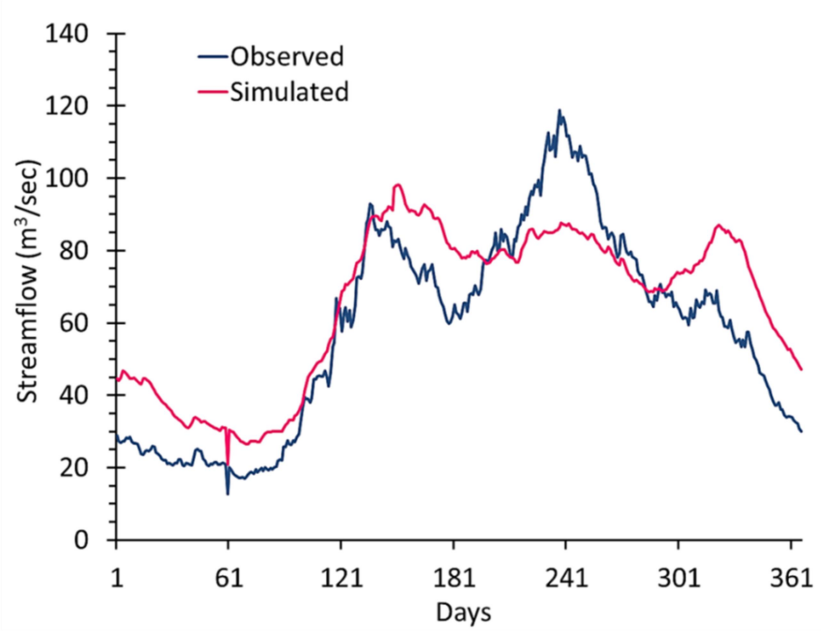

Figure 4.5: Hydrograph for mean observed and simulated daily stream flow for the entire simulation period (1973-1998).

4.1.3 Parameter uncertainty

The parameter uncertainty is illustrated in Figure 4.6. The figure shows the observed and simulated mean daily flows and the 95% uncertainty bound obtained by the SUFI-2 algorithm. Based on the results, a high parameter uncertainty is evident across the year and especially for the high flow period. This increase in uncertainty with increase in discharge was also observed by Tian et al. (2014) who attributed it mainly to model parameters. Generally, higher uncertainty was displayed during the May to November period. This corresponds with the peak flows during May-June, August–September, and November–December. The observed flow is generally enveloped by the uncertainty bound although some of the flow events are not well captured by the model.

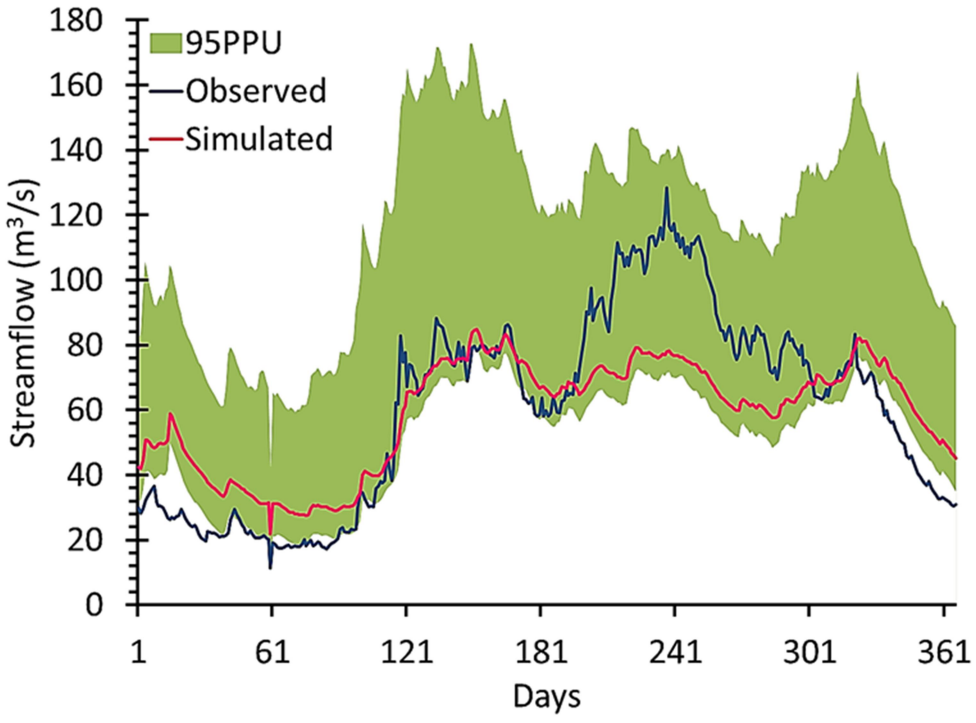

Figure 4.6: Streamflow uncertainty during calibration period (1986-1998)

4.2 Future climate scenarios

In the analysis of future climate and hydrological scenarios, '2020s' indicates the results for 2011-2040, '2050s' indicates the results for 2041-2070, and '2080s' indicates the results for 2071-2100. The different seasons are represented by DJF (December-February), MAM (March-May), JJA (June-August) and SON (September-November).

4.2.1 Annual and seasonal scenarios

The projected changes in annual and seasonal precipitation for the three future periods are shown in Figure 4.7. The projected changes in rainfall by Hulme et al. (2001) and IPCC (2001) indicate that the east Africa region is likely to get wetter in the future. In this study, similar results were obtained whereby projected shifts in annual rainfall vary from 1.4-4.6% by the 2020s; 3.3-6.4% by the 2050s and 7.3-11.1% by the 2080s, depending on the scenario. The largest shifts are projected to occur under the A2 scenario followed by A1B and B1. However, by the 2020s, the largest increase in annual average rainfall (about 4.6%) is projected under the B1 scenario. Under the A1B and A2 scenarios, the projected increase by the 2020s is 2.5% and 1.4% respectively. Rainfall projections for the 2050s show an increasingly wetter climate relative to the baseline period (6.4%, 4.5% and 3.3% increase for the A1B, A2 and B1 scenarios respectively). During the 2080, the projected increase in annual rainfall is even more significant (11.1%, 15.1% and 7.3%) compared to the baseline.

Seasonal rainfall amount and variability is a significant site factor for agricultural production. However, previous assessments of precipitation projections over the East Africa region have exhibited the complexity of likely rainfall change in the region (Kent et al., 2015). As shown in Figure 4.7, greater variability is expected in the future seasonal precipitation change compared to the annual change. During the baseline period, observed rainfall in DJF, MAM, JJA, and SON accounts for 10.9%, 34.9%,

29.9%, and 24.4% respectively of the annual rainfall. All the scenarios analyzed project increased DJF and SON rainfall by 4.0-7.3% and 2.1-4.7% by the 2020s, 9.1-11.3% and 3.1-11.1% by the 2050s, and 9.8-25.1% and 9.3-24.0% by the 2080s, respectively. Under scenario B1, JJA rainfall projections indicate decrease in rainfall by 2.0% by the 2020s, 4.6% by the 2050s and 5.6% by the 2080s. Scenario A1B shows a persistent increase in rainfall across the time periods in all the seasons. The relative changes in DJF and SON precipitation for the different scenarios display a larger spread than the other seasons.

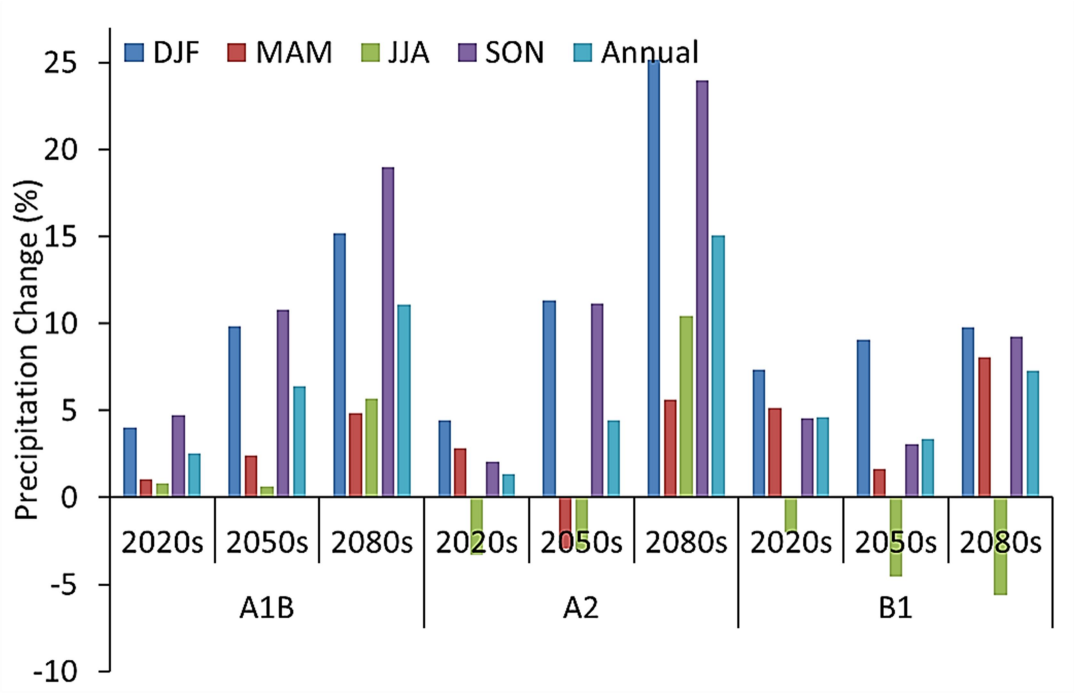

Figure 4.7: Seasonal and annual precipitation changes by the 2020s, 2050s and 2080s under climate scenarios A1B, A2 and B1.

The projected annual and seasonal temperature changes based on the climate scenarios analyzed are shown in Figure 4.8. The magnitude of projected temperature change shows a significant increasing trend over time as also indicated by Hulme et al. (2001). On average, annual temperatures are projected to increase by 1.1˚C by the 2020s, 2.1˚C by the 2050s, and 3.0˚C by the 2080s. Based on the analyzed scenarios, the annual mean

warming from the baseline climate varies from 0.6 to 1.5˚C by the 2020s, 1.3 to 2.8˚C by the 2050s, and from 1.5 to 4.4˚C by the 2080s. This is comparable to conclusion by Hulme et al. (2001) that the average warming in Africa continent towards the year 2100 is likely to be 2-5°C compared to 1961-1990 baseline period. On a seasonal basis, all models show generally similar increasing trends of warming. In addition, the uncertainty in the projected shifts increases over time. The projected seasonal temperature shifts vary from 0.5 to 1.9˚C by the 2020s, 1.2 to 3.7˚C by the 2050s, and 1.2 to 5.5˚C by the 2080s, depending on the season, GHGs emissions scenario and climate models. Depending on the future time period and GHGs emissions scenario, the projected warming is greatest in JJA (1.1 to 4.3˚C) and lowest in DJF (1.0 to 3.6˚C) while in both SON and MAM projected temperature increases range from 1.1 to 3.7˚C. The uncertainty in seasonal temperature change is largely due to different projections of climate models.

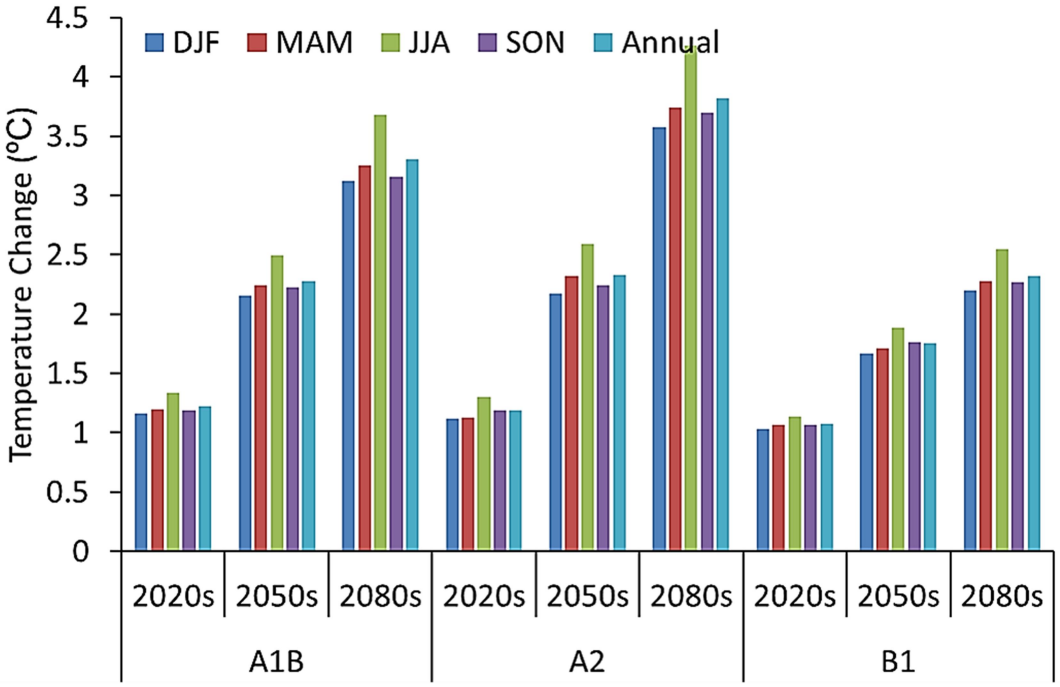

Figure 4.8: Seasonal and annual temperature changes by the 2020s, 2050s and 2080s under climate scenarios A1B, A2 and B1.

4.2.2 Monthly scenarios

Figure 4.9 shows the projected monthly precipitation anomalies. The severe drought of 2010-2011 experienced in the east Africa region was the worst to occur in the region for the last 60 years. The recorded significant decrease in the March-May "long rains" in the region has been attributed to Pacific-centered multi-decadal natural variability due to sea surface temperature variations over the Pacific Ocean (Kent et al., 2015; Lyon et al., 2013; Lyon & DeWitt, 2012; Lyon, 2014; Yang et al., 2014) and westward extension of an anthropogenic-based relatively rapid Indio-Pacific warm pool and related Walker circulation (Williams & Funk, 2011). According to Hulme et al. (2001), future projections in east Africa region indicate a likely rainfall increase (5-20%) during the wet months (December to February) and a decrease (5- 10%) during the dry months (June to August).

In this study, the intra-annual pattern of projected precipitation changes is also multi-modal whereby across the time periods, the majority of the analyzed models and scenarios generally show an increase in December to March, decrease in April to July, and increase again in August to November. By the 2020s, under scenario A1B, a major increase in monthly precipitation is projected in February (14.2%) and September (32.5%), while a decrease is expected in April (-0.6%) and May (-1.6%). Under the B1 scenario, the projected mean monthly changes by the 2020s are greater than by the 2050s, but lower compared to the 2080s. The projected increase in April (6.6%), and May (4.0%) for the 2020s, reverses to a negative change in the 2050s (-2.2% and -1.5% for April and May, respectively), and again shows an increase to 7.7% and 3.3% by the 2080s.

Figure 4.10 shows the projected monthly temperature changes. Unlike the precipitation anomalies, monthly temperature anomalies show a fairly consistent increasing trend in all climate scenarios. Projected temperature change ranges between 0.2 to 2.4˚C for the

2020s, 0.9 to 4.0˚C for the 2050s and 1.0 to 5.9˚C for the 2080s depending on the emissions scenario and climate model. All the models indicate greater warming from April to September than during the rest of the year.

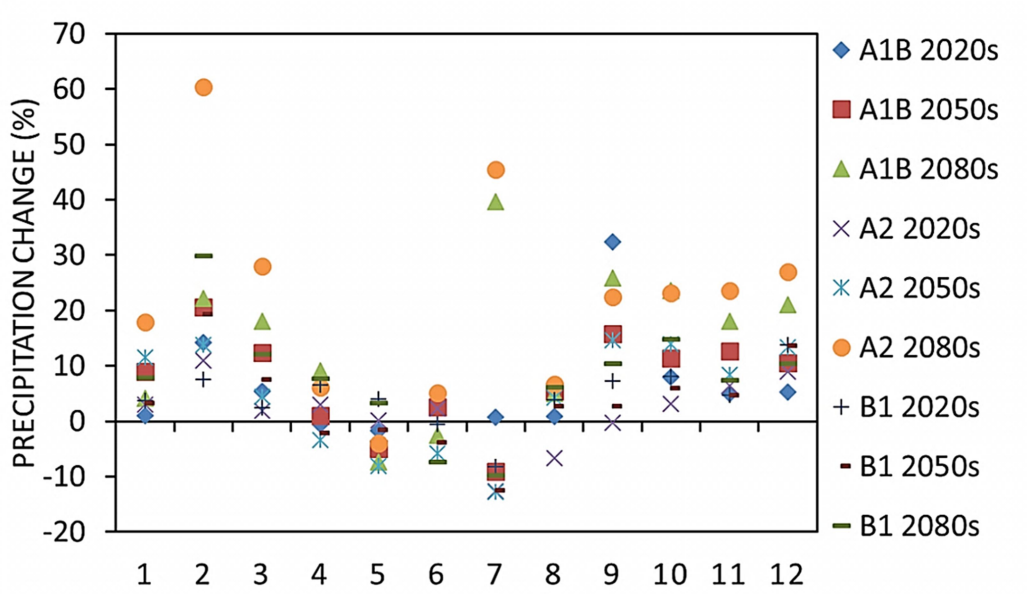

Figure 4.9: Monthly precipitation changes by the 2020s, 2050s and 2080s relative to the baseline period (1961–1990) under climate scenarios A1B, A2 and B1.

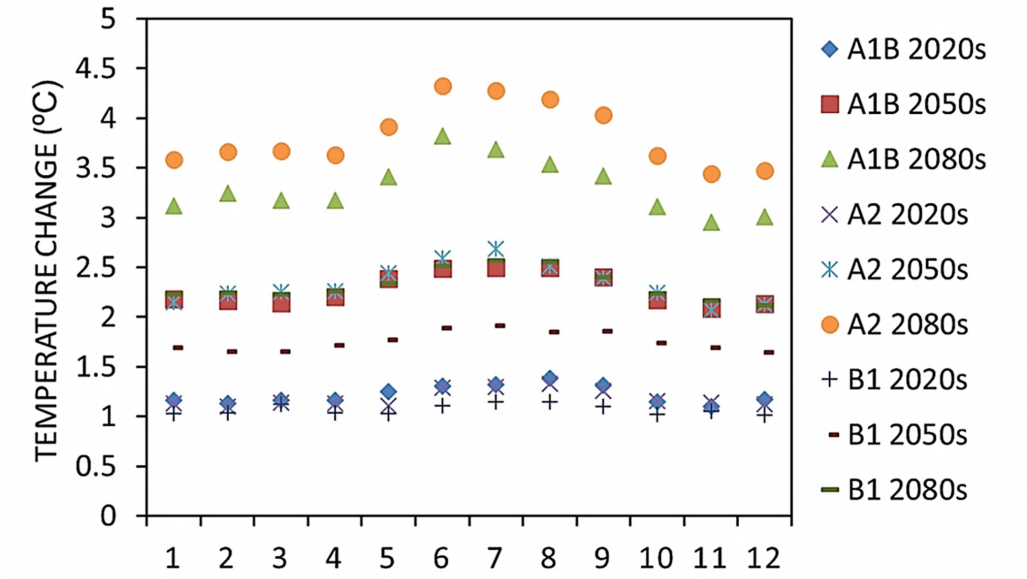

Figure 4.10: Monthly temperature changes by the 2020s, 2050s and 2080s relative to the baseline period (1961–1990) under climate scenarios A1B, A2 and B1.

4.2.3 Uncertainty in climate projections

Uncertainty in the projected climate scenarios was evaluated using box plots derived from the GCMs projections. Figure 4.11 and Figure 4.12 show the uncertainty in the projected changes in annual precipitation and temperature for the future three periods under the three emission scenarios relative to the reference period. As shown in the figures, there is considerable larger uncertainty in the projected annual precipitation compared to temperature changes. This was also shown by Woldemeskel et al. (2012) who noted that it could be due to large variability in the minimum temperature compared to precipitation where it is usually zero; and the small difference between minimum and maximum temperature values compared to precipitation values. For each of the future periods, the box and whisker plots show the upper and lower quartile, maximum, median and minimum of annual values within each emissions scenario. An increasing trend is depicted over time in both temperature and precipitation. In addition, the uncertainty in projected precipitation change increases over time. The relative changes in precipitation and temperature under the A1B and A2 scenarios show a wider range of uncertainty than for the B1 scenario, with the A2 scenario showing the highest uncertainty.

The monthly and seasonal uncertainties are depicted by the box plots shown in Appendices 3 to 6. As shown in the figures, the general anomalies in average monthly and seasonal precipitation and temperature are different in the three future periods. As expected, the range of monthly anomalies for 2080s is much higher than those for 2020s and 2050s. Therefore, the expected impacts are likely to be time dependent and may be influenced by the future period considered. Precipitation in October to January shows a considerably lower uncertainty compared to other months across the time periods and emission scenarios. The relative change in SON precipitation shows a wider range than the other seasons under all the emission scenarios in the three future periods. For temperature, the DJF and MAM seasons shows the largest range of expected changes.

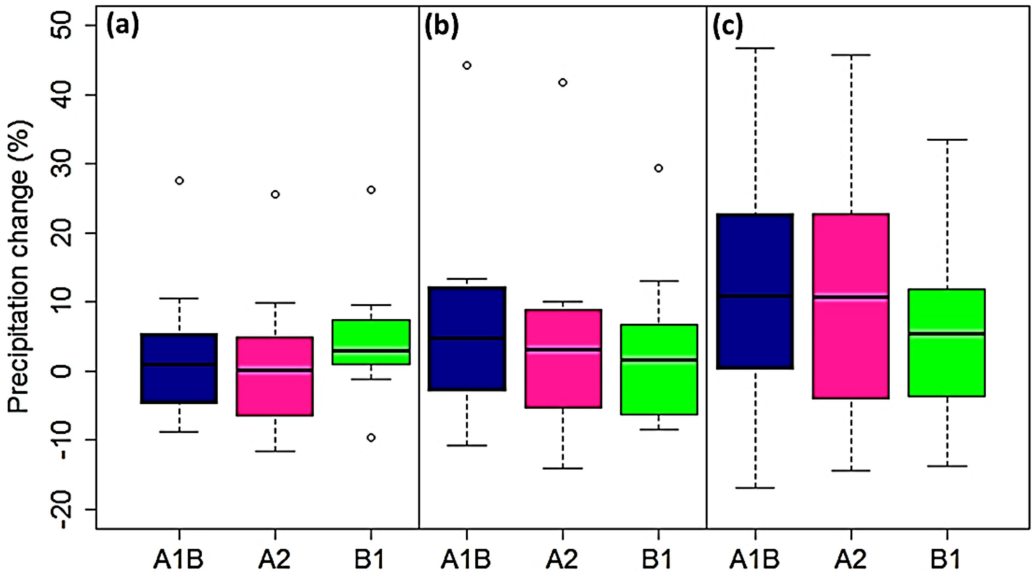

Figure 4.11: Box plots depicting the uncertainty in projected annual precipitation change for the A1B, A2 and B1 emissions scenarios by the (a) 2020s, (b) 2050s, and (c) 2080s.

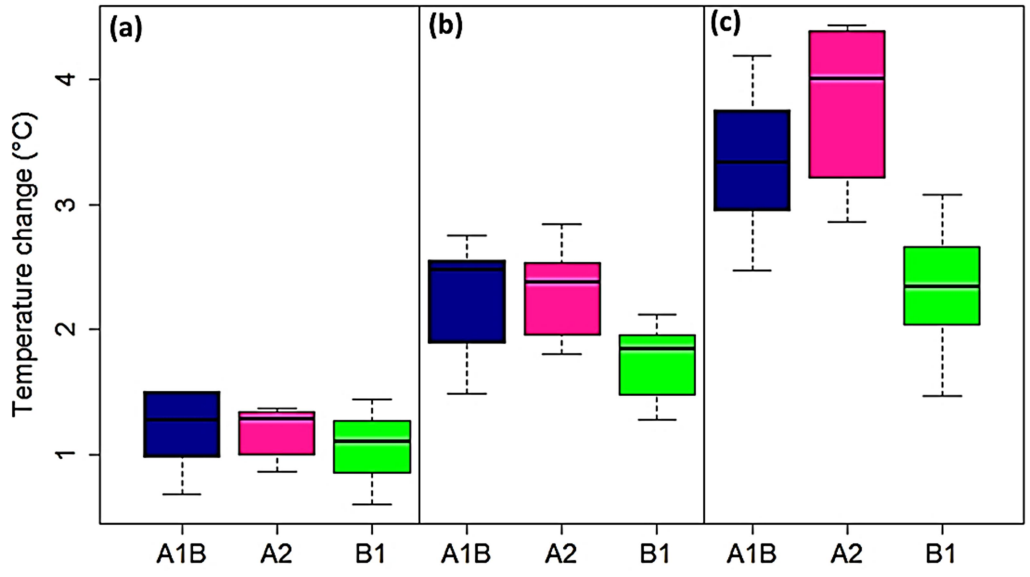

Figure 4.12: Box plots depicting the uncertainty in projected annual temperature change for the A1B, A2 and B1 emissions scenarios by the (a) 2020s, (b) 2050s, and (c) 2080s.

4.3 Projected hydrological impacts

In this study, the main drivers of hydrological impacts were mean monthly changes in precipitation and temperature for all climate models per emission scenario and future period. The impact was analyzed taking the 1970-1998 simulated flow as the baseline flow against which the future flows for the 2020s, 2050s and 2080s were compared. The projected climate change impacts on flow were analyzed on annual, seasonal and monthly basis.

4.3.1 Annual streamflow changes

The mean annual response of streamflow to the climate scenarios is summarized in Table 4.3. Generally, this table shows that the percent changes of mean annual stream flow exhibit a large variability when the projected temperature and precipitation changes were used in the SWAT model. As expected, stream flow responses to climate change signals do not follow an obvious trend partly due to projected increases and decreases of precipitation as well as natural variability. However, although periods of increased and decreased annual mean flows are expected in future, all climate scenarios project increased annual mean flow toward the end of the 21st century except in Kuywa sub-watershed.

In the Koitobos sub-watershed, all scenarios project an increase in mean annual stream flow except scenario A2 which projects a 1.4% decrease by the 2020s. The annual mean flow in the Rongai sub-watershed is expected to increase in the future under all emissions scenarios. In this sub-watershed, a large increase of about 40% is expected by the 2080s under the A2 scenario. Under the A1B scenario, stream flow in Rongai is expected to increase by 21.2% by the 2020s, 13.7% by the 2050s, and by 32.3% by the 2080s. Under the B1 scenario, flow in this sub-watershed is expected to increase by 13.8% by the 2020s, 3.6% by the 2050s, and 15.6% by the 2080s.

Table 4.3: Simulated relative changes in mean annual stream flow (negative changes are in bold)

Emission Scenario	Time Period	% stream flow change per sub-watershed			
		Koitobos	Rongai	Kimilili	Kuywa
A1B	2020s	18.56	21.20	6.71	**-13.15**
	2050s	14.53	13.73	3.07	**-30.12**
	2080s	53.30	32.32	11.63	**-20.09**
A2	2020s	**-1.42**	2.81	**-9.86**	**-23.17**
	2050s	2.93	4.77	**-12.31**	**-36.64**
	2080s	64.62	40.16	19.95	**-14.46**
B1	2020s	11.70	13.81	5.03	**-15.79**
	2050s	0.36	3.59	**-4.01**	**-35.27**
	2080s	17.14	15.60	0.61	**-28.00**

The projected stream flow changes in the Kimilili and Kuywa sub-watersheds differ in magnitude and direction despite their proximity. This can be attributed to the differences in the physical characteristics of the sub-watersheds as well as spatial estimation of the climate variables in SWAT. The mean annual streamflow in Kimilili is projected to decrease by 9.9% and 12.3% under scenarios A2 for the 2020s and 2050s respectively and by 4% under scenario B1 for the 2050s. Other scenarios show a possible increase in the annual mean flow. In Kuywa sub-watershed, all scenarios show a possible decrease in annual streamflow. The projected decline ranges between 13%- 23% by the 2020s, 30%-36% by the 2050s and 14 %-28% by the 2080s.

4.3.2 Seasonal streamflow changes

The temporal distribution of discharge is a significant component in the hydrological cycle. Figure 4.13 shows the changes in seasonal flow projected under different scenarios in Koitobos and Rongai sub-watersheds. The analysis of the projected seasonal streamflow changes in these sub-watersheds indicated that mean JJA, SON and DJF flows are likely to be altered by climate change. The majority of the projected seasonal changes in mean discharge in these sub-watersheds range between -10% and +50%. In

Koitobos, the mean DJF discharge is likely to increase by an average of 5.9% (ranging from -1.7% to +11.8%) for the 2020s, by 3.5% (ranging from -1.9% to +8.8%) for 2050s and by 20.4% (ranging from +6.3% to +30.8%) for the 2080s.In Rongai watershed, all scenarios project an increase in streamflow during the DJF season except B1 (2050s) scenario which projects a decrease of about 0.1%.

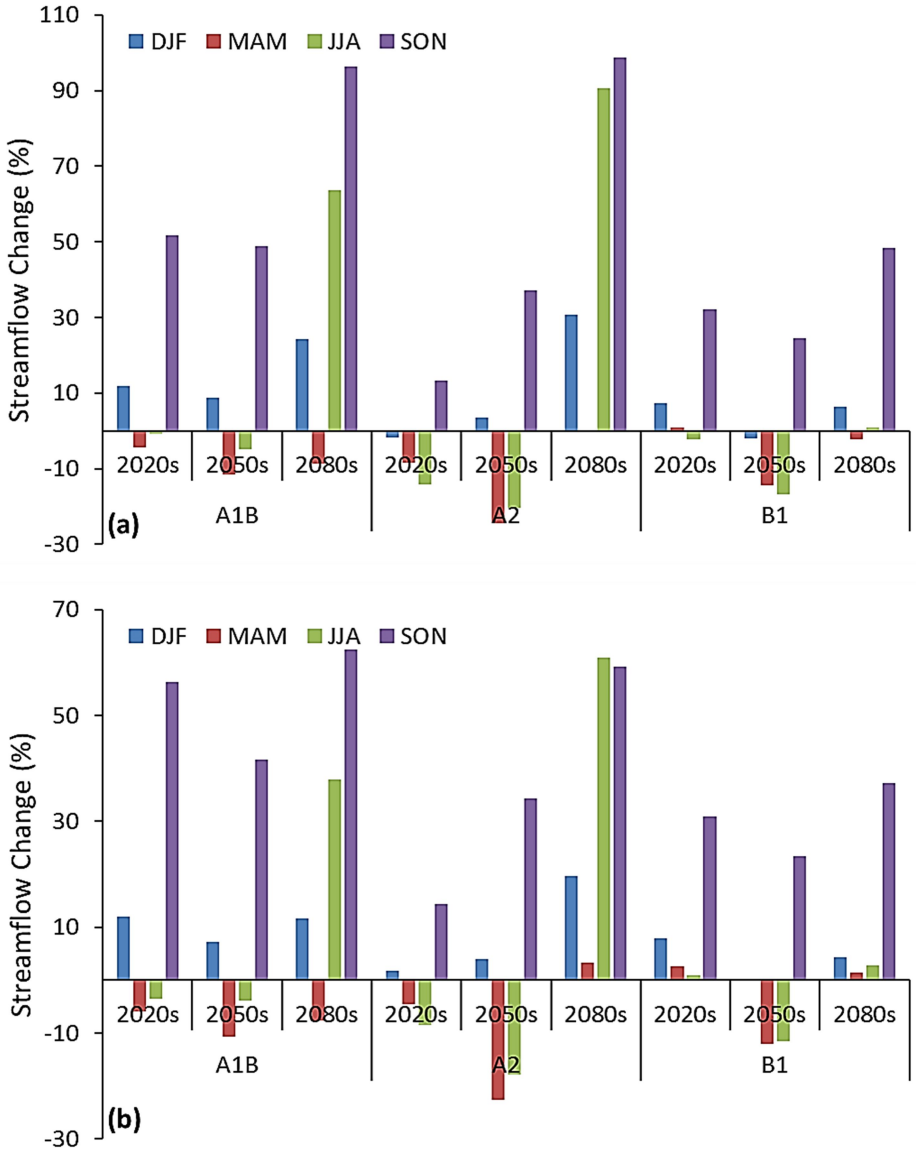

Figure 4.13: Projected seasonal streamflow changes in (a) Koitobos and (b) Rongai sub-watersheds.

The projected changes in the MAM season in both sub-watersheds indicate a likely decrease under all scenarios and future periods except for scenarios A2 for the 2080s and B1 for the 2020s. For the SON season, projected changes under all scenarios and time periods indicate likely streamflow increase in both Koitobos and Rongai sub-watersheds. The mean SON discharge in Koitobos and Rongai sub-watersheds is projected to increase by an average of 32.4% and 33.9% by the 2020s, 36.8% and 32.2% by the 2050s, 81.1% and 53.0% by the 2080s, respectively.

The projected changes in seasonal flow projected under different scenarios in Kimilili and Kuywa sub-watersheds are shown in Figure 4.14. Under the A2 scenario, streamflow in Kimilili is projected to decrease in 2020s and 2050s in all seasons. Under the A1B scenario, all seasons show a decrease by the 2020s and 2050s except the SON season. All the seasons show an increase in A1B for the 2080s, A2 for the 2080s and B1 for the 2020s. In Kuywa all scenarios show a likely decrease in seasonal streamflow. The highest decrease is expected in the JJA season under all scenarios except A2 for the 2020s where the SON season shows the highest decrease.

4.3.3 Monthly streamflow changes

The projected monthly streamflow changes in Koitobos by the 2020s, 2050s and 2080s are shown in Figure 4.15. By the 2020s, under the A1B scenario, stream flow in Koitobos is expected to increase in all months except April, May, June, and July. In this period an increase up to 75.6% (October) and a decrease of up to 11% (May) in monthly flow volume is projected. For the A2 scenario, in the same period and sub-watershed, all months show a decrease in streamflow except March, September, October and November. In this scenario, the increase in monthly streamflow is likely to reach up to 25.6% in October while the decrease is expected to reach up to 19% in July. The B1 scenario projections for this sub-watershed for the 2020s period indicate that discharge is likely to decrease in May, June and July.

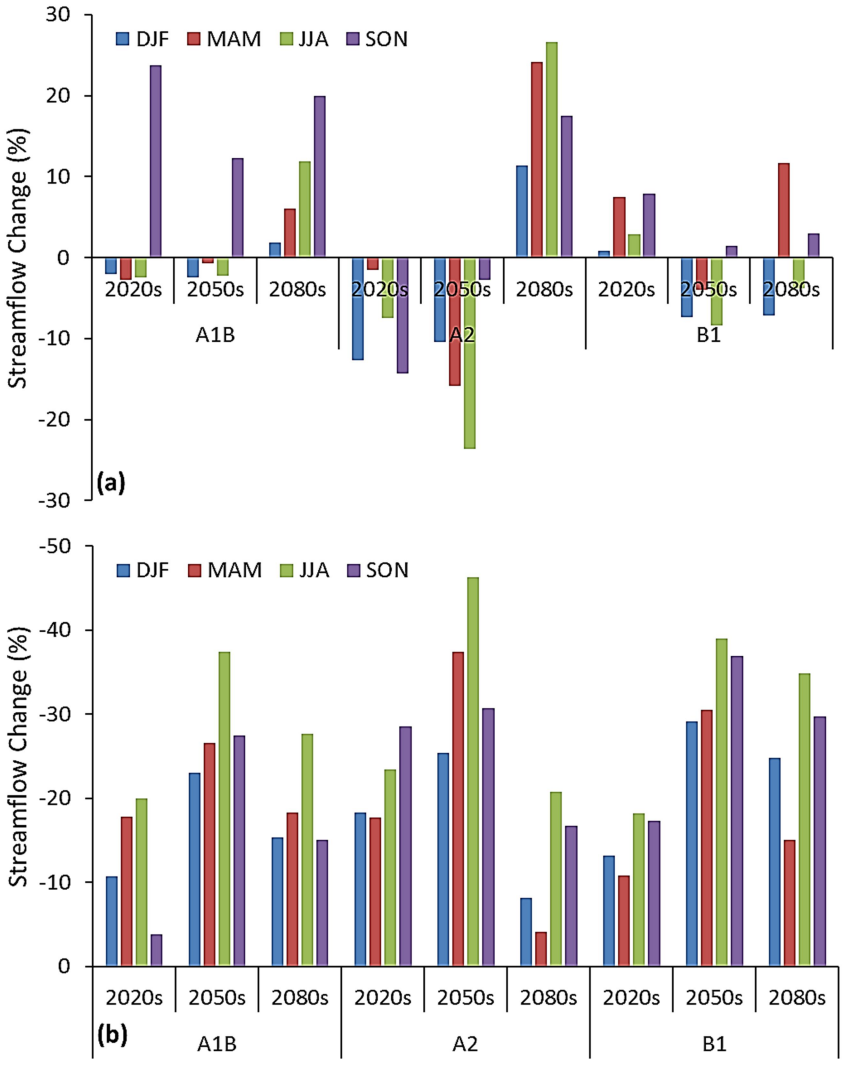

Figure 4.14: Projected seasonal streamflow change in (a) Kimilili and (b) Kuywa sub-watersheds

By the 2050s, the A1B scenario shows a similar pattern of streamflow change as the 2020s period but the magnitude of projected changes is bigger. Scenario A2 also show a similar pattern but greater magnitude of changes by the 2050s compared to 2020s, except that the flow is expected to increase in January, February and August (by 2.6% and 2.7% respectively) while decreases are expected by the 2020s. Scenario B1 in this

period projects that flow is likely to decrease in all months except March, September, October, and November.

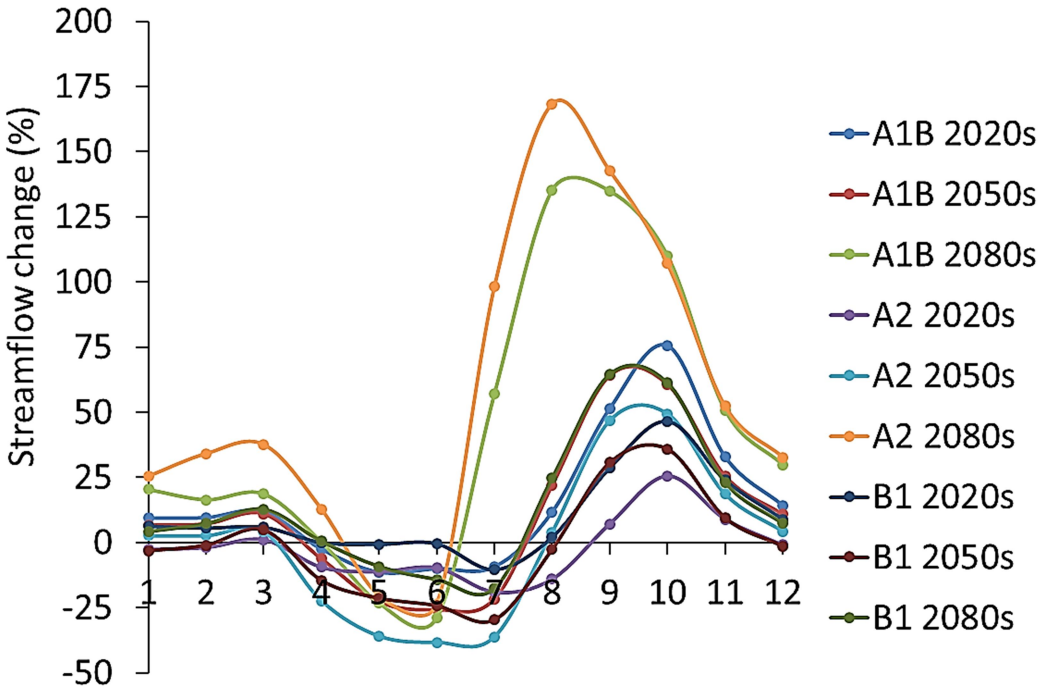

Figure 4.15: Projected monthly stream flow change in Koitobos sub-watershed by the 2020s, 2050s and 2080s under the A1B, A2 and B1 emission scenarios.

By the 2080s, for scenario A1B, a similar pattern of change as for the 2050s is expected, except that the flow in April and July is expected to increase by 0.2% and 57.1% respectively. An increase of up to 135.2% forAugust and a decrease of up to 28.8% in June are expected in this period. Under the A2 scenario, flow is expected to decrease in May (-23.2%) and June (-28.8%) while under the B2 scenario, a decrease is likely in May to July (-9.2%, -14.2% and -17.6%, respectively).

The pattern of stream flow change in Rongai, as shown in Figure 4.16, is similar to that of Koitobos sub-watershed. However the largest increases by the 2020s are expected in September (78.0%, A1B), October (19.7%, A2) and September (41.1%, B1). During this

period, the largest decrease are expected in June (13.9%, A1B), July (10.2%, A2) and July (4.8%, B1). By the 2050s, low flows are expected between April and July under all scenarios. During this period, very high flows are expected in August to November under all scenarios. By the 2080s, decreases are expected in May and June (under the A1B and A2 scenarios) and May to July (under the B1 scenario).

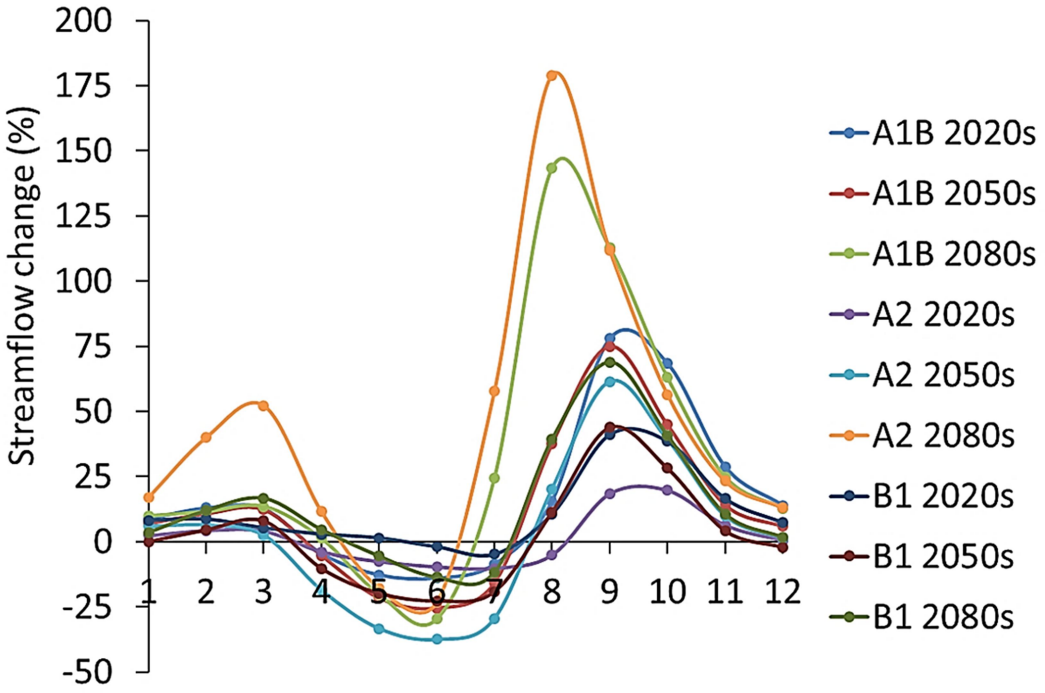

Figure 4.16: Projected monthly streamflow change in Rongai sub-watershed by the 2020s, 2050s and 2080s under the A1B, A2 and B1 emission scenarios.

The projected monthly flow changes in Kimilili sub-watershed are shown in Figure 4.17. By the 2020s, scenarios A1B and A2 show a likely decrease in all months except February, March, September, October and November (for the A1B scenario), and May (for the A2 scenario). Scenario B1 shows a likely increase in all months except August. The major increases are 32.8% (October, A1B), and 12.4% (May, B1). By the 2050s, scenario A1B projects a decrease in January, May, June, July and December. Scenarios

A2 and B1 project a decrease in all months except October (under A2) and March, September and October (under B1). By the 2080s, all scenarios project an increase in all months except January and June under the A1B scenario, June under A2 and September to January and June, July under B1 scenario.

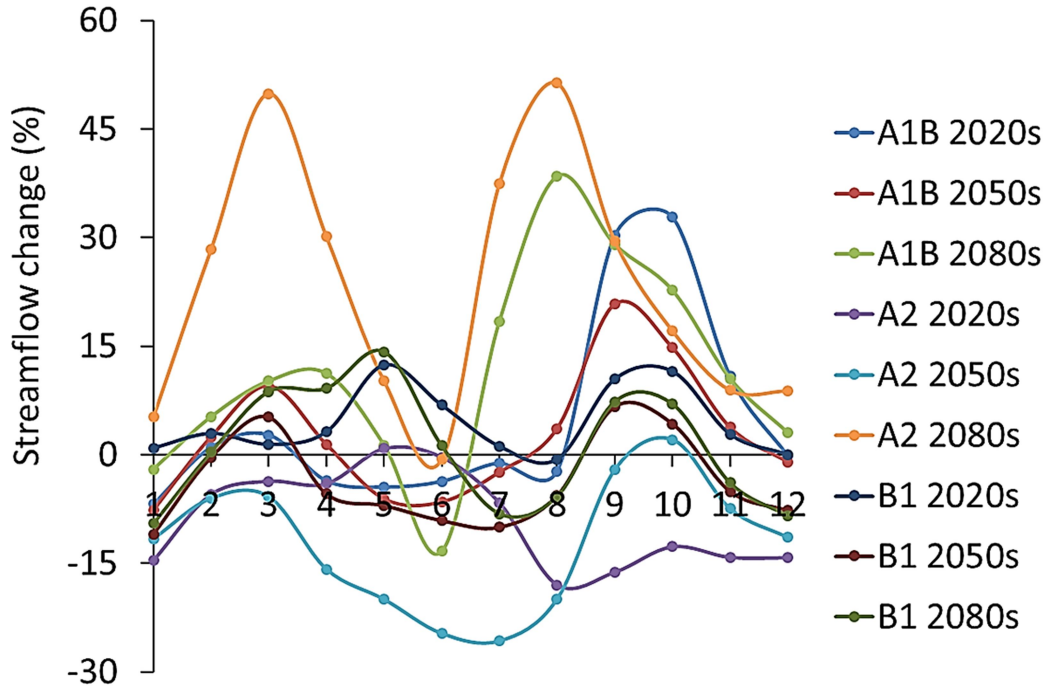

Figure 4.17: Projected monthly streamflow change in Kimilili sub-watershed by the 2020s, 2050s and 2080s under the A1B, A2 and B1 emission scenarios

As shown in Figure 4.18, all scenarios project flow decrease in Kuywa in all months across the three future periods except in October (A1B 2020s), and February and March (A2, 2080s). By the 2020s, major decreases are expected in August (-24.8%), September (-35.1%) and August (-26.5%) under the A1B, A2 and B1 scenarios respectively. By the 2050s, the largest decline is expected in August under all scenarios while by the 2080s, the largest decline is likely in June (-34.2% and -27.6% under the A1B and A2 scenarios respectively) and August (-36.1% under the B1 scenario).

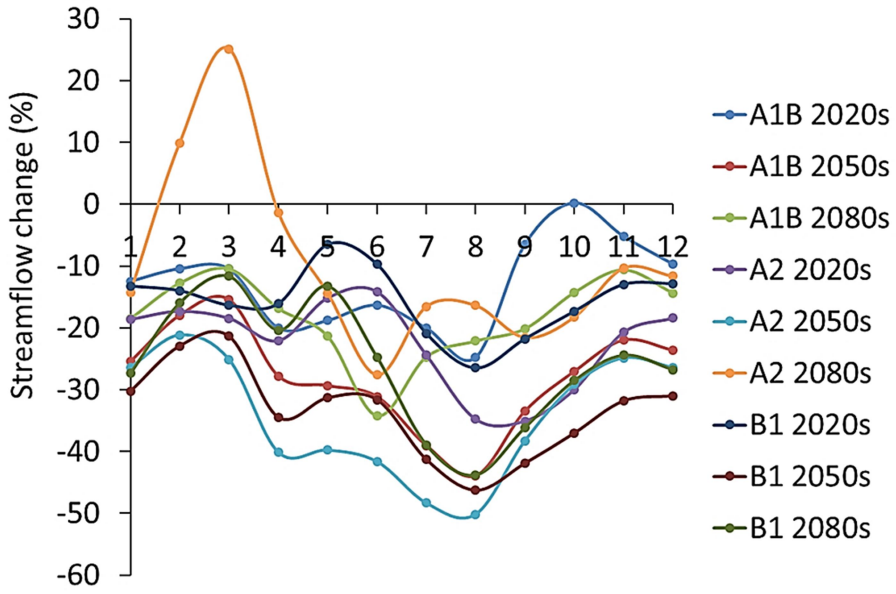

Figure 4.18: Projected monthly stream flow change in Kuywa sub-watersheds by the 2020s, 2050s and 2080s under the A1B, A2 and B1 emission scenarios

4.3.4 Analysis of extreme flows

The expected changes in precipitation and temperature will certainly affect high and low flows hence upsetting aquatic ecosystems as well as hydrologic regimes. Figure 4.19 shows the FDC for the annual maximum streamflow at the 1DD01A discharge station. Most of the scenarios show that annual maximum daily streamflow is likely to increase. The highest streamflow magnitudes shows likely increase. This implies that floods are likely to be a major concern in water management in and downstream of the area. Nevertheless, since the downscaling method did not account for the possible changes in precipitation frequency and magnitude, deterministic predictions of floods frequency and magnitude in the area can not be simulated. The exceedance probability of 50% during the baseline time period has a magnitude of about 170 m^3/s. During 2020s, the 50% exceedance probability shows magnitudes of approximately 175, 160, and 176 m^3/s for the A1B, A2 and B1 scenarios. By 2050s, this exceedance probability shows

magnitudes of approximately 164, 142, and 156 m^3/s for the A1B, A2 and B1 scenarios. The FDC for the annual manimum streamflow is shown in Figure 4.20. The lowest annual minimum streamflow magnitudes show a likely decrease.

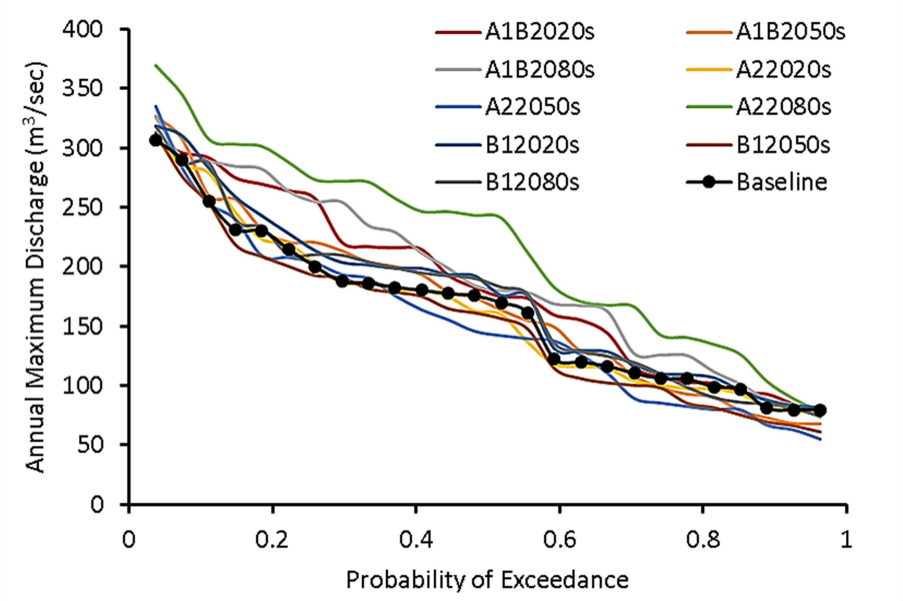

Figure 4.19: Exceedance probabilities of maximum annual streamflow for the baseline and future simulations

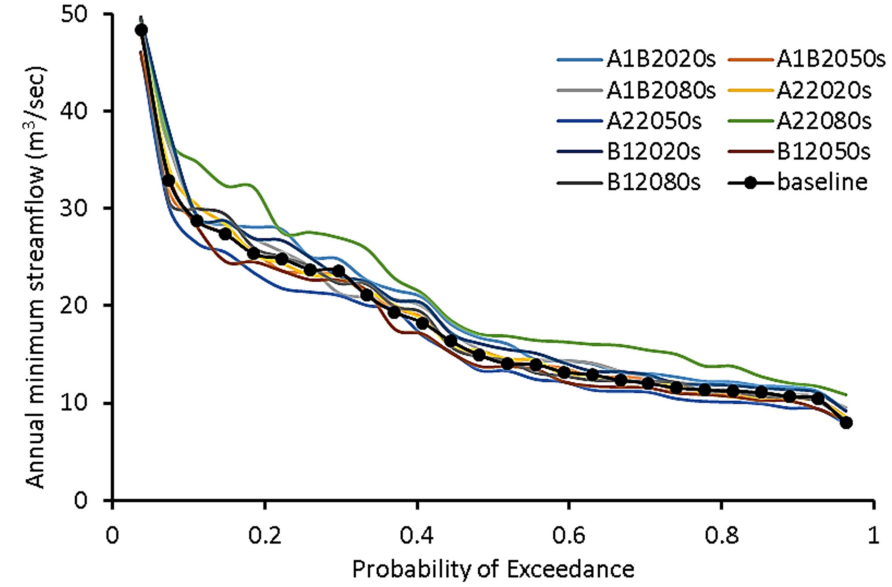

Figure 4.20: Exceedance probabilities of minimum annual streamflow for the baseline and future simulations

CHAPTER FIVE

CONCLUSIONS AND RECOMMENDATIONS

5.0 A brief on the chapter

This chapter comprises of a summary in section 5.1 while conclusions derived from the study are outlined in section 5.2. Section 5.3 comprises recommendations for future studies and climate change adaptation based on the results of the study.

5.1 Summary

The main goal of this study was to assess the hydrological impacts of climate change in Mt. Elgon sub-watersheds using the SWAT model. In order to achieve this goal, three specific objectives were formulated: to calibrate and validate Soil and Water Assessment Tool (SWAT) model for the watershed, to develop climate change scenarios for the sub-watersheds using delta change approach, and to assess the hydrological impacts of climate change scenarios in the sub-watersheds.

Prior to auto-calibration of SWAT model, manual calibration of the most sensitive parameters was undertaken by manually varying the parameter values to achieve better fit between observed and simulated flows. The SUFI2 algorithm included in the SWATCUP software was used for auto-calibration. The simulated flow corresponded well with the observed flow at daily and monthly time scales with R^2 and NSE values greater than 0.5 for both calibration (1986-1998) and validation (1973-1985) periods.

Rainfall and temperature scenarios reflecting the projected changes under the A1B, A2 and B1 emissions scenarios were generated for three different future periods namely the 2020s (2011–2040), the 2050s (2041-2070) and the 2080s (2071-2100). Climate change impact was assessed based on monthly relative shifts of rainfall and temperature

predicted by GCMs. The consideration of uncertainty in the climate change scenarios was based on the use of averaged climate projections of ten GCMs, three different emission scenarios, and three future periods. The projected changes indicated that annual rainfall is likely to change by 1.4-4.6% by the 2020s; 3.3-6.4% by the 2050s and 7.3-11.1% by the 2080s, depending on the emissions scenario. The projected annual mean warming varied from 0.6 to 1.5˚C by the 2020s, 1.3 to 2.8˚C by the 2050s, and from 1.5 to 4.4˚C by the 2080s depending on the emissions scenario.

The analysis of potential hydrological impacts of climate change focused on the changes in mean monthly, seasonal and annual streamflow. The projected streamflow changes varied strongly depending on emissions scenario and time period. In the Koitobos sub-watershed, all scenarios project an increase in mean annual streamflow except scenario A2 which projects a 1.4% decrease by the 2020s. The annual mean flow in the Rongai sub-watershed is expected to increase in the future under all emissions scenarios. The mean annual streamflow in Kimilili is projected to decrease by 9.9% and 12.3% under scenarios A2 for the 2020s and 2050s respectively and by 4% under scenario B1 for the 2050s. All scenarios project flow decrease in Kuywa in all months across the three future periods except in October (under A1B, 2020s scenario), and February and March (under A2, 2080s scenario).

The study demonstrates diverse monthly streamflow responses in Mt. Elgon sub-watersheds under climate change. The projected monthly streamflow changes vary throughout the year. The results indicate that August to December streamflow is likely to be highly altered in Koitobos, Rongai and Kimilili sub-watersheds while in Kuywa sub-watershed June to September flows are likely to change considerably due to climate change. Streamflow variability in the four sub-watersheds was different suggesting varied buffering capabilities in response to climate forcing in the four sub-watersheds.

5.2 Conclusions

Based on the results of the study, the following conclusions were derived.

i. The SWAT model can adequately simulate streamflow in the upper Nzoia Basin. A strong correlation between simulated and observed flows was noted both at daily and monthly time scales. R^2 values of 0.68 and 0.70 and NSE values of 0.58 and 0.70 were achieved for the calibration (1986-1998) and validation (1973-1985) periods, respectively. In addition, the SUFI2 sensitivity and uncertainty analysis algorithm in the SWATCUP software was identified as an efficient tool for auto-calibration and validation of the SWAT model.

ii. Large uncertainties in the precipitation, temperature and streamflow changes are expected due to varied projections of the different climatic models and emissions scenarios. Annual precipitation changes range from 1.4 to 4.6% by the 2020s; 3.3 to 6.4% by the 2050s and 7.3 to 11.1% by the 2080s, depending on the emissions scenario. Annual temperature changes range from 0.6 to 1.5˚C by the 2020s, 1.3 to 2.8˚C by the 2050s, and from 1.5 to 4.4˚C by the 2080s depending on the emissions scenario. At sub-basin level, the streamflow response to precipitation and temperature change was nonlinear. However, projected streamflow changes showed high dependence on the direction of projected precipitation changes, as concluded also by Shrestha et al. (2013) and Kingston et al. (2011).

iii. This study provided useful insights into the potential implications of climate change for water resource management in the study area. Generally, in the Koitobos, Rongai and Kimilili sub-watersheds, streamflow in August to March is likely to increase, while in the Kuywa sub-watershed, June to September flows are likely to decrease. The quantitative impacts of these changes will have significant implications for development and ecosystems in the sub-watersheds and downstream. Climate change would lead to alteration of streamflow in the Mt. Elgon sub-watersheds. However, this study does not make deterministic

predictions of the potential impacts but only projects possible hydrological responses under climate change scenarios.

iv. Despite the uncertainty in the projections, the study presents useful insights for long-term basin-wide strategic planning and implementation of development projects, disaster preparedness strategies and water resources management in this important basin. The projections show increases in streamflow, particularly between August and November, which ought to sound an alarm for reassessment of the design and sustainability of flood and landslide disaster management and mitigation measures in the area. The significance of a multi-model approach in climate change impacts assessment has also been highlighted. The use of multiple climate models to force different hydrological models would provide a detailed picture of expected uncertainties as well as possible hydrological responses and trends in the basin.

5.3 Recommendations

i. The calibration of the SWAT model was done based on data from a downstream station. It is therefore recommended that future studies in the sub-watersheds be based on calibration data collected from outlets of individual sub-watersheds. In addition, the calibrated model parameters were assumed to remain constant in future climatic conditions although previous authors have argued that change in climatic conditions is likely to alter model parameters (Merz et al., 2011). It is therefore recommended that parameter instability and non-uniqueness across time periods be considered in future studies. In addition, consideration of the spatial-temporal patterns in climatic data is recommended in case of generalization of results from this study to broader geographic and temporal contexts.

ii. The downscaling approach used in this study assumes that the GCM uncertainties in the baseline period remain similar across future periods. Since

this may not be the case, it is recommended that, in future research in the area, a more advanced downscaling method be used, as different downscaling methods may produce different future climate projections. In addition, consideration of a different set of GCMs is recommended as different climate models show different projections.

iii. The projected streamflow changes depicted a wide uncertainty. As a result, future studies in the sub-watersheds should consider advanced uncertainty analysis techniques. Due to the interplay nature in the different components of the water cycle, an assessment of the potential impacts on other hydrological components and sectors should also be considered.

iv. Further research in the livelihood strategies among the communities in the area is recommended to assess their contribution in the enhancing or mitigating adverse environmental change in the area. In addition, suitable adaptation strategies should be assessed to enhance the ability of the communities to cope with the potential climate change impacts in the Mt. Elgon area.

REFERENCES

Abbaspour, K. C., van Genuchten, M. T., Schulin, R., and Schläppi, E. (1997). A sequential uncertainty domain inverse procedure for estimating subsurface flow and transport parameters. *Water Resources Research*, *33*(8), 1879–1892. doi:10.1029/97WR01230

Abbaspour, K. C., Yang, J., Maximov, I., Siber, R., Bogner, K., Mieleitner, J., … Srinivasan, R. (2007). Modelling hydrology and water quality in the pre-alpine/alpine Thur watershed using SWAT. *Journal of Hydrology*, *333*(2-4), 413–430. doi:10.1016/j.jhydrol.2006.09.014

Adhikari, P., and Hong, Y. (2013). Will Nzoia basin in Kenya see water deficiency in coming decades as a result of climate change. *British Journal of Environment and Climate Change*, *3*(1), 67–85.

Akotsi, E. F. N. (2006). *Changes in Forest Cover in Kenya's Five "water Towers" 2003-2005*. Kenya Forests Working Group.

Akurut, M., Willems, P., and Niwagaba, C. (2014). Potential Impacts of Climate Change on Precipitation over Lake Victoria, East Africa, in the 21st Century. *Water*, *6*(9), 2634–2659. doi:10.3390/w6092634

Anand, S., Mankin, K. R., Mcvay, K. A., Janssen, K. A., Barnes, P. L., and Pierzynski, G. M. (2007). Calibration and validation of ADAPT and SWAT for field-scale runoff prediction. *J. American Water Resour. Assoc.*, *43*(4), 899–910.

Andreassian, V., Perrin, C., Michel, C., Usart-sanchez, I., and Lavabre, J. (2001). Impact of imperfect rainfall knowledge on the efficiency and the parameters of watershed models. *Journal of Hydrology*, *250*, 206–223.

Andréasson, J., Bergström, S., Carlsson, B., Graham, L. P., and Lindström, G. (2004). Hydrological Change – Climate Change Impact Simulations for Sweden. *AMBIO: A J. Hum. Environ.*, *33*(4), 228–234. doi:10.1579/0044-7447-33.4.228

Anyah, R. O., and Semazzi, F. H. M. (2007). Variability of East African rainfall based on multiyear RegCM3 simulations. *Int. J. Climatol.*, *27*, 357–371. doi:10.1002/joc

Arnell, N. W. (2011). Uncertainty in the relationship between climate forcing and hydrological response in UK catchments. *Hydrology and Earth System Sciences*, *15*(3), 897–912. doi:10.5194/hess-15-897-2011

Arnold, J., and Allen, P. M. (1996). Estimating hydrologic budgets for three Illinois watersheds. *Journal of Hydrology*, *176*, 57–77. doi:10.1016/0022-1694(95)02782-3

Arnold, J., Kiniry, J., Srinivasan, R., Williams, J., Haney, E. B., and Neitsch, S. L. (2011). *Soil and Water Assessment Tool Input/Output File Documentation Version 2009*. *Texas Water Resources Institute Technical Report No. 365*.

Arnold, J., Srinivasan, R., Muttiah, R. S., and Williams, J. (1998). Large-area hydrologic modeling and assessment: Part I. Model development. *J. American Water Resour. Assoc.*, *34*(1), 73–89.

Bae, D.-H., Jung, I.-W., and Lettenmaier, D. P. (2011). Hydrologic uncertainties in climate change from IPCC AR4 GCM simulations of the Chungju Basin, Korea. *Journal of Hydrology*, *401*(1-2), 90–105. doi:10.1016/j.jhydrol.2011.02.012

Bahremand, A., and De Smedt, F. (2008). Distributed Hydrological Modeling and Sensitivity Analysis in Torysa Watershed, Slovakia. *Water Resources Management*, *22*, 393–408. doi:10.1007/s11269-007-9168-x

Bastola, S., Murphy, C., and Sweeney, J. (2011). The role of hydrological modelling uncertainties in climate change impact assessments of Irish river catchments. *Advances in Water Resources*, *34*(5), 562–576. doi:10.1016/j.advwatres.2011.01.008

Bates, B. C., Kundzewicz, Z. W., Wu, S., and Palutikof, J.P., E. (2008). *Climate change and water. Technical Paper of the Intergovernmental Panel on Climate Change*. Geneva.

Bekiaris, I., Panaopoulos, in, and Mimikou, M. (2005). Application of the SWAT (soil and water assessment tool) model in the Ronnea Catchment of Sweden. *Global NEST Journal*, *7*(3), 252–257. Retrieved from https://www.gnest.org/Journal/Vol7_No3/paper_4_bekiaris_343.pdf

Benaman, J., and Shoemaker, C. a. (2005). An analysis of high-flow sediment event data for evaluating model performance. *Hydrological Processes*, *19*(3), 605–620. doi:10.1002/hyp.5608

Bergström, S., and Forsman, A. (1973). Development of a conceptual deterministic rainfall-runoff model. *Nordic Hydrology*, *4*, 147–170.

Beven, K., and Binley, A. (1992). The future of distributed models: Model calibration and uncertainty prediction. *Hydrological Processes*, *6*(3), 279–298. doi:10.1002/hyp.3360060305

Blasone, R. S., Madsen, H., and Rosbjerg, D. (2007). Parameter estimation in distributed hydrological modelling: comparison of global and local optimisation techniques. *Nordic Hydrology*, *38*(4-5), 451. doi:10.2166/nh.2007.024

Borah, D. K., and Bera, M. (2003). Watershed-scale hydrologic and nonpoint-source pollution models: review of mathematical bases. *Transactions of the ASAE*, *46*(6), 1553–1566. doi:Article

Bouraoui, F., Galbiati, L., and Bidoglio, G. (2002). Climate change impacts on nutrient loads in the Yorkshire Ouse catchment (UK). *Hydrology and Earth System Sciences*, *6*(2), 197–209. doi:10.5194/hess-6-197-2002

Boyer, C., Chaumont, D., Chartier, I., and Roy, A. G. (2010). Impact of climate change on the hydrology of St. Lawrence tributaries. *Journal of Hydrology*, *384*(1-2), 65–83. doi:10.1016/j.jhydrol.2010.01.011

Boyle, D. P., Gupta, H. V., Sorooshian, S., Koren, V., Zhang, Z., and Smith, M. (2001). Toward improved streamflow forecasts: value of semidistributed modeling. *Water Resources Research*, *37*(11), 2749–2759. doi:10.1029/2000WR000207

Braga, A. C. F. M., Silva, R. M. Da, Santos, C. A. G., Galvão, C. D. O., and Nobre, P. (2013). Downscaling of a global climate model for estimation of runoff, sediment yield and dam storage: A case study of Pirapama basin, Brazil. *Journal of Hydrology*, *498*, 46–58. doi:10.1016/j.jhydrol.2013.06.007

Brigode, P., Oudin, L., and Perrin, C. (2013). Hydrological model parameter instability: A source of additional uncertainty in estimating the hydrological impacts of climate change? *Journal of Hydrology*, *476*, 410–425. doi:10.1016/j.jhydrol.2012.11.012

Butts, M., Payne, J. T., Kristensen, M., and Madsen, H. (2004). An evaluation of the impact of model structure on hydrological modelling uncertainty for streamflow simulation. *Journal of Hydrology*, *298*(1-4), 242–266. doi:10.1016/j.jhydrol.2004.03.042

Chang, H., and Jung, I.-W. (2010). Spatial and temporal changes in runoff caused by climate change in a complex large river basin in Oregon. *Journal of Hydrology*, *388*, 186–207. doi:10.1016/j.jhydrol.2010.04.040

Chaponniere, A., Boulet, G., Chehbouni, A., Aresmouk, M., Chaponnière, A., Boulet, G., … Aresmouk, M. (2008). Understanding hydrological processes with scarce data in a mountain environment. *Hydrological Processes*, *22*(12), 1908–1921. doi:10.1002/hyp

Chen, H., Xu, C.-Y., and Guo, S. (2012). Comparison and evaluation of multiple GCMs, statistical downscaling and hydrological models in the study of climate change impacts on runoff. *Journal of Hydrology*, *434-435*, 36–45. doi:10.1016/j.jhydrol.2012.02.040

Chen, J., Brissette, F., Chaumont, D., and Braun, M. (2013). Performance and uncertainty evaluation of empirical downscaling methods in quantifying the climate change impacts on hydrology over two North American river basins. *Journal of Hydrology*, *479*, 200–214. doi:10.1016/j.jhydrol.2012.11.062

Chen, J., Brissette, F., and Leconte, R. (2011). Uncertainty of downscaling method in quantifying the impact of climate change on hydrology. *Journal of Hydrology*, *401*(3-4), 190–202. doi:10.1016/j.jhydrol.2011.02.020

Chien, H., Yeh, P. J.-F., and Knouft, J. H. (2013). Modeling the potential impacts of climate change on streamflow in agricultural watersheds of the Midwestern United States. *Journal of Hydrology*, *491*, 73–88. doi:10.1016/j.jhydrol.2013.03.026

Chiew, F., Kirono, D., Kent, D., Frost, A., Charles, S., Timbal, B., … Fu, G. (2010). Comparison of runoff modelled using rainfall from different downscaling methods

for historical and future climates. *Journal of Hydrology*, *387*(1-2), 10–23. doi:10.1016/j.jhydrol.2010.03.025

Christy, J. R., Norris, W. B., and McNider, R. T. (2009). Surface Temperature Variations in East Africa and Possible Causes. *Journal of Climate*, *22*(12), 3342–3356. doi:10.1175/2008JCLI2726.1

Clark, M., Slater, A. G., Rupp, D. E., Woods, R. A., Vrugt, J. A., Gupta, H. V., … Hay, L. E. (2008). Framework for Understanding Structural Errors (FUSE): A modular framework to diagnose differences between hydrological models. *Water Resources Management*, *44*(12), n/a–n/a. doi:10.1029/2007WR006735

Conway, D., Hanson, C. E., Doherty, R., and Persechino, A. (2007). GCM simulations of the Indian Ocean dipole influence on East African rainfall: Present and future. *Geophysical Research Letters*, *34*(3), 1–6. doi:10.1029/2006GL027597

Daniel, E. B., Camp, J. V, Leboeuf, E. J., Penrod, J. R., Dobbins, J. P., and Abkowitz, M. D. (2011). Watershed Modeling and its Applications : A State-of-the-Art Review. *The Open Hydrology Journal*, *5*, 26–50.

Dibike, B., and Coulibaly, P. (2005). Hydrologic impact of climate change in the Saguenay watershed: comparison of downscaling methods and hydrologic models. *Journal of Hydrology*, *307*(1-4), 145–163. doi:10.1016/j.jhydrol.2004.10.012

Duan, Q., Sorooshian, S., Gupta, H. V., and Gupta, V. (1992). Effective and efficient global optimization for conceptual rainfall-runoff models. *Water Resources Research*, *28*(4), 1015–1031. doi:10.1029/91WR02985

Efstratiadis, a., Nalbantis, I., Koukouvinos, A., Rozos, E., and Koutsoyiannis, D. (2008). HYDROGEIOS: a semi-distributed GIS-based hydrological model for modified

river basins. *Hydrology and Earth System Sciences*, *12*(4), 989–1006. doi:10.5194/hess-12-989-2008

Engeland, K., Gottschalk, L., and Tallaksen, L. (2001). Estimation of Regional Parameters in a Macro Scale Hydrological Model. *Nordic Hydrology*, *32*, 161–180.

Faramarzi, M., Yang, H., Schulin, R., and Abbaspour, K. C. (2010). Modeling wheat yield and crop water productivity in Iran: Implications of agricultural water management for wheat production. *Agricultural Water Management*, *97*(11), 1861–1875. doi:10.1016/j.agwat.2010.07.002

Ficklin, D., Luo, Y., Luedeling, E., and Zhang, M. (2009). Climate change sensitivity assessment of a highly agricultural watershed using SWAT. *Journal of Hydrology*, *374*(1-2), 16–29. doi:10.1016/j.jhydrol.2009.05.016

FitzHugh, T. W., and Mackay, D. S. (2000). Impacts of input parameter spatial aggregation on an agricultural nonpoint source pollution model. *Journal of Hydrology*, *236*(1-2), 35–53. doi:10.1016/S0022-1694(00)00276-6

Fowler, H., Blenkinsop, S., and Tebaldi, C. (2007). Linking climate change modelling to impacts studies : recent advances in downscaling techniques for hydrological. *International Journal of Climatology*, *27*, 1547–1578. doi:10.1002/joc

Franczyk, J., and Chang, H. (2009). The effects of climate change and urbanization on the runoff of the Rock Creek basin in the Portland metropolitan area , Oregon , USA. *Hydrological Processes*, *23*, 805–815. doi:10.1002/hyp

Galván, L., Olías, M., Izquierdo, T., Cerón, J. C., and Villarán, R. F. De. (2014). Rainfall estimation in SWAT : An alternative method to simulate orographic

precipitation. *Journal of Hydrology*, *509*, 257–265. doi:10.1016/j.jhydrol.2013.11.044

Gan, T. Y., and Biftu, G. F. (1996). Automatic Calibration of Conceptual Rainfall-Runoff Models: Optimization Algorithms, Catchment Conditions, and Model Structure. *Water Resources Research*, *32*(12), 3513–3524. doi:10.1029/95WR02195

Gan, T. Y., Dlamini, E. M., and Biftu, G. F. (1997). Effects of model complexity and structure, data quality, and objective functions on hydrologic modeling. *Journal of Hydrology*, *192*(1-4), 81–103. doi:10.1016/S0022-1694(96)03114-9

Gao, P., Geissen, V., Ritsema, C. J., Mu, X.-M., and Wang, F. (2013). Impact of climate change and anthropogenic activities on stream flow and sediment discharge in the Wei River basin, China. *Hydrology and Earth System Sciences*, *17*(3), 961–972. doi:10.5194/hess-17-961-2013

Gassman, P. W., Reyes, M. R., Green, C. H., and Arnold, J. (2007). The soil and water assessment tool: historical development, applications and future research directions. *Transactions of the ASABE*, *50*(4), 1211–1250.

Georgakakos, K. P., Seo, D.-J., Gupta, H., Schaake, J., and Butts, M. (2004). Towards the characterization of streamflow simulation uncertainty through multimodel ensembles. *Journal of Hydrology*, *298*(1-4), 222–241. doi:10.1016/j.jhydrol.2004.03.037

Geza, M., Poeter, E. P., and McCray, J. E. (2009). Quantifying predictive uncertainty for a mountain-watershed model. *Journal of Hydrology*, *376*(1-2), 170–181. doi:10.1016/j.jhydrol.2009.07.025

Ghosh, S., and Misra, C. (2010). Assessing Hydrological Impacts of Climate Change : Modeling Techniques and Challenges. *The Open Hydrology Journal*, *4*, 115–121.

Githui, F., Gitau, W., and Bauwens, W. (2009). Climate change impact on SWAT simulated streamflow in western Kenya. *International Journal of Climatology*, *29*, 1823–1834. doi:10.1002/joc

Hagg, W., Braun, L. N., Kuhn, M., and Nesgaard, T. I. (2007). Modelling of hydrological response to climate change in glacierized Central Asian catchments. *Journal of Hydrology*, *332*(1-2), 40–53. doi:10.1016/j.jhydrol.2006.06.021

Hargreaves, G., Hargreaves, G., and Riley, J. (1985). Agricultural Benefits for River Senegal Basin. *J. Irrig. Drain Eng.*, *111*(2), 113–124.

Hawkins, E., and Sutton, R. (2009). The Potential to Narrow Uncertainty in Regional Climate Predictions. *Bulletin of the American Meteorological Society*, *90*(8), 1095–1107. doi:10.1175/2009BAMS2607.1

Hewitson, B. C., and Crane, R. G. (1996). Climate downscaling : techniques and application. *Climate Research*, *7*, 85–95.

Hijmans, R. J., Cameron, S. E., Parra, J. L., Jones, P. G., and Jarvis, A. (2005). Very high resolution interpolated climate surfaces for global land areas. *Int. J. Climatol.*, *25*(15), 1965–1978. doi:10.1002/joc.1276

Hulme, M., Doherty, R., Ngara, T., New, M., and Lister, D. (2001). African climate change: 1900-2100. *Climate Research*, *17*, 145–168. doi:10.3354/cr017145

Im, E.-S., Jung, I.-W., Chang, H., Bae, D.-H., and Kwon, W.-T. (2009). Hydroclimatological response to dynamically downscaled climate change

simulations for Korean basins. *Climatic Change*, *100*(3-4), 485–508. doi:10.1007/s10584-009-9691-2

Immerzeel, W. W., van Beek, L. P. H., and Bierkens, M. F. P. (2010). Climate change will affect the Asian water towers. *Science*, *328*(5984), 1382–5. doi:10.1126/science.1183188

IPCC. (2001). Impact, Adaptation and vulnerability. In M. L. Parry, O. F. Canziani, J. P. Palutikof, P. J. van der Linden, & C. E. Hanson (Eds.), *Contribution of Working Group II to the Fourth Assessment Report of the Intergovernmental Panel on Climate Change, 2007*. Cambridge University Press, Cambridge, United Kingdom and New York, NY, USA. Retrieved from http://www.ipcc.ch/publications_and_data/ar4/wg2/en/contents.html

IPCC. (2007). Summary for Policymakers. In S. Solomon, D. Qin, M. Manning, Z. Chen, M. Marquis, K. B. Averyt, … H. L. Miller (Eds.), *Contribution of Working Group I to the Fourth Assessment Report of the Intergovernmental Panel on Climate Change, 2007*. Cambridge University Press, Cambridge, United Kingdom and New York, NY, USA. Retrieved from http://www.ipcc.ch/publications_and_data/ar4/wg1/en/contents.html

Jajarmizadeh, M., Harun, S., Ghahraman, B., and Mokhtari, M. (2012). Modeling daily stream flow using plant evapotranspiration method. *International Journal of Water Resources and Environmental Engineering*, *4*(6), 218–226. doi:10.5897/IJWREE12.019

Jajarmizadeh, M., Harun, S., and Salarpour, M. (2012). A Review on Theoretical Consideration and Types of Models in Hydrology. *Journal of Environmental Science and Technology*, *5*(5), 249–261.

Jeong, J., Kannan, N., Arnold, J., Glick, R., Gosselink, L., and Srinivasan, R. (2010). Development and Integration of Sub-hourly Rainfall-Runoff Modeling Capability Within a Watershed Model. *Water Resources Management*, *24*(15), 4505–4527. doi:10.1007/s11269-010-9670-4

Jha, M., Gassman, P. W., Secchi, S., Gu, R., and Arnold, J. (2004). Effect of watershed subdivision on swat flow, sediment, and nutrient predictions. *J. American Water Resour. Assoc.ournal Of The American Water Resources Association*, *40*(3), 811–825.

Jha, M. K. (2011). Evaluating Hydrologic Response of an Agricultural Watershed for Watershed Analysis. *Water*, *3*(4), 604–617. doi:10.3390/w3020604

Jiang, T., Chen, Y. D., Xu, C., Chen, X., Chen, X., and Singh, V. P. (2007). Comparison of hydrological impacts of climate change simulated by six hydrological models in the Dongjiang Basin, South China. *Journal of Hydrology*, *336*(3-4), 316–333. doi:10.1016/j.jhydrol.2007.01.010

Jung, I.-W., Moradkhani, H., and Chang, H. (2012). Uncertainty assessment of climate change impacts for hydrologically distinct river basins. *Journal of Hydrology*, *466-467*, 73–87. doi:10.1016/j.jhydrol.2012.08.002

Kavetski, D., Kuczera, G., and Franks, S. W. (2006). Bayesian analysis of input uncertainty in hydrological modeling: 1. Theory. *Water Resources Research*, *42*(3), W03407. doi:10.1029/2005WR004376

Kay, L., Davies, H., Bell, V., and Jones, R. (2009). Comparison of uncertainty sources for climate change impacts: flood frequency in England. *Climatic Change*, *92*(1-2), 41–63. doi:10.1007/s10584-008-9471-4

Kent, C., Chadwick, R., and Rowell, D. P. (2015). Understanding Uncertainties in Future Projections of Seasonal Tropical Precipitation. *Journal of Climate*, *28*, 4390–4413. doi:http://dx.doi.org/10.1175/JCLI-D-14-00613.1

Kienzle, S. W., Nemeth, M. W., Byrne, J. M., and MacDonald, R. J. (2012). Simulating the hydrological impacts of climate change in the upper North Saskatchewan River basin, Alberta, Canada. *Journal of Hydrology*, *412-413*, 76–89. doi:10.1016/j.jhydrol.2011.01.058

Kilsby, C. G., Tellier, S. S., Fowler, H. J., and Howels, T. R. (2007). Hydrological impacts of climate change on the Tejo and Guadiana Rivers. *Hydrology and Earth System Sciences*, *11*(3), 1175–1189. doi:10.5194/hess-11-1175-2007

King, K. W., Arnold, J., and Bingner, R. L. (1999). Comparison of Green-Ampt and Curve number methods on Goodwin Creek Watershed using SWAT. *American Society of Agricultural Engineers*, *42*(1978), 919–925.

Kingston, D. G., and Taylor, R. G. (2010). Sources of uncertainty in climate change impacts on river discharge and groundwater in a headwater catchment of the Upper Nile Basin, Uganda. *Hydrology and Earth System Sciences*, *14*(7), 1297–1308. doi:10.5194/hess-14-1297-2010

Kingston, D. G., Thompson, J. R., and Kite, G. (2011). Uncertainty in climate change projections of discharge for the Mekong River Basin. *Hydrology and Earth System Sciences*, *15*(5), 1459–1471. doi:10.5194/hess-15-1459-2011

Kitanidis, P. K., and Bras, R. L. (1980). Real-time forecasting with a conceptual hydrologic model: 2. Applications and results. *Water Resources Research*, *16*(6), 1034–1044. doi:10.1029/WR016i006p01034

Kite, G. W., Dalton, A., and Dion, K. (1994). Simulation of streamflow in a macroscale watershed using general circulation model data. *Water Resources Research*, *30*(5), 1547–1559. doi:10.1029/94WR00231

Krause, P., Boyle, D. P., and F, B. (2005). Comparison of different efficiency criteria for hydrological model assessment. *Advances in Geosciences*, *5*, 89–97.

Kuczera, G., Kavetski, D., Franks, S., and Thyer, M. (2006). Towards a Bayesian total error analysis of conceptual rainfall-runoff models: Characterising model error using storm-dependent parameters. *Journal of Hydrology*, *331*(1-2), 161–177. doi:10.1016/j.jhydrol.2006.05.010

Labat, D., Goddéris, Y., Probst, J. L., and Guyot, J. L. (2004). Evidence for global runoff increase related to climate warming. *Advances in Water Resources*, *27*(6), 631–642. doi:10.1016/j.advwatres.2004.02.020

Larose, M., Heathman, G. C., Norton, L. D., and Engel, B. (2003). Hydrologic and atrazine simulation of the Cedar Creek Watershed using the SWAT model. *Journal of environmental quality*, *36*(2), 521–531. doi:10.2134/jeq2006.0154

Lastoria, B. (2008). *Hydrological processes on the land surface: A survey of modelling approaches*. *FORALPS Technical Report, 9*. Trento, Italy.

Lee, A., Cho, S., Kang, D. K., and Kim, S. (2013). Analysis of the effect of climate change on the Nakdong river stream flow using indicators of hydrological alteration. *J. Hydro-environment Res.*, 1–14. doi:10.1016/j.jher.2013.09.003

Liang, X., and Guo, J. (2003). Intercomparison of land-surface parameterization schemes: sensitivity of surface energy and water fluxes to model parameters. *Journal of Hydrology*, *279*, 182–209. doi:10.1016/S0022-1694(03)00168-9

Lindström, G., Johansson, B., Persson, M., Gardelin, M., and Bergström, S. (1997). Development and test of the distributed HBV-96 hydrological model. *Journal of Hydrology*, *201*, 272–288.

Liu, Y. B., Batelaan, O., Smedt, F. De, Poórová, J., and Velcická, L. (2005). Automated calibration applied to a GIS-based flood simulation model using PEST. In V. Alphen, V. Beek, & Taal (Eds.), *Floods, from Defence to Management* (pp. 317–326). London: Taylor & Francis Group.

Loaiciga, H. A., Valdes, J. B., Vogel, R., Garvey, J., and Schwarz, H. (1996). Global warming and the hydrologic cycle. *Journal of Hydrology*, *174*(1), 83–127. Retrieved from http://www.sciencedirect.com/science/article/pii/002216949502753X

Lu, E., Takle, E. S., and Manoj, J. (2010). The Relationships between Climatic and Hydrological Changes in the Upper Mississippi River Basin: A SWAT and Multi-GCM Study. *Journal of Hydrometeorology*, *11*(2), 437–451. doi:10.1175/2009JHM1150.1

Lubini, A., and Adamowski, J. (2013). Assessing the Potential Impacts of Four Climate Change Scenarios on the Discharge of the Simiyu River, Tanzania Using the SWAT Model. *International Journal of Water Sciences*, *2*, 1. doi:10.5772/56453

Luo, Y., Ficklin, D. L., Liu, X., and Zhang, M. (2013). Assessment of climate change impacts on hydrology and water quality with a watershed modeling approach. *Science of the Total Environment*, *450-451*, 72–82. doi:10.1016/j.scitotenv.2013.02.004

Lyon, B. (2014). Seasonal Drought in greater horn of Africa and its Recent Increase During the March-May Long Rains. *Journal of Climate*, *27*, 7953–7975. doi:10.1175/JCLI-D-13-00459.1

Lyon, B., Barnston, A., and DeWitt, D. G. (2013). Tropical Pacific forcing of a 1998-99 climate shift: Observational analysis and climate model results for the boreal spring season. *Climate Dynamics*, 1–17. doi:10.1007/s00382-013-1891-9

Lyon, B., and DeWitt, D. G. (2012). A recent and abrupt decline in the East African long rains. *Geophysical Research Letters*, *39*(2).

Madsen, H., Wilson, G., and Ammentorp, H. C. (2002). Comparison of different automated strategies for calibration of rainfall-runoff models. *Journal of Hydrology*, *261*, 48–59. doi:10.1016/S0022-1694(01)00619-9

Mango, L. M., Melesse, a. M., McClain, M. E., Gann, D., and Setegn, S. G. (2011). Land use and climate change impacts on the hydrology of the upper Mara River Basin, Kenya: results of a modeling study to support better resource management. *Hydrology and Earth System Sciences*, *15*(7), 2245–2258. doi:10.5194/hess-15-2245-2011

Marshall, L., Nott, D., and Sharma, A. (2004). A comparative study of Markov chain Monte Carlo methods for conceptual rainfall-runoff modeling. *Water Resources Research*, *40*(2). doi:10.1029/2003WR002378

Matalas, N. (1967). Mathematical assessment of synthetic hydrology. *Water Resources Research*, *3*(4), 937–945.

Matondo, J. I., Peter, G., and Msibi, K. M. (2004). Evaluation of the impact of climate change on hydrology and water resources in Swaziland: Part II. *Physics and Chemistry of the Earth*, *29*(15-18), 1193–1202. doi:10.1016/j.pce.2004.09.035

Maurer, E. P., and Hidalgo, H. G. (2008). Utility of daily vs . monthly large-scale climate data : an intercomparison of two statistical downscaling methods. *Hydrology and Earth System Sciences*, *12*, 551–563.

McHugh, M. J. (2005). Multi-model trends in East African rainfall associated with increased CO2. *Geophysical Research Letters*, *32*(1), 1–4. doi:10.1029/2004GL021632

Melching, C. S. (1992). An improved first-order reliability approach for assessing uncertainties in hydrologic modeling. *Journal of Hydrology*, *132*, 157–177. Retrieved from http://www.sciencedirect.com/science/article/pii/002216949290177W

Mengistu, D. T., and Sorteberg, a. (2012). Sensitivity of SWAT simulated streamflow to climatic changes within the Eastern Nile River basin. *Hydrology and Earth System Sciences*, *16*(2), 391–407. doi:10.5194/hess-16-391-2012

Merritt, W. S., Alila, Y., Barton, M., Taylor, B., Cohen, S., and Neilsen, D. (2006). Hydrologic response to scenarios of climate change in sub watersheds of the Okanagan basin, British Columbia. *Journal of Hydrology*, *326*(1-4), 79–108. doi:10.1016/j.jhydrol.2005.10.025

Merz, R., Parajka, J., and Blöschl, G. (2011). Time stability of catchment model parameters: Implications for climate impact analyses. *Water Resources Research*, *47*(2). doi:10.1029/2010WR009505

Minville, M., Brissette, F., and Leconte, R. (2008). Uncertainty of the impact of climate change on the hydrology of a nordic watershed. *Journal of Hydrology*, *358*(1-2), 70–83. doi:10.1016/j.jhydrol.2008.05.033

Montanari, A., and Brath, A. (2004). A stochastic approach for assessing the uncertainty of rainfall-runoff simulations. *Water Resources Research*, *40*(1), n/a–n/a. doi:10.1029/2003WR002540

Moradkhani, H., Hsu, K.-L., Gupta, H., and Sorooshian, S. (2005). Uncertainty assessment of hydrologic model states and parameters: Sequential data assimilation using the particle filter. *Water Resources Research*, *41*(5). doi:10.1029/2004WR003604

Moriasi, D. N., Arnold, J., Liew, M. W. Van, Bingner, R. L., Harmel, R. D., and Veith, T. L. (2007). Model Evaluation Guidelines for Systematic Quantification of Accuraccy in Watershed Simulations. *Transactions of the ASABE*, *50*(3), 885–900.

Muleta, M. K., and Nicklow, J. W. (2005). Sensitivity and uncertainty analysis coupled with automatic calibration for a distributed watershed model. *Journal of Hydrology*, *306*(1-4), 127–145. doi:10.1016/j.jhydrol.2004.09.005

Murphy, J. (1998). An Evaluation of statistical and dynamical techniques for downscaling local climate. *Journal of Climate*, *12*, 2256–2284.

Najafi, M., Moradkhani, H., and Jung, I. (2011). Assessing the uncertainties of hydrologic model selection in climate change impact studies. *Hydrological Processes*, *25*(18), 2814–2826. doi:10.1002/hyp.8043

Nash, J. E., and Sutcliffe, J. V. (1970). River flow forecasting through conceptual models part I — A discussion of principles. *Journal of Hydrology*, *10*(3), 282–290.

Neitsch, S. L., Arnold, J., Kiniry, J. R., and Williams, J. (2011). *Soil and Water Assessment Tool Theoretical Documentation Version 2009*. *Texas Water Resources Institute Technical Report No. 406*.

Nicks, A. D. (1974). Stochastic generation of the occurrence, pattern, and location of maximum amount of daily rainfall. In *Proceedings Symposium on Statistical Hydrology, United States Department of Agriculture, Misc. Publication No. 1275, Tucson, AZ 31 August-2 September 1971*.

Nie, W., Yuan, Y., Kepner, W., Nash, M. S., Jackson, M., and Erickson, C. (2011). Assessing impacts of Landuse and Landcover changes on hydrology for the upper San Pedro watershed. *Journal of Hydrology*, *407*(1-4), 105–114. doi:10.1016/j.jhydrol.2011.07.012

Nunes, P., and Pacheco, N. R. (2008). Vulnerability of water resources , vegetation productivity and soil erosion to climate change in Mediterranean watersheds. *Hydrological Processes*, *22*, 3115–3134. doi:10.1002/hyp

Ogiramoi, P. (2011). *Climate change impacts on hydrological extremes and water resources in Lake Victoria catchments, upper Nile basin*. Katholieke Universiteit Leuven.

Orellana, B., Pechlivanidis, I. G., Mcintyre, N., Wheater, H. S., and Wagener, T. (2008). A Toolbox for the Identification of Parsimonious Semi-Distributed Rainfall-Runoff Models : Application to the Upper Lee Catchment. In *Integrating Sciences and Information Technology for Environmental Assessment and Decision Making* (pp. 670–677).

Pechlivanidis, I. G., Jackson, B. M., Mcintyre, N. R., and Wheater, H. S. (2011). Catchment scale hydrological modelling : A review of model types , calibration

approaches and uncertainty analysis methods in the context of recent developments in technology and applications. *Glob. NEST J.*, *13*(3), 193–214.

Petursson, J. G., Pal, V., and Kaboggoza, J. (2006). *Transboundary biodiversity management challenges; the case of Mt. Elgon, Uganda and Kenya*.

Prudhomme, C., and Davies, H. (2009). Assessing uncertainties in climate change impact analyses on the river flow regimes in the UK. Part 2: future climate. *Climatic Change*, *93*(1-2), 197–222. doi:10.1007/s10584-008-9461-6

Rahman, M., Bolisetti, T., and Balachandar, R. (2012). Hydrologic modelling to assess the climate change impacts in a Southern Ontario watershed. *Canadian Journal of Civil Engineering*, *39*, 91–103. doi:10.1139/L11-112

Roosmalen, L. van. (2009). *The effects of future climate change on groundwater and stream discharge in Denmark*. Copenhagen.

Rosbjerg, D., and Madsen, H. (2006). 10 Concepts of Hydrologic Modeling. *Encyclopedia of Hydrological Sciences*. doi:10.1002/0470848944

Saltelli, A., Tarantola, S., and Chan, K. P.-S. (1999). A Quantitative Model-Independent Method for Global Sensitivity Analysis of Model Output. *Technometrics*, *41*(1), 39–56.

Schreck, C. J., and Semazzi, F. H. M. (2004). Variability of the recent climate of eastern Africa. *International Journal of Climatology*, *24*(6), 681–701. doi:10.1002/joc.1019

Setegn, S. G., Srinivasan, R., and Dargahi, B. (2008). Hydrological Modelling in the Lake Tana Basin, Ethiopia Using SWAT Model. *The Open Hydrology Journal*, *2008*(2), 49–62.

Sharpley, A. N., and Williams, J. (1990). *Erosion/Productivity Impact Calculator, 1. Model Documentation, USDA–ARS Technical Bulletin 1768*.

Shongwe, M. E., van Oldenborgh, G. J., van den Hurk, B., and van Aalst, M. (2011). Projected Changes in Mean and Extreme Precipitation in Africa under Global Warming. Part II: East Africa. *Journal of Climate*, *24*(14), 3718–3733. doi:10.1175/2010JCLI2883.1

Shrestha, B., Babel, M. S., Maskey, S., van Griensven, A., Uhlenbrook, S., Green, A., and Akkharath, I. (2013). Impact of climate change on sediment yield in the Mekong River basin: a case study of the Nam Ou basin, Lao PDR. *Hydrology and Earth System Sciences*, *17*, 1–20. doi:10.5194/hess-17-1-2013

Sieber, A., and Uhlenbrook, S. (2005). Sensitivity analyses of a distributed catchment model to verify the model structure. *Journal of Hydrology*, *310*, 216–235. doi:10.1016/j.jhydrol.2005.01.004

Singh, J., Knapp, H. V., Arnold, J. G., and Demissie, M. (2005). Hydrological modeling of the Iroquois River watershed using HSPF and SWAT. *Journal of the American Water Resources Association*, *41*(2), 343–360. doi:10.1111/j.1752-1688.2005.tb03740.x

Singh, V. P., and Frevert, D. K. (2006). *Watershed Models*. Boca Raton, FL: CRC Press.

Singh, V. P., and Woolhiser, D. A. (2002). Mathematical Modeling of Watershed Hydrology. *Journal of Hydrologic Engineering*, *7*(4), 270–292.

Solomatine, D. P., and Shrestha, D. L. (2009). A novel method to estimate model uncertainty using machine learning techniques. *Water Resources Research*, *45*(12), W00B11. doi:10.1029/2008WR006839

Strauch, M., Bernhofer, C., Koide, S., Volk, M., Lorz, C., and Makeschin, F. (2012). Using precipitation data ensemble for uncertainty analysis in SWAT streamflow simulation. *Journal of Hydrology*, *414-415*, 413–424. doi:10.1016/j.jhydrol.2011.11.014

Tang, Y., Reed, P., Wagener, T., and VanWerkhoven, K. (2007). Comparing sensitivity analysis methods to advance lumped watershed model identification and evaluation. *Hydrology and Earth System Sciences*, *11*, 793–817. doi:10.5194/hess-11-793-2007

Taye, M. T., Ntegeka, V., Ogiramoi, N. P., and Willems, P. (2010). Assessment of climate change impact on hydrological extremes in two source regions of the Nile River Basin. *Hydrology and Earth System Sciences*, *7*(4), 209–222. doi:10.5194/hessd-7-5441-2010

Tebaldi, C., Smith, R., Nychka, D., and Linda, M. (2005). Quantifying Uncertainty in Projections of Regional Climate Change : A Bayesian Approach to the Analysis of Multimodel Ensembles. *Journal of Climate*, *18*, 1524–1540.

Teng, J., Vaze, J., Chiew, F. H. S., Wang, B., and Perraud, J.-M. (2012). Estimating the Relative Uncertainties Sourced from GCMs and Hydrological Models in Modeling Climate Change Impact on Runoff. *Journal of Hydrometeorology*, *13*(2009), 122–139. doi:10.1175/JHM-D-11-058.1

Thiemann, M., Trosset, M., Gupta, H., and Sorooshian, S. (2001). Bayesian recursive parameter estimation for hydrologic models. *Water Resources Research*, *37*(10), 2521–2535. doi:10.1029/2000WR900405

Thyer, M., Kuczera, G., and Bates, B. C. (1999). Probabilistic optimization for conceptual rainfall-runoff models: A comparison of the shuffled complex evolution

and simulated annealing algorithms. *Water Resources Research*, *35*(3), 767–773. doi:10.1029/1998WR900058

Tian, Y., Booij, M. J., and Xu, Y. (2014). Uncertainty in high and low flows due to model structure and parameter errors. *Stochastic Environmental Research and Risk Assessment*, *28*(2), 319–332. doi:10.1007/s00477-013-0751-9

Tian, Y., Xu, Y., Booij, M. J., and Wang, G. (2015). Uncertainty in Future High Flows in Qiantang River Basin, China. *Journal of Hydrometeorology*, *16*, 363–380. doi:http://dx.doi.org/10.1175/JHM-D-13-0136.1

Tripathi, M. P., Raghuwanshi, N. S., and Rao, G. P. (2006). Effect of watershed subdivision on simulation of water balance components. *Hydrological Processes*, *20*(5), 1137–1156. doi:10.1002/hyp.5927

Uhlenbrook, S., Seibert, J., Leibundgut, C., and Rodhe, A. (1999). Prediction uncertainty of conceptual rainfall-runoff models caused by problems in identifying model parameters and structure. *Hydrological Sciences Journal*, *44*(5), 779–797. doi:10.1080/02626669909492273

US-Soil Conservation Service Engineering Department. (1972). Section 4: Hydrology. In *National Engineering Handbook*.

Van Griensven, A., Meixner, T., Grunwald, S., Bishop, T., Diluzio, M., and Srinivasan, R. (2006). A global sensitivity analysis tool for the parameters of multi-variable catchment models. *Journal of Hydrology*, *324*(1-4), 10–23. doi:10.1016/j.jhydrol.2005.09.008

Varis, O., Kajander, T., and A, R. L. (2004). Climate and water : From climate models to water resources management and vice versa Water. *Climate Change*, *66*, 321–344.

Viner, D. (2002). A qualitative assessment of the sources of uncertainty in climate change impacts assessment studies. In M. Beniston (Ed.), *Climatic Change: implications for the hydrological cycle and for water management* (Vol. 10, pp. 139–149). Dordrecht: Springer Netherlands. doi:10.1007/0-306-47983-4

Viviroli, D., Dürr, H. H., Messerli, B., Meybeck, M., and Weingartner, R. (2007). Mountains of the world, water towers for humanity: Typology, mapping, and global significance. *Water Resources Research*, *43*(7), n/a–n/a. doi:10.1029/2006WR005653

Vrugt, J. A., Gupta, H. V., Bouten, W., and Sorooshian, S. (2003). A Shuffled Complex Evolution Metropolis algorithm for optimization and uncertainty assessment of hydrologic model parameters. *Water Resources Research*, *39*(8). doi:10.1029/2002WR001642

Vrugt, J. A., and Robinson, B. A. (2007). Treatment of uncertainty using ensemble methods: Comparison of sequential data assimilation and Bayesian model averaging. *Water Resources Research*, *43*(1), 1–15. doi:10.1029/2005WR004838

Vrugt, J. A., ter Braak, C. J. F., Clark, M., Hyman, J. M., and Robinson, B. A. (2008). Treatment of input uncertainty in hydrologic modeling: Doing hydrology backward with Markov chain Monte Carlo simulation. *Water Resources Research*, *44*(12). doi:10.1029/2007WR006720

Wagener, T., Boyle, D. P., Lees, M. J., Wheater, H. S., and Hoshin, V. (2001). A framework for development and application of hydrological models. *Hydrology and Earth System Sciences*, *5*(1), 13–26.

Wetterhall, F., Halldin, S., and Xu, C.-Y. (2007). Seasonality properties of four statistical-downscaling methods in central Sweden. *Theoretical and Applied Climatology*, *87*(1-4), 123–137. doi:10.1007/s00704-005-0223-3

Wilby, R. L., and Harris, I. (2006). A framework for assessing uncertainties in climate change impacts: Low-flow scenarios for the River Thames, UK. *Water Resources Research*, *42*(2). doi:10.1029/2005WR004065

Williams, A., and Funk, C. (2011). A westward extension of the warm pool leads to a west-ward extension of the Walker circulation, drying eastern Africa. *Climate Dynamics*, *37*(11-12), 2417–2435.

Williams, J. (1969). Flood routing with variable travel time or variable storage coefficients. *Transactions of the ASABE*, *12*(1), 100–103.

Williams, J. (1995). Charpter 25: The EPIC Model. In *Computer Models of Watershed Hydrology* (pp. 909– 1000).

Willmott, C. J., Ackleson, S. G., Davis, R. E., Feddema, J. J., Klink, K. M., Legates, D. R., … Rowe, C. M. (1985). Statistics for the evaluation and comparison of models. *Journal of Geophysical Research*, *90*(C5), 8995–9005. doi:10.1029/JC090iC05p08995

Wilson, C. O., and Weng, Q. (2011). Simulating the impacts of future land use and climate changes on surface water quality in the Des Plaines River watershed, Chicago Metropolitan Statistical Area, Illinois. *Science of the Total Environment*, *409*(20), 4387–4405. doi:10.1016/j.scitotenv.2011.07.001

Woldemeskel, F. M., Sharma, a., Sivakumar, B., and Mehrotra, R. (2012). An error estimation method for precipitation and temperature projections for future climates.

Journal of Geophysical Research: Atmospheres, *117*(22), 1–13. doi:10.1029/2012JD018062

Xu, C. (1999). From GCMs to river flow : a review of downscaling methods and hydrologic modelling approaches. *Prog. Phys. Geo.*, *23*(2), 229–249.

Xu, C. (2000). Modelling the Effects of Climate Change on Water Resources in Central Sweden. *Water Resources Management*, *14*, 177–189.

Xu, H., Taylor, R. G., and Xu, Y. (2011). Quantifying uncertainty in the impacts of climate change on river discharge in sub-catchments of the Yangtze and Yellow River Basins, China. *Hydrology and Earth System Sciences*, *15*(1), 333–344. doi:10.5194/hess-15-333-2011

Xu, Y., Zhang, X., Ran, Q., and Tian, Y. (2013). Impact of climate change on hydrology of upper reaches of Qiantang River Basin, East China. *Journal of Hydrology*, *483*, 51–60. doi:10.1016/j.jhydrol.2013.01.004

Yang, J., Reichert, P., Abbaspour, K. C., Xia, J., and Yang, H. (2008). Comparing uncertainty analysis techniques for a SWAT application to the Chaohe Basin in China. *Journal of Hydrology*, *358*(1-2), 1–23. doi:10.1016/j.jhydrol.2008.05.012

Yang, W., Seager, R., Cane, M. A., and Lyon, B. (2014). The East African Long Rains in Observations and Models. *Journal of Climate*, *27*, 7185–7202. doi:http://dx.doi.org/10.1175/JCLI-D-13-00447.1

Yapo, P. O., Gupta, H. V., and Sorooshian, S. (1996). Automatic calibration of conceptual rainfall-runoff models: sensitivity to calibration data. *Journal of Hydrology*, *181*, 23–48.

Zhang, X., Liu, Y., Fang, Y., Liu, B., and Xia, D. (2012). Modeling and assessing hydrologic processes for historical and potential land-cover change in the Duoyingping watershed, southwest China. *Physics and Chemistry of the Earth, Parts A/B/C*, *53-54*, 19–29. doi:10.1016/j.pce.2011.08.021

APPENDICES

Appendix 1: Projected changes (%) in (i) MAM (long rains), and (ii) OND (short rains) for East Africa region during the 2051–2200: (a) mean precipitation rates, (b) 10-year driest events, and (c) 10-year wettest events in each climatic zone. In the three plotted values, the middle number indicates the projected average change while the number above (below) the mean change shows the distance to the upper (lower) critical value at 5% level of significance. The grey shaded values are significant at 5% level while those marked with two asterices are significant at 1%. The regions marked by XX could not be adequately resolved by the lowest-resolution AR4 CGCMs hence were omitted in the analyses (Source: Shongwe et al., 2011).

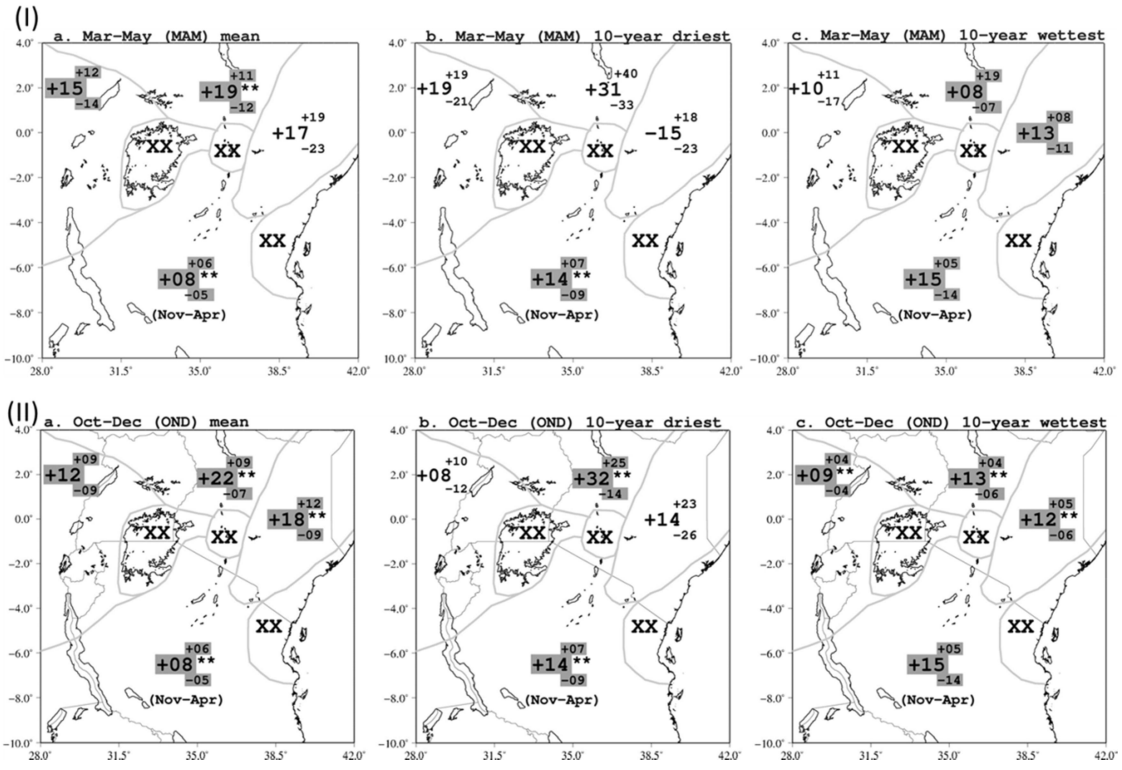

Appendix 1: Projected seasonal precipitation changes (%) in East Africa

Appendix 2: Precipitation anomalies (standard deviation) for October- December (OND) rainfall season (a-c) in east Africa regions, during austral summer–autumn (November–April; NDJFMA) for much of Tanzania and MAM precipitation (e-f) based on the 1961-1990 base period. The black dotted lines indicate the CRU data precipitation, the darker and lighter shaded areas show 50% (q0.25, q075) and 95% (q0.025, q0.975) of the distribution respectively while the white lines show the ensemble mean (Source: Shongwe et al., 2011).

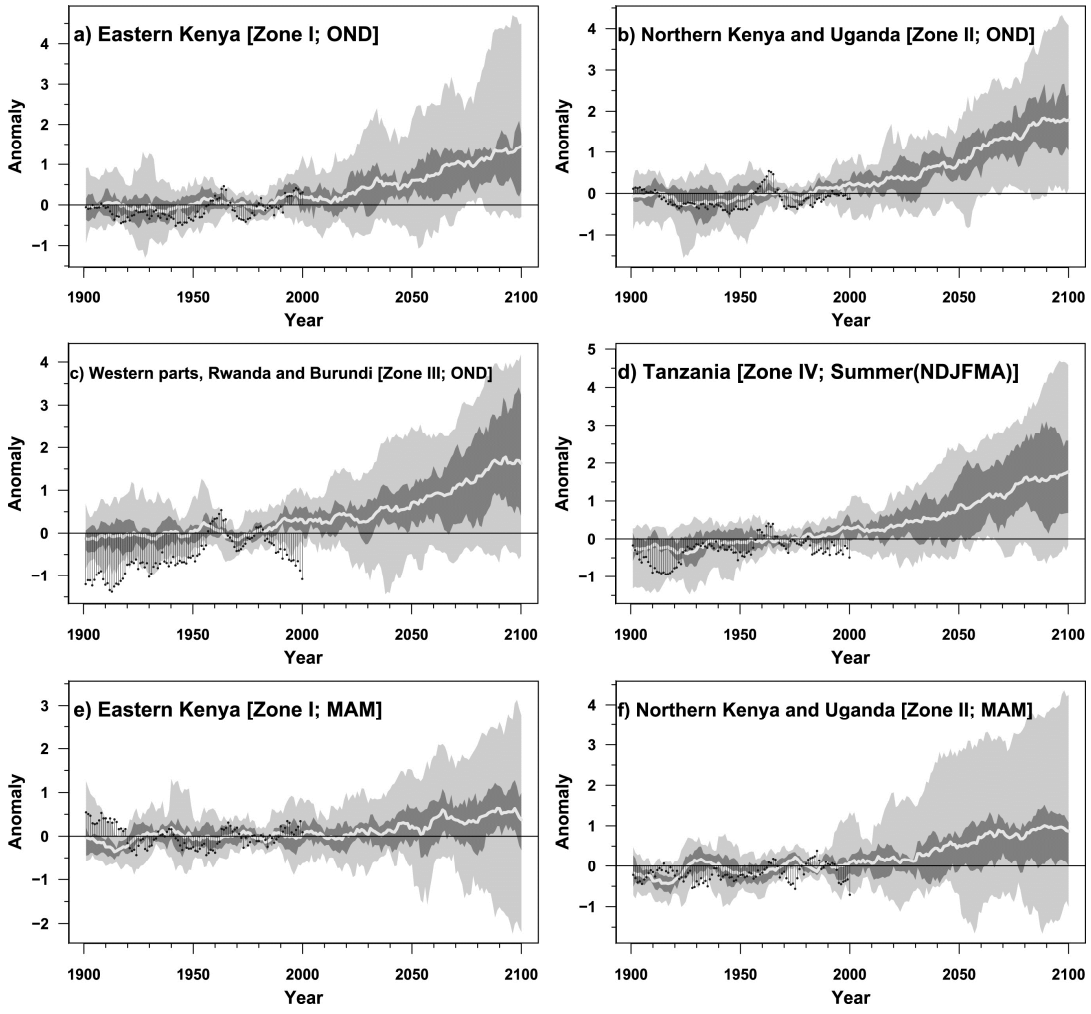

Appendix 2: Projected seasonal precipitation changes (standard deviation) in East Africa

Appendix 3: Box-and-whisker plots for monthly precipitation change factors from the 10 GCMs used in this study for the time periods (a) 2020s, (b) 2050s, and (c) 2080s for emissions scenarios A1B, A2 and B1.

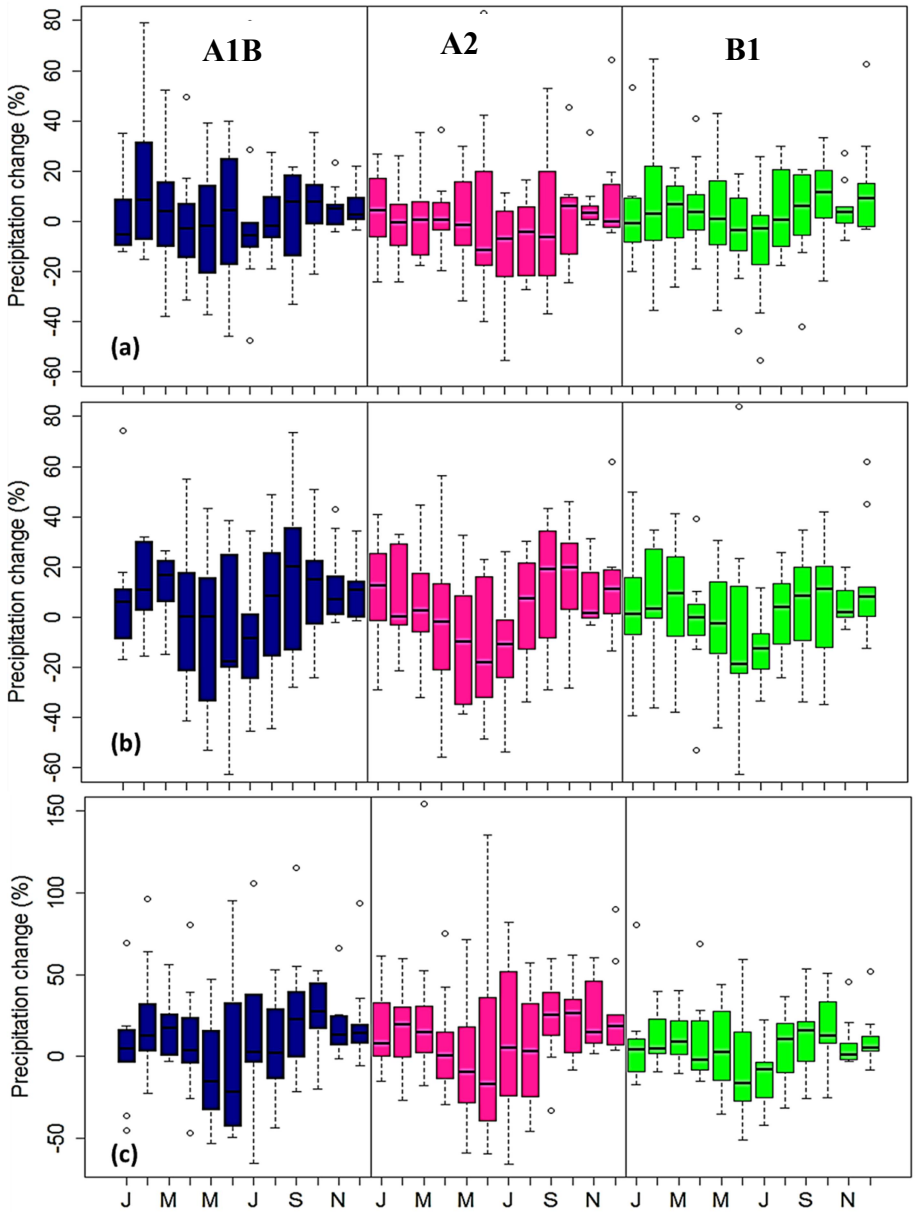

Appendix 3: Projected monthly precipitation changes in Mt. Elgon sub-watersheds

Appendix 4: Box-and-whisker plots for monthly temperature change factors from the 10 GCMs used in this study for the time periods (a) 2020s, (b) 2050s, and (c) 2080s for emissions scenarios A1B, A2 and B1.

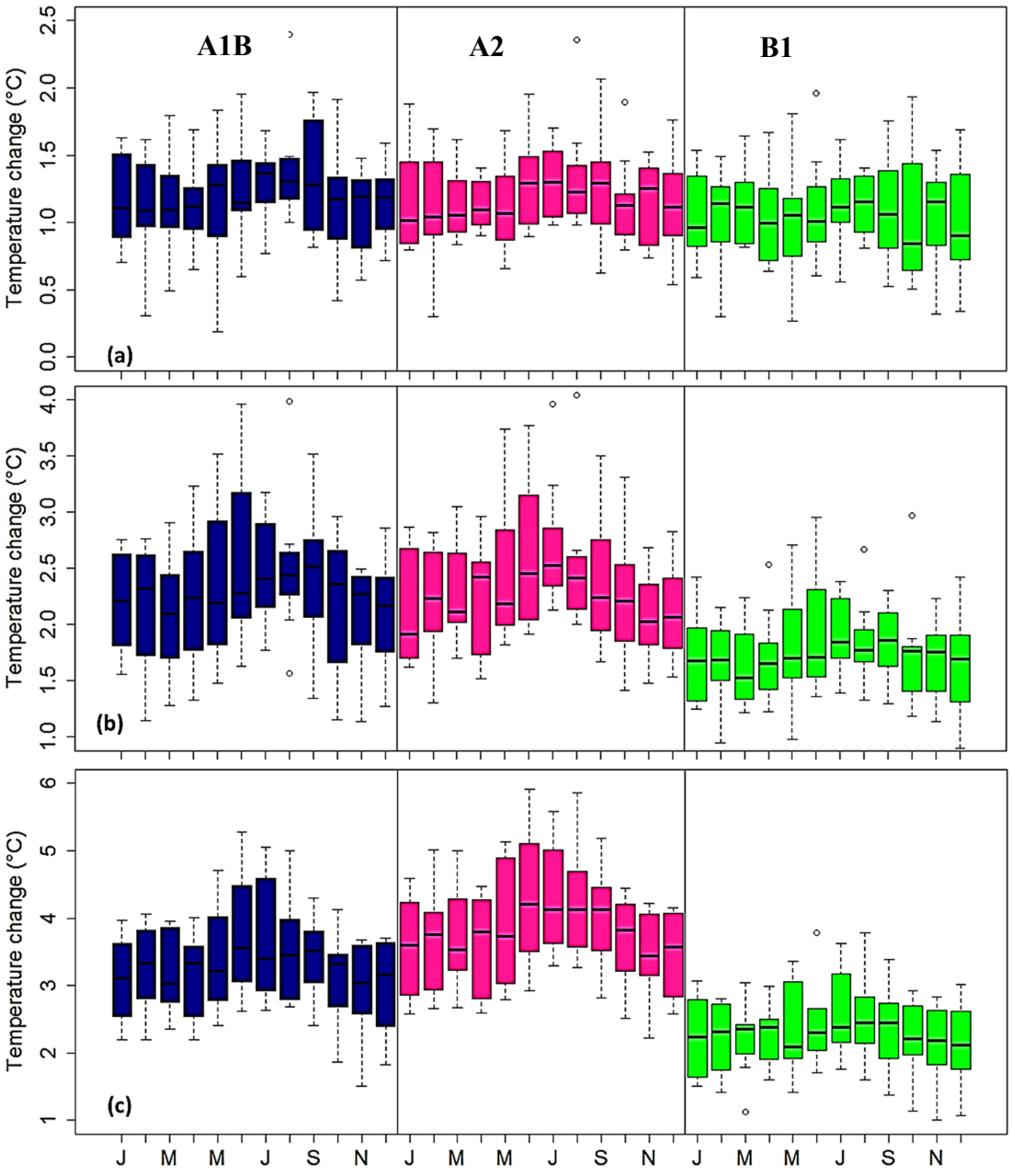

Appendix 4: Projected monthly temperature changes in Mt. Elgon sub-watersheds

Appendix 5: Box-and-whisker plots for seasonal temperature change factors from the 10 GCMs used in this study for the time periods (a) 2020s, (b) 2050s, and (c) 2080s for emissions scenarios A1B, A2 and B1.

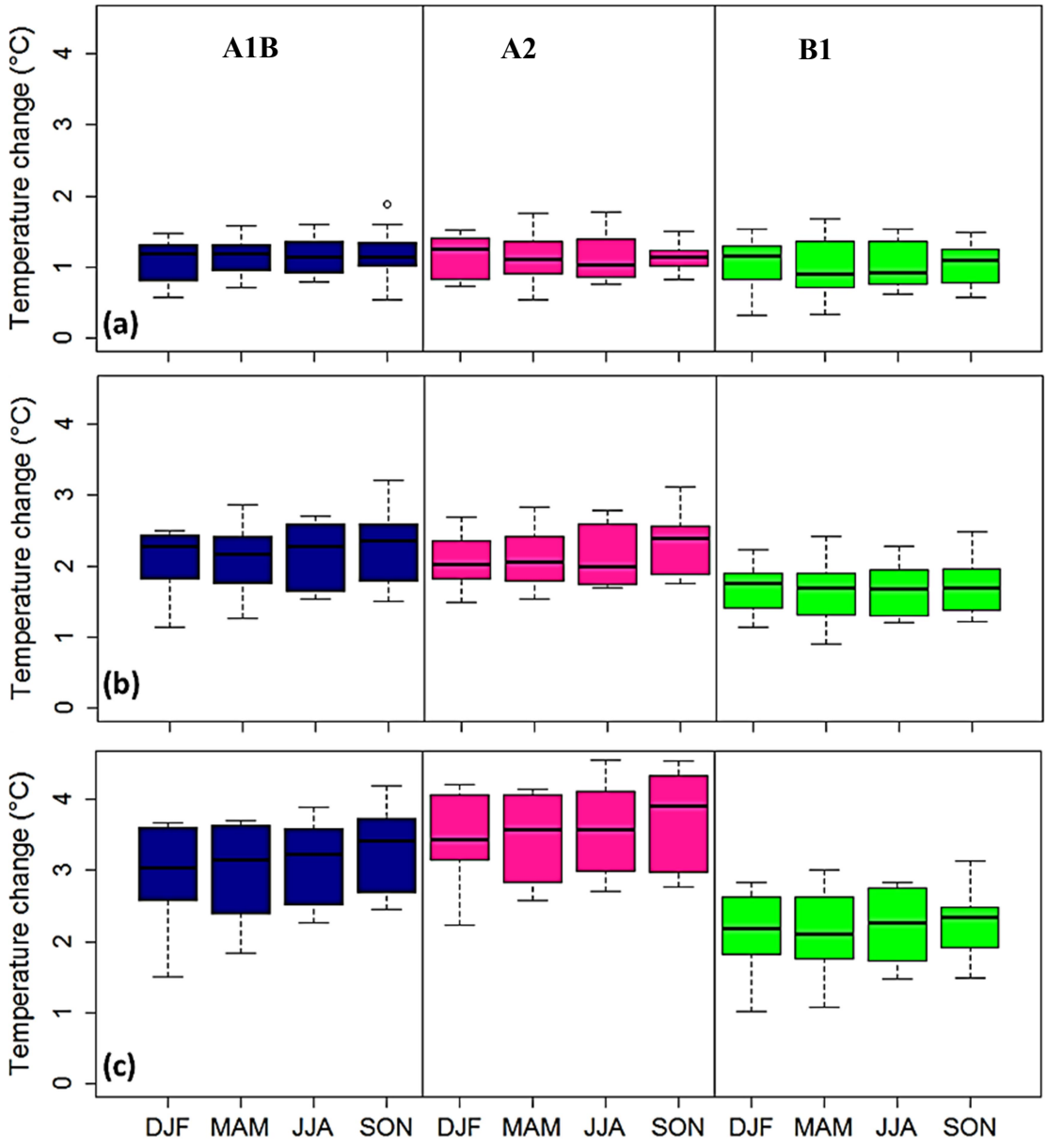

Appendix 5: Projected seasonal temperature changes in Mt. Elgon sub-watersheds

Appendix 6: Box-and-whisker plots for seasonal precipitation change factors from the 10 GCMs used in this study for the time periods (a) 2020s, (b) 2050s, and (c) 2080s for emissions scenarios A1B, A2 and B1.

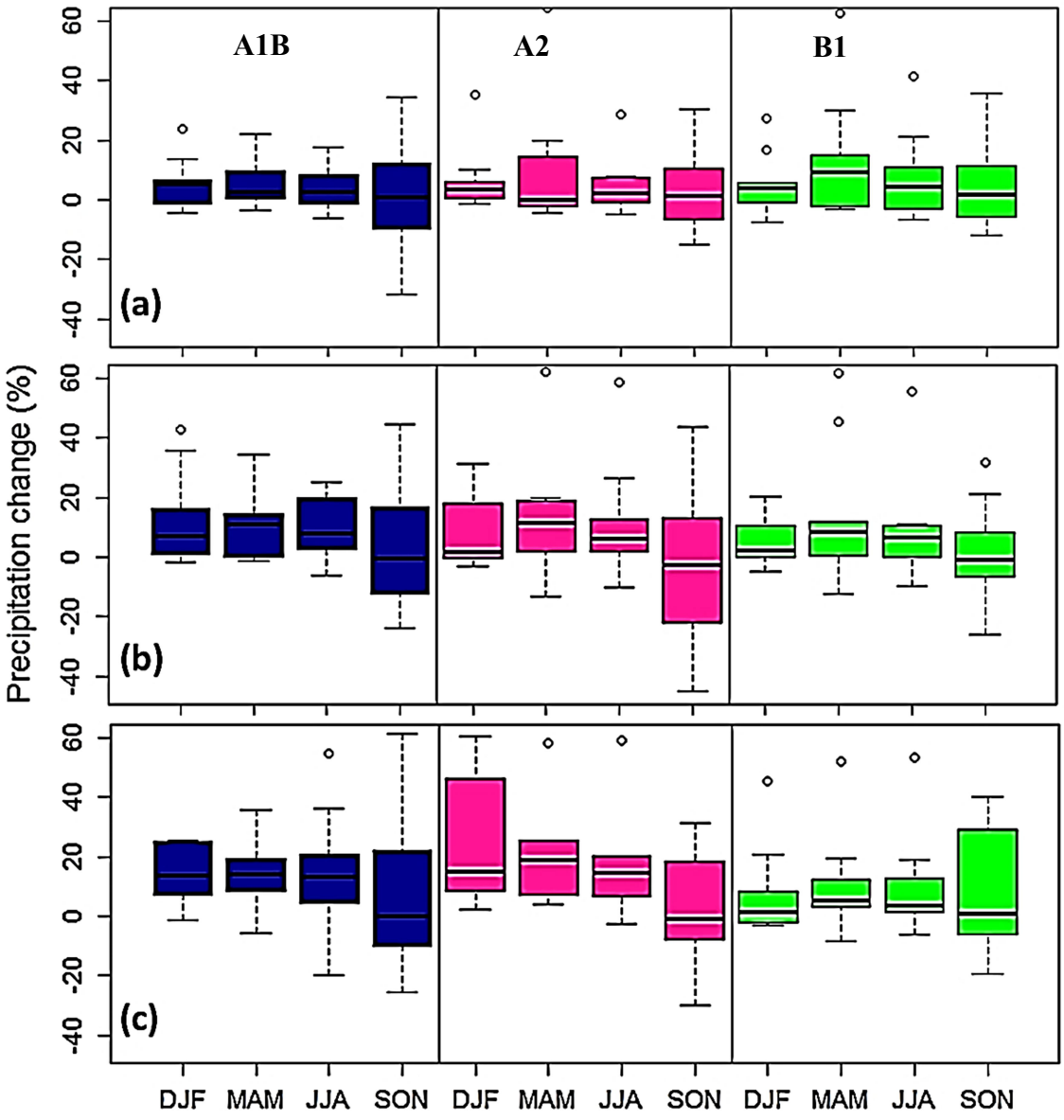

Appendix 6: Projected seasonal precipitation changes in Mt. Elgon sub-watersheds